

UC San Diego

UC San Diego Electronic Theses and Dissertations

Title

Further genetic identification of genes and pathways associated with axon growth and regeneration

Permalink

<https://escholarship.org/uc/item/8cw3j20d>

Author

Carter, Patricia

Publication Date

2012

Peer reviewed|Thesis/dissertation

UNIVERSITY OF CALIFORNIA, SAN DIEGO

Further Genetic Identification of Genes and Pathways Associated with Axon Growth and
Regeneration

A Thesis submitted in partial satisfaction of the requirements for the degree Master of
Science

in

Biology

by

Patricia Carter

Committee in Charge:

Professor Yishi Jin, Chair
Professor Andrew Chisholm
Professor Nigel Crawford

2012

The Thesis of Patricia Carter is approved, and it is acceptable in quality and form for publication on microfilm and electronically:

Chair

University of California, San Diego

2012

TABLE OF CONTENTS

Signature Page.....	iii
Table of Contents.....	iv
List of Tables.....	v
List of Graphs.....	vi
List of Figures.....	x
Acknowledgements.....	xi
Abstract.....	xii
I. Introduction	1
II. Materials and Methods.....	9
III. Results.....	14
Chapter 1 – Testing Genetic Interactions Via Double Mutants	15
Chapter 2 – Testing Conservation of Molecular Function in PDE Dopaminergic Neurons	24
Chapter 3 – Testing New Genes For Molecular Function in Axon Growth and Regeneration	27
IV. Discussion	32
V. Tables, Graphs, and Figures	41
References	129

LIST OF TABLES

Table 1: List of Strains Used in Experiments	39
Table 2: List of Primers Used in Experiments	44
Table 3: List of Average Branch Numbers For Each Axotomy Group (Done By Zilu Wu).....	57

LIST OF GRAPHS

Graph 1: AVM Guidance Growth Defect for double mutant <i>zdis5 I unc-57 (e1190); pxn-2(ju358)</i>	74
Graph 2: ALM Guidance Growth Defect for double mutant <i>zdis5 I unc-57 (e1190); pxn-2(ju358)</i>	75
Graph 3: PVM Guidance Growth Defect for double mutant <i>zdis5 I unc-57 (e1190); pxn-2 (ju358)</i>	76
Graph 4: PLM Overshoot Growth Defect for double mutant <i>zdis5 I unc-57 (e1190); pxn-2(ju358)</i>	77
Graph 5: Axotomy Data: Vesicle Associated Protein/ Development Double mutant <i>zdis5 I unc-57 (e1190); pxn-2 (ju358)</i>	78
Graph 6: PLM Overshoot Growth Defect for double mutant <i>zdis5 I; arf-6 (tm1447); pxn-2(ju358)</i>	79
Graph 7: ALM (ALM Wavy) Growth Defect for double mutant <i>zdis5 I; arf-6 (tm1447); pxn-2(ju358)</i>	80
Graph 8: AVM Guidance Growth Defect for double mutant <i>zdis5 I; arf-6 (tm1447); pxn-2(ju358)</i>	81
Graph 9: Axotomy Data: for double mutant <i>zdis5 I; arf-6 (tm1447); pxn-2(ju358)</i>	82
Graph 10: PLM Overshoot Growth Defect for double mutant <i>mul32 II; arf-6 (tm1447) IV; sec-22 (ok3053) X</i>	83
Graph 11: Axotomy Data: for the double mutant <i>mul32 II; arf-6 (tm1447) IV; sec-22 (ok3053) X</i>	84

Graph 12: PLM Overshoot Growth Defect for double mutant	
<i>muIs32 II; snb-1 (md247) V, sec-22 (ok3053) X</i>	85
Graph 13: ALM Bent Growth Defect for double mutant	
<i>muIs32 II; snb-1 (md247) V, sec-22 (ok3053) X</i>	86
Graph 14: Axotomy Data: for the double mutant	
<i>muIs32 II; snb-1 (md247) V, sec-22 (ok3053) X</i>	87
Graph 15: PLM Overshoot Growth Defect: Rescue	
<i>muIs32 II; unc-26 (e205) IV arf- 6 (tm1447) IV</i>	88
Graph 16: ALM Wavy Growth Defect: Rescue	
<i>zdis5 I; arf-6 (tm1447) IV; unc-51 (ky347) V</i>	89
Graph 17: PLM Overshoot Growth Defect: Rescue	
<i>zdis5 I; arf-6 (tm1447) IV; unc-51 (ky347) V</i>	90
Graph 18: PLM Overshoot Growth Defect: Rescue	
<i>zdis5 I; arf-6 (tm1447) IV; unc-51 (ky347) V</i>	91
Graph 19: Axotomy Data: Rescue:	
<i>muIs32 II; unc-26 (e205) IV arf- 6 (tm1447) IV; juEx4082</i>	92
Graph 20: Axotomy Data: Rescue:	
<i>zdis5 I; arf-6 (tm1447) IV; unc-51 (ky347) V; juEx4082</i>	93
Graph 21: Axotomy Data: Rescue:	
<i>muIs32 II; unc-26 (e205) IV arf- 6 (tm1447) IV; juEx4084</i>	94
Graph 22: Axotomy Data: Rescue:	
<i>zdis5 I; arf-6 (tm1447) IV; unc-51 (ky347) V; juEx4082</i>	95
Graph 23: ADE Anterior Migration Defect: <i>otIs181</i> Single Mutants	96

Graph 24: ADE Anterior Migration Defect: <i>otIs181</i> Double Mutants	97
Graph 25: AIY Posterior Migration Defect: <i>otIs181</i>	98
Graph 26: Axotomy Data: <i>otIs181</i> Single Mutants	99
Graph 27: Axotomy Data: <i>otIs181</i> Double Mutants	100
Graph 28: PLM Overshoot Defect: Temperature Sensitive 25 degrees	
PLM Overshoot Defect: Temperature Sensitive 25 degrees (Cont.)	101
Graph 29: PLM Overshoot Defect: New Temperature Sensitive	102
Graph 30: <i>mulS32 II; dnc-4(or633) IV</i> Temperature Sensitive	103
Graph 31: <i>zdlS5 I; dnc-4(or633) IV</i> Temperature Sensitive	104
Graph 32: <i>mulS32 II; lit-1 (or393) III</i> Temperature Sensitive	105
Graph 33: <i>mulS32 II; par-2 (or640)</i> Temperature Sensitive	106
Graph 34: <i>mulS32 II; par-2 (or373)</i> Temperature Sensitive	107
Graph 35: <i>zdlS5 I; par-2 (or373)</i> Temperature Sensitive	108
Graph 36: <i>mulS32 II; plk-1 (or683) III</i> Temperature Sensitive	109
Graph 37: <i>zdlS5 I; plk-1 (or683) III</i> Temperature Sensitive	110
Graph 38: <i>spd-2 (or492) I; mulS32 II</i> Temperature Sensitive	111
Graph 39: <i>spd-2 (or293) I; mulS32 II</i> Temperature Sensitive	112
Graph 40: <i>zdlS5 I; zyg-1 (or297) II</i> Temperature Sensitive	113
Graph 41: <i>zdlS5 I; zyg-1 (or409) II</i> Temperature Sensitive	114
Graph 42: <i>rsa-1 (or598) I; mulS32 II</i> Temperature Sensitive	115
Graph 43: <i>zdlS5 I; rsa-1 (or598) I</i> Temperature Sensitive	116
Graph 44: <i>mei-1 (or642) I; mulS32 II</i> Temperature Sensitive	117
Graph 45: <i>spd-5 (or213) I; mulS32 II</i> Temperature Sensitive	118

Graph 46: <i>dnc-1 (or404) I; mul32 II</i> Temperature Sensitive	119
Graph 47: <i>zds5 I dnc-1 (or404) I</i> Temperature Sensitive	120
Graph 48: <i>mel-26 (or543) I; mul32 II</i> Temperature Sensitive	121
Graph 49: PLM Overshoot Defect: Reticulon (RET) associated	122
Graph 50: PLM Overshoot Defect: Reticulon (RET) with vesicle- associated genes	123
Graph 51: Axotomy Data: Reticulon (RET) associated	124
Graph 52: PLM Overshoot Defect: Reticulon (RET) associated 2	125
Graph 53: Axotomy Data: Reticulon (RET) associated 2	126
Graph 54: PLM Overshoot Defect: <i>pinn-1</i> and <i>svh-2</i>	127
Graph 55: Axotomy Data: <i>pinn-1</i> and <i>svh-2</i>	128

LIST OF FIGURES

Figure 1: DLK-1 MAPKKK and JNK MAPK Pathway.....	71
Figure 2: Proper Growth of ALM, AVM, PLM, and PVM Neurons	72
Figure 3: Proper Growth of CEP, AIY, ADE, and PDE Neurons.....	73

ACKNOWLEDGEMENTS

First, I would like to thank the members of my committee who have been there for me when I have needed them. Most of all I would like to thank my chair, Dr. Yishi Jin, for providing me this great opportunity to actively participate in the world of science and for pushing me to be the best I can be. I would also like to thank every person in the Jin and Chisholm labs for everything they have done for me. Thank you for not only helping me with my experiments, but for being my friend. I have enjoyed getting to know each and every single one of you. Last but not least, I would also like to give a special thank you to Zhiping Wang for being an amazing mentor, who not only taught me the basic techniques, but also guided me throughout this process and provided me many pep talks. I owe a lot of my success I have accomplished in the lab to her.

ABSTRACT OF THE THESIS

Further Genetic Identification of Genes and Pathways Associated with Axon Growth and Regeneration

by

Patricia Carter

Master of Science in Biology

University of California, San Diego, 2012

Professor Yishi Jin, Chair

To understand how to fix damages to the central nervous system, the genes and pathways associated with axon growth and regeneration must be determined. Although significant progress has been made in understanding axon growth and regeneration in vitro, demonstrating in vivo roles requires intense effort. My project consisted of three goals that would help us gain better understanding of axon growth and regeneration. The project was performed using the model animal *Caenorhabditis elegans*. The first goal of this project was to test the in vivo interactions among genes known to be moderately involved in axon regeneration via double mutants. We found that some of the genes appear to work together, while others do not. The second goal was to test genes previously determined to have significant affects on PLM axon regeneration to see if

their role is conserved in the PDE, a different neuron type. We found that for axon regeneration, gene function do not appear to be conserved in the PDE. The last goal was to determine the function of not previously tested genes on axon growth and regeneration. Of the genes tested, some showed affects on axon growth or regeneration alone, while some showed affects in both. Overall, we have determined pathways and function conservation of genes known to be involved in axon growth and regeneration, while also determining the functions of new genes. Further studies need to be done to determine genetic interactions of the genes with the pathways that guide proper axon growth and regeneration.

I.

Introduction

Understanding axon growth and regeneration remains still a work in progress

The nervous system is comprised of a network of neurons, which are cells that can be activated by electrical and chemical signals. The signals travel down the axon at great rates where they leave the neuron, via the synapse, to go on to the target. Axons can be various lengths and extend to various places in an organism's body. Severe damage or severing of the axons in the central nervous system of mammals has shown failure to heal or regenerate, leading to neurodegeneration or different levels of paralysis. This has been a topic of extreme interest since knowledge of the subject can prove to help millions who are plagued with neurological diseases, such as Alzheimer's disease, or neuronal injuries, such as spinal cord crush injuries.

To be able to understand how to fix damages to the central nervous system, the genes and pathways associated with axon growth and regeneration must be determined. Although progress has been made in understanding axon growth and regeneration in vivo, demonstrating the in vivo role requires intense effort. For the genes that have already been discovered to function in axon growth or regeneration, further study needs to be done in order to understand how those genes work in a pathway and to learn if the functions of those genes are conserved in different neurons. Also, further studies need to be done in order to see if untested genes have any control over axon growth and regeneration.

C. elegans as a model for axon growth and regeneration

Research studies have used animals as research models due to the fact that human research has ethical issues. Certain animal models have advantages over human model-based research, which may include larger brood sizes, faster reproductive cycles, or genomes that are easily manipulated. Also, with the use of animal models, research can be completed at faster rates leading to greater rates of discovery. Of the many different animal models, the nematode *Caenorhabditis elegans*, or *C. elegans*, has recently emerged as a great animal model for studying axon growth and post-injury regeneration ([Yanik et al., 2004], [Wang and Jin, 2011], and [Wu et al., 2007]).

In *C. elegans*, we can label specific groups of neurons with fluorescent protein transgenes such as GFP or RFP. For this experiment, we used *mec-7-GFP (muIs32)* or *mec-4-GFP (zdIs5)*, which marks the ALM, AVM, PLM, and the PVM. We also used *dat-1mch; ptx-3 mch (otIs181)*. *dat-1* marks the ADE, CEP, and PDE, while *pttx-3* marks the AIY. In doing so, we can then visualize the axons of the neuron groups and observe the effects of different mutants, in comparison to a wild type animal, on axon growth patterns. From this data, we can determine what defect each mutant strain has and what genes are essential for proper axon growth. We can also visualize the axons for femtosecond laser axotomy, which is the efficient severing of the axons with a precise, high-speed laser (Yanik et al., 2004). In our axotomy experiments, the PLM or the PDE, both located in the tail region, were severed for observations. Axotomy mimics neuronal injuries and provides a way to study whether or not genes are essential for axon regeneration and whether the essential genes inhibit or promote regeneration.

Many factors, genes, and pathways have already been identified in *C. elegans* to have effects on axon regeneration. For example, the genes in the DLK-1 MAPKKK pathway were determined to be part of this cascade and essential for axon regeneration in *C. elegans* ([Hammarlaund et al., 2009] and [Yan et al., 2009]). Without *dlk-1*, the axon was not able to initiate growth cone formation after the axon was severed. The same pathway is required, but not essential, in *Drosophila* (Xiong et al., 2010) and in mice (Itoh et al., 2009) for axon regeneration (Chen et al., 2011). The previous data suggests that molecular pathways for axon regeneration can be conserved in different models; and therefore, *C. elegans* can be used as a valuable, in vivo model for studying axon growth and regeneration with hopes of applying the knowledge to find therapeutics to help prevent or alleviate neurodegeneration or neuronal injuries in humans.

Our project aims to further study genes associated with axon growth and regeneration

Of what we know about axon growth and regeneration in mammals has been tested in vitro in cell cultures. For example, the protein NOGO- a product of the gene TRN4- has been tested in vitro and has shown inhibitory roles in neuronal regrowth (Schwab M., 2010). Although significant progress has been made with in-vitro studies, the factors affecting axon growth and regeneration in vivo is a less known topic of study. Our lab performed a large-scale screen for genes that play a role in axon regeneration in vivo by using a mutation-based screen. From the screen, many genes not previously known to be involved in axon regeneration were identified to be required for axon regrowth. Upon generating double mutants and analyzing the axotomy data, our lab was able to determine the affects the genes had on each other (Chen et al., 2011). Our current

interest is to continue the work done by the lab to gain further knowledge of axon growth and regeneration and the mechanisms behind both. For the genes that we already know to have some affect on axon regeneration, meaning the genes that do not complete block or promote regeneration, we are testing the genes together to figure out the genetic interactions since we already know they work in parallel pathways.

We made double mutants for *efa-6*, *arf-6*, *snb-1*, *unc-26*, *unc-57*, *sec-22* and *pxn-2*; with *pxn-2* being the developmental gene. Previous axotomy data showed that *pxn-2*, *efa-6*, and *arf-6* showed significant increase in PLM regrowth, meaning that these genes normally inhibit regeneration in wild type animals ([Chen et al., 2011] and [Gotenstein et al., 2010]). *pxn-2* is a peroxidase that is essential in development, specifically for embryonic morphogenesis and basement membrane function (Gotenstein et al., 2010). *efa-6* is an exchange factor for ARF-6 that negatively regulates DHC-1 (O'Rourke et al., 2007). *arf-6* is a GTPase that functions in receptor-mediated endocytosis (Dang et al., 2003). Previous axotomy data also showed that *unc-26*, *unc-57*, and *sec-22* showed significant decrease in PLM regrowth, meaning that these genes normally promote axon regeneration in wild type animals. Also, *unc-51* was shown to be required for growth of axonal processes and elongation of developing neurons ([Ogrua et al., 1994] and [Chen et al., 2011]). *unc-51* has also been shown in *Drosophila* to be involved in membrane vesicle trafficking. *unc-26* is a synaptic vesicle recycling associated protein that encodes synaptojanin (Harris et al., 2000). *unc-57* is also required for synaptic vesicle recycling and is similar to *unc-26* with indication that the two genes work in the same genetic pathway (Schuske et al., 2003). *sec-22* is a yeast sec homolog involved in membrane trafficking (Chen et al., 2011), but not much else is known about the gene.

We also continued the work by testing previously determined genes, from the large-scale screen and other experiments, to see if their role in axon growth and regeneration is conserved in different neurons. As we know in vertebrates, the roles of a gene in a specific type of neuron may not be conserved in another type of neuron. For example, the peripheral nervous system (PNS) shows regeneration of damaged axons, while the central nervous system (CNS) does not. Normally, we test regeneration in the *mec-7-GFP (muIs32)* or *mec-4-GFP (zdIs5)* backgrounds. However, to test conservation of the genes that showed strong results in the *muIs32* or *zdIs5* background, we decided to use *dat-1mch; pttx-3 mch (otIs181)* background. The strains we made in the *otIs181* background include: *arf-6*, *efa-6*, *unc-26*, *unc-57*, *mlk-1*, *dlk-1*, *cebp-1*, *kgb-1*, and *kgb-1 kgb-2*. Once again the previously mentioned genes code for vesicle associated proteins. The genes not previously mentioned, *mlk-1*, *dlk-1*, *cebp-1*, *kgb-1*, and *kgb-1 kgb-2*, are all part of the previously talked about DLK-1 MAPKKK pathway and its parallel JNK MAPK pathway that regulates axon regeneration by promoting regeneration ([Hammarlaund et al., 2009] and [Yan et al., 2009]). See Figure 1. Upon finishing the single mutants in the *otIs181* background, we also made double mutants to see if the pathways were conserved in different neurons as well. The double mutant strains we made were: *dlk-1 (tm4024) I; otIs181 III*; *kgb-1 (um3) IV* and *dlk-1 (tm4024) I; otIs181 III; kgb-1 (um3) kgb-2 (km16) IV*.

Lastly, we also continued the work done in the lab by testing genes that were not previously tested to see their effect on axon growth and regeneration. The first group of new genes tested were temperature-sensitive genes. O'Rourke et al. wanted to determine what the maternal gene requirements were of early embryos so they bypassed early

essential gene requirements in the larval and adult germline development stages. They did this by doing a screen for temperature-sensitive, embryonic lethal mutations that would allow for the bypass of early gene requirements. At 15 degrees, the proteins in the temperature sensitive strains remain active. Upon shifting the L1 mutants up to 25 degrees, the proteins become inactive because the mutations are single amino acid changes within the hydrophobic core of the folded proteins (O'Rourke et al., 2011), so the proteins becomes destabilized. We decided to test some of the genes from their screen, specifically the ones that deal with microtubules, to see if the essential maternal genes have any effect on adult axon growth and regeneration. We chose the genes that deal with microtubules because microtubules span the axon providing cytoskeleton paths for transport. If we knock out the genes that deal with microtubules, then the microtubules in the axon may be affected leading to defects in axon growth and regeneration. We also tested a few other genes that have previously shown interactions with some of the temperature- sensitive genes we decided to test. The genes tested include: *dnc-4*, *lit-1*, *par-2*, *plk-1*, *spd-2*, *zyg-1*, *rsa-1*, *mei-1*, *dnc-1*, *mel-26*, and *spd-5*.

The next group of new genes tested coded for vesicle-associated proteins. The genes tested included: *ret-1*, *lnp-1*, and *yop-1*. The genes were selected because *ret-1* is a member of the reticulon family and homologous to NOGO, which was previously stated to inhibit regeneration, in invertebrates. *yop-1* was selected because it has been shown to associate with *ret-1* to interfere with the formation of the endoplasmic reticulum during mitosis (Audhya et al., 2007). Reticulons have also shown to function in intracellular trafficking, which is related to vesicle formation and recycling (Yang et al., 2007). Upon

finishing the single mutants, we also constructed double mutants for *ret-1* and *lnp-1* in order to test the genes genetic interactions with each other and *arf-6*.

The last two of the new genes tested were *pinn-1* and *svh-2*. Of the two genes, *svh-2* was selected for testing because it has been shown to activate the JNK MAPK cascade, which is the pathway that works in parallel with the DLK-1 MAPKKK pathway. The pathway does not control the DLK-1 pathway (Li et al., 2011). *pinn-1* is part of the peptidyl-prolyl *cis/trans* isomerases enzyme family and has been shown to be involved in Alzheimer's disease and other neurodegenerative diseases in mammals. PIN1 binds specifically to tau and restores its function, which is to stabilize microtubules. Without *pinn-1*, the microtubules tangle forming neurofibrillary tangles, which leads to the progression of neurodegenerative diseases (Poli et al., 2005). *pinn-1* can be a target for therapeutics for neurodegeneration. Upon finishing the single mutants, we also constructed the double mutant for *pinn-1* and *svh-2*. (See Table 1 for full list of constructed strains)

II:

Materials and Methods

Worm Maintenance and Genetics

C. elegans animals were grown, at 15 or 20°C, on NGM agar plates seeded with OP50 *E. coli* lawns, as described (Brenner, 1974). Wild type control worms are N2 Bristol. Mutant strains were identified by PCR to detect deletion and insertion mutations. All substitution mutations were identified by DNA sequencing. However, if the strain had an obvious phenotype, mutant strains were identified by that specific phenotype. Table 1 provides a list of mutant strain numbers, genotypes, and starting strain genotypes. Table 2 provides genotyping and sequencing primer sequences and amplicon band sizes.

Crosses (single mutants)

Cross 10 mutant hermaphrodites to 20 wild type (N2/ *zdl5/ mul32*) males to get heterozygous mutant F1 hermaphrodites carrying the marker. Next, 8 F1 heterozygous hermaphrodites with the marker are put on a plate and allowed to produce F2 progeny. From the plate, 16 F2 progeny with the marker are singled and allowed to produce progeny. To determine the genotype of the plates, a lysis is done on the F3 worms and a PCR is done. If a strain had an obvious phenotype, mutant strains were identified by that specific phenotype.

For mutants with transgenes, the above cross was preformed. However, the hermaphrodites from the cross contained an integrated transgene [for this project: *Prgef-1-arf-6::gfp (juEx4082)* or *Pmec-7-arf-6::gfp (juEx4084)*].

Crosses (double mutants)

First, cross 10 mutant hermaphrodites to 20 wild type (N2/ *zdl5/ mul32*) males to get heterozygous mutant males carrying the marker. Next, using the dissection scope, pick 20 heterozygous males with markers and crossed them to 10 hermaphrodites of next

mutant strain. From there, 8 F1 double heterozygous hermaphrodites with the marker are put on a plate and allowed to produce F2 progeny. From the plate, 32-50 F2 progeny with the marker are singled and allowed to produce progeny. To determine the genotype of the plates, a lysis is done on the F3 worms and a PCR is done. If a strain had an obvious phenotype, mutant strains were identified by that specific phenotype.

For mutants with transgenes, the above crosses were preformed. However, the hermaphrodites from the first cross contained an integrated transgene [for this project: *Prgef-1-arf-6::gfp* (*juEx4082*) or *Pmec-7-arf-6::gfp* (*juEx4084*)].

Worm lysis

From each of the plates that were assumed to be mutant homozygous, 10-20 worms were picked and 2 μ L 10X PCR buffer (no Mg²⁺), 2 μ L 25mM MgCl₂, 16 μ L ddH₂O, and 2.2 μ L proteinase K were added to PCR tubes. The mixtures were run at 65°C for 60 minutes, 95°C for 15 minutes, and 4°C for 5 minutes. Worm lysis was also done on the original mutant and wild type worms as positive and negative controls, respectively.

Polymerase Chain Reaction (PCR)- Phusion Polymerase

To amplify the product, a PCR was done by adding 14.75 μ L ddH₂O, 5 μ L 5X Phusion Buffer, 2 μ L dNTPs, 1.5 μ L primers (.5 μ L forward, .5 μ L internal, and .5 μ L reverse), 1.5 μ L template (worm lysis), and .25 μ L phusion polymerase. The phusion polymerase was added last since the PCR mixture needed to be in the correct environment for the polymerase to not get denatured. The temperatures used for the PCR are 98°C for 4 minutes to denature the DNA, 55-62°C for 20 seconds to anneal the primers, and 72°C for 2-6 minutes to elongate and extend the new DNA. The reaction

was repeated 39 times to get enough products to visualize on DNA agarose gel. (See table 2 for primer list and estimated band sizes)

Polymerase Chain Reaction (PCR)- TAQ

To amplify the product, a PCR was done by adding 10 μ L ddH₂O, 2 μ L 10X PCR Buffer, 1 μ L dNTPs, ~1 μ L primers (.33 μ L forward, .33 μ L internal, and .33 μ L reverse), 4 μ L template (worm lysis) and .5 μ L TAQ. The temperatures used for the PCR are 95°C for 4 minutes to denature the DNA, 55-62°C for 20 seconds to anneal the primers, and 72°C for 2-6 minutes to elongate and extend the new DNA. The reaction was repeated 39 times to get enough products to visualize on DNA agarose gel. (See table 2 for primer list and estimated band sizes)

Gel electrophoresis

To check if the PCR product was correct, a gel electrophoresis was done, and the bands for potential homozygous mutant worms were compared to the band for mutant positive control. A 2% gel was used and loaded with each of the samples and a 1X KB Ladder. The gel was run in the machine for 30 minutes at 120mV. Then, a UV box was used to visualize the bands. (See table 2 for estimated band sizes)

Sequencing

For any mutants that have a substitution mutation, the PCR products then sent to sequencing to verify the substitution mutation. To prepare samples for sequencing, the PCR primers in the PCR solution needed to first be destroyed using ExoSAP-It reagent. 5 μ L of PCR product and 2 μ L of ExoSAP- IT reagent were mixed and incubated at 37°C for 15 minutes followed by 80°C for 15 minutes. The mixture was then sent to sequencing with sequencing primers (forward or reverse) already added to the tubes.

Final worm selection

The plates that have samples that come back showing mutant homozygous are then checked under the dissection scope to check that 100% of the progeny have GFP marker. The plates that are correct for mutant and marker are used for axon growth and regeneration projects.

Temperature Sensitive Shift

Strains plus controls are maintained at 15 degrees. The day before scoring or axotomy, L1 worms are shifted onto pre-warmed plates and moved to 25 degrees and left over night. The next day L4 worms are scored or cut using the protocols described above.

Scoring

20-40 L4 worms (controls or mutants) are chosen each time and observed under the compound scope on slides. 5mM levamisole is used to paralyze the worms. The mutant worms are observed for any defects and compared to the control worms for significance of the defects seen. Scoring is repeated three times.

Axotomy

Laser axotomy experiments were performed by Zilu Wu as discussed (Wu et al., 2007).

III.
Results

Chapter 1 – Testing Genetic Interactions Via Double Mutants

As previously stated in earlier sections, for the genes that we already know to have some affect on axon regeneration, we are now testing the genes together to figure out the genetic interactions. We know the genes must work in parallel pathways or in the same pathways since they all have an affect on axon regeneration. To determine the interactions of the genes, the ALM, AVM, PLM, and PVM were observed for defects in axon growth in the wild type, single mutant controls, and the double mutant and compared to one another. The defects seen in the study for the ALM were that the ALM was wavy. The defects seen in the AVM and PVM were guidance defects. The axon did not properly move ventrally to the ventral cord and turn moving anteriorly towards the head. Instead, the axon turned early before reaching the ventral cord. The defects seen in the PLM were overshooting defects- the PLM would overshoot the ALM. To see how the axons develop in a wild type worm see Figure 2. To determine the interactions of the genes in axon regeneration, the PLM was cut in the wild type, single mutants, and double mutant and compared to one another.

Of the double mutants, *mec-4-GFP (zdIs5) unc-57 (e1190) I; pxn-2 (ju358) X* and *mec-4-GFP (zdIs5) I; arf-6 (tm1447) IV; pxn-2 (ju358) X* were made in order to see if the genes interacted in the same pathways as each other. To figure out the interactions between *unc-57 (e1190)* and *pxn-2 (ju358)* in axon regrowth, we first determined the growth defects in the single mutants and then compared it to the double mutants. *mec-4-GFP (zdIs5) I unc-57 (e1190) I* show no or no significant increase in defects in the AVM, ALM, PVM, and PLM when compared to the zdIs5 wild type control. However, *mec-4-GFP (zdIs5) I; pxn-2 (ju358) X* shows significant (**) increase in defects in AVM

guidance defect and PLM overshoot defect compared to the wild type. *mec-4-GFP (zdIs5) I; pxn-2 (ju358) X* also shows significant (***) increase in ALM (the axon is wavy) growth defect and no significant increase PVM guidance growth defect. For the AVM, the double mutant *mec-4-GFP (zdIs5) I unc-57 (e1190) I; pxn-2 (ju358) X* shows no significant increase in guidance defect compared to the *pxn-2 (ju358)* single mutant, but shows significant (***) increase in guidance defect when compared to the *unc-57 (e1190)* single mutant. (See Graph 1.) For the ALM, the double mutant shows no significant decrease in defect compared to *pxn-2 (ju358)*, but shows significant (***) increase in guidance defect when compared to *unc-57 (e1190)*. (See Graph 2.) For the PVM, the double mutant shows no significant increase in guidance defect compared to both single mutants. (See Graph 3.) For the PLM, the double mutant shows significant (*) increase in overshooting defect when compared to *pxn-2 (ju358)* and showed significant (***) increase in defect when compared to *unc-57 (e1190)*. (See Graph 4.)

To figure out the interactions between *unc-57 (e1190)* and *pxn-2 (ju358)* in axon regeneration, we performed axotomy on the wild type, single mutants, and double mutants and compared the regrowth data. The axotomy data shows that *mec-4-GFP (zdIs5) I unc-57 (e1190) I* shows a significant (***) decrease in regrowth and *mec-4-GFP (zdIs5) I; pxn-2 (ju358) X* shows a slight increase in regrowth that is not significant when compared to the *zdIs5* wild type control. When comparing the *unc-57 (e1190)* single mutant to *mec-4-GFP (zdIs5) I unc-57 (e1190) I; pxn-2 (ju358)*, the double mutant shows significant increase in re-growth (**). Also when the double mutant is compared to the *pxn-2 (ju358)* single mutant, the double mutant shows significant (*) decrease in re-growth. (See Graph 5.)

To figure out the interactions between *arf-6 (tm1447)* and *pxn-2 (ju358)* in axon regrowth, we once again determined the growth defects in the single mutants and then compared it to the double mutants. *mec-4-GFP (zdIs5) I; arf-6 (tm1447) IV* strain showed no or no significant increase in defects compared to the wild type control. When comparing *mec-4-GFP (zdIs5) I; pxn-2 (ju358) X* strain showed significant (*) increase in ALM growth (ALM wavy) and PLM overshooting defects. The double mutant *mec-4-GFP (zdIs5) I; arf-6 (tm1447) IV; pxn-2 (ju358) X* shows no significant change in PLM overshooting (See Graph 6) or AVM guidance defects (See Graph 7) when compared to the two single mutants. However, the double mutant does show a significant (*) increase in ALM growth (ALM wavy) defect (See Graph 8) when compared to the *arf-6 (tm1447)* single mutant, but not the *pxn-2 (ju358)* single mutant. To look further into the interactions between *arf-6 (tm1447)* and *pxn-2 (ju358)* in axon regeneration, we performed axotomy on the wild type, single mutants, and double mutants and compared the regrowth data. The axotomy data shows that the single and double mutant show no significant increase between each other and the wild type control (See Graph 9).

In testing other double mutants to see if the genes interacted in the same pathways as each other, we also tested *mec-7-GFP(muIs32) II; arf-6 (tm1447) IV; sec-22 (ok3053) X* and *mec-4-GFP(zdIs5)I; snb-1 (md247)V; sec-22 (ok 3053) X*. For *mec-7-GFP(muIs32) II; arf-6 (tm1447) IV; sec-22 (ok3053) X*, the *arf-6 (tm1447)* single mutant showed no significant decrease in PLM overshooting defect. While the *sec-22 (ok3053)* single mutant showed a similar percentage of PLM overshoot defect as the wild type control. The double mutant showed no significant increase in PLM overshoot defect compared to the *arf-6 (tm1447)* single mutant and showed a similar percentage of PLM overshoot

defect as the wild type control and the *sec-22 (ok3053)* X single mutant (See Graph 10). To see how *arf-6 (tm1447)* and *sec-22 (ok3053)* interact together in axon regeneration, we once again compared the single and double mutants. The *arf-6 (tm1447)* single mutant showed significant (**) increase in axon regrowth and the *sec-22 (ok3053)* single mutant showed significant (***) increase in axon regrowth. Comparing the double mutant to the single mutants, the strain showed no significant change in axon regrowth.

For *mec-4-GFP (zdIs5) I; snb-1 (md247) V; sec-22 (ok 3053) X*, the single mutants both showed a significant (***) increase in PLM overshoot defect compared to wild type control. They showed no other defects in the AVM, ALM, or PVM. Comparing the double mutant to *sec-22 (ok3053)* single mutant, the strain showed no significant increase in PLM overshooting defects. However, when the double mutant is compared to the *snb-1 (md247)* single mutant, the strain shows a significant (***) increase in PLM overshooting defect (See Graph 12). Also, when the double mutant is compared to both single mutants, the strain shows a significant (**) increase in ALM defect (See Graph 13)- the ALM is bent at an angle near the cell body. As for how the genes interact together in axon regeneration, the *snb-1 (md247)* single mutant showed no significant increase in axon regrowth and the *sec-22 (ok3053)* single mutant showed significant (**) increase in axon regrowth, when compared to the wild type control. In comparing the double mutant to the *snb-1 (md247)* single mutant, the strain showed a significant (*) decrease in axon regrowth. While comparing the double mutant to the *sec-22 (ok3053)* single mutant, the strain showed a significant (***) increase in axon regrowth (See graph 14).

Lastly, in unpublished data from Lizhen Chen and Zilu Wu, the double mutants *mec-7-GFP (muIs32) II; unc-26 (e205) IV arf-6 (tm1447) IV* and *mec-4-GFP (zDIs5)I; arf-6(tm1447) IV; unc-51 (ky347) V* suggested that *arf-6* suppressed *unc-26* and *unc-51*. We then went on to see if the results could be rescued by the transgenes *Prgef-1-arf-6::gfp (juEx4082)* or *Pmec-7-arf-6::gfp (juEx4084)*. The purpose of the rescue is to see if the mutants were actually the reason for the results seen, so in this case that *arf-6* suppresses *unc-26* and *unc-51*. We do this by inserting back in one of the genes into the double mutant, in this case *arf-6*, and see if the strain rescues back to similar results as the other single mutant. We also went to see if the transgenes could rescue any defects seen axon growth. For the first group of rescues, we used the transgene *Prgef-1-arf-6::gfp (juEx4082)*, which is expressed pan- neuronally.

For *muIs32; unc-26 (e205) IV arf-6 (tm1447) IV; Prgef-1-arf-6::gfp (juEx4082)*, no single mutants were ever scored for the strain. However, compared to the *muIs32* control, *muIs32; unc-26 (e205) IV arf-6 (tm1447) IV* showed no or no significant increase in growth defects in the ALM, AVM, PLM, and PVM. Also, compared to *muIs32* control, *muIs32; Prgef-1-arf-6::gfp (juEx4082)* showed no or no significant increase in growth defects in the ALM, AVM, and PVM. However, *muIs32; juEx4082* showed significant (**) increase in PLM overshoot defect. In comparing *muIs32; unc-26 (e205) IV arf-6 (tm1447) IV; juEx4082*, to both *muIs32; unc-26 (e205) IV arf-6 (tm1447) IV* and *muIs32; juEx4082*, the rescue strain showed no significant decrease in PLM overshooting defect (See Graph 15). For *zDIs5; arf-6 (tm1447) IV; unc-51 (ky347) V; juEx4082*, no single mutants were ever scored for the strain as well. However, *zDIs5; arf-6 (tm1447) IV; unc-51 (ky347) V* showed no or no significant increase in growth

defects in the ALM, AVM, PLM, and PVM when compared to the *zdis5* control. When comparing the rescue strain *zdis5; arf-6 (tm1447) IV; unc-51 (ky347) V; Prgef-1-arf-6::gfp (juEx4082)* to *zdis5; arf-6 (tm1447) IV; unc-51 (ky347) V*, the strain showed similar results in ALM (wavy) defect, no significant decrease in PVM guidance defect, no significant increase in PLM termination defect, and significant (**) increase in PLM overshooting defect (See Graphs 16, 17, and 18).

For conclusions if the transgene could rescue *muIs32; unc-26 (e205) IV arf-6 (tm1447) IV* in axon regeneration, we looked at the single mutants and saw that the *unc-26 (e205) IV* single mutant showed no significant decrease and *arf-6 (tm1447) IV* single mutant showed no significant increase in axon regrowth when compared to wild type control. Comparing the double mutant to the *unc-26 (e205)* single mutant, the strain showed no significant increase in axon regrowth. While compared to the *arf-6 (tm1447)* single mutant, the double mutant showed significant (**) decrease in axon regrowth. Comparing *muIs32; unc-26 (e205) IV arf-6 (tm1447) IV; juEx4082* to the double and single mutants, it appears that the transgene, *Prgef-1-arf-6::GFP(juEx4082)*, did not rescue *arf-6(tm1447) IV*. *muIs32; unc-26 (e205) IV arf-6 (tm1447) IV; juEx4082* actually showed a slight non-significant increase in total average regrowth when compared to *muIs32; unc-26 (e205) IV arf-6 (tm1447) IV* (See graph 19). Also, to see if the transgene could rescue *zdis5; arf-6 (tm1447) IV; unc-51 (ky347) V* in axon regeneration, we looked at these single mutants and saw that the *unc-51 (ky347)* single mutant showed significant (***) decrease and the *arf-6 (tm1447)* single mutant showed no significant increase in axon regrowth when compared to wild type control. Comparing the double mutant to both single mutants, the double mutant showed no significant increase in axon regrowth.

In comparing *muIs32; unc-51 (ky347) V; arf- 6 (tm1447) IV; juEx4082* the double and single mutants, it appears that the transgene, *Prgef-1-arf-6::GFP(juEx4082)*, did not rescue *arf-6(tm1447) IV*. The rescue strain actually showed a non-significant increase in total average regrowth when compared to *muIs32; unc-51 (ky347) V; arf- 6 (tm1447) IV* (See Graph 20).

For the next group of rescues, we used the transgene *Pmec-7-arf-6::GFP(juEx4084)*, which is expressed by (β -tubulin in the six touch receptor neurons. For *muIs32; unc-26 (e205) IV arf- 6 (tm1447) IV; Pmec-7-arf-6::GFP(juEx4084)*, once again, no single mutants were ever scored for the strain. However, the double mutant showed no or no significant increase in growth defects in the ALM, AVM, PLM, and PVM. Also, compared to the wild type control, *muIs32; juEx4084* showed no or no significant increase in growth defects in the ALM, AVM, and PVM. However, *muIs32; juEx4084* showed significant (**) increase in PLM overshoot defect (See Graph 15). In comparing the rescue strain, to both *muIs32; unc-26 (e205) IV arf- 6 (tm1447) IV* and *muIs32; juEx408*, the rescue strain showed no significant decrease in PLM overshooting defect. For *zdIs5; arf-6 (tm1447) IV; unc-51 (ky347) V; Pmec-7-arf-6::gfp(juEx4084)*, once again no single mutants were ever scored. The double mutant showed no or no significant increase in growth defects in the ALM, AVM, PLM, and PVM compared to the wild type control. Comparing the rescue strain to *zdIs5; arf-6 (tm1447) IV; unc-51 (ky347) V*, the rescue strain showed no significant decrease in ALM (wavy) defect, PVM guidance defect and PLM overshooting defect (See Graph 16, 17, and 18). However, compared to the double mutant, the rescue strain did showed significant (**) increase in PLM termination defect (See Graph 18).

To see if the transgene could rescue *muIs32; unc-26 (e205) IV arf- 6 (tm1447) IV* in axon regeneration, we looked at these single mutants and saw that the *unc-26 (e205)* single mutant showed significant (***) decrease and the *arf- 6 (tm1447)* single mutant showed no significant increase in axon regrowth when compared to wild type control. Comparing *muIs32; unc-26 (e205) IV arf- 6 (tm1447) IV* to *unc-26 (e205)* single mutant, the strain showed significant (**) increase in axon regrowth. However the double mutant to the *arf- 6 (tm1447)* single mutant, the strain showed no significant decrease in axon regrowth. Comparing *muIs32; unc-26 (e205) IV arf- 6 (tm1447) IV; juEx4084* to the single and double mutants, it appears that the transgene, *Pmec-7-arf-6::GFP(juEx4084)*, did potentially rescue *arf-6(tm1447) IV. muIs32; unc-26 (e205) IV arf- 6 (tm1447) IV; juEx4084* actually showed a non-significant decrease in total average regrowth when compared to *muIs32; unc-26 (e205) IV arf- 6 (tm1447) IV* (See Graph 21). In looking at *muIs32; unc-51 (ky347) V; arf- 6 (tm1447) IV; juEx4082* to see if the transgene could rescue the strain, we saw that the *unc-51 (ky347)* single mutant showed significant (***) decrease and the *arf- 6 (tm1447)* single mutant showed no significant increase in axon regrowth when compared to wild type control. Comparing *muIs32; unc-51 (ky347) V; arf- 6 (tm1447) IV* to the *unc-51 (ky347) V* single mutant, the double mutant showed significant (*) increase in axon regrowth. When the double mutant was compared to the *arf-6 (tm1447)* single mutant, the double mutant showed significant (***) decrease in axon regrowth. In comparing *muIs32; unc-51 (ky347) V; arf- 6 (tm1447) IV; juEx4084* to the single and double mutants, it appears that the transgene, *Pmec-7-arf-6::GFP(juEx4084)*, did potentially rescue *arf-6(tm1447) IV. muIs32; unc-51 (ky347) V; arf- 6 (tm1447) IV; juEx4082* actually showed a non-significant increase in total average

regrowth when compared to *muIs32; unc-51 (ky347) V; arf- 6 (tm1447) IV* (See Graph 22).

Chapter 2: Testing Conservation of Molecular Function in PDE Dopaminergic Neurons

As previously stated, there are genes that are known to have significant affects on axon regeneration, we are now testing the genes in different neurons to see if the gene function is conserved in the new neurons. In order to do so, we used the *dat-1mch; pttx-3 mch (otIs181)* background, with *dat-1* marking the ADE, CEP, and PDE, and *pttx-3* marking the AIY. We will look at the defects in the new neurons as well as the regeneration results and compare that data to previous data on those genes. The defects seen in the study for the ADE were migration defect where the ADE migrated anteriorly. The defects seen in the AIY were migration defects where the AIY showed posterior migration. In our study, we did not see any mutants with defects of the CEP or the PDE. To see how the axons develop in a wild type worm see Figure 3. To determine the interactions of the genes in axon regeneration, the PDE was cut in the wild type, single mutants, and double mutant and compared to one another.

For the genes in the DLK-1 MAPKKK and JNK MAPK pathway, which include *cebp-1 (tm2807)*, *dlk-1(tm4024)*, *kgb-1(um3)*, *mlk-1(ok2471)*, and *kgb-1(um3) kgb-2(km16)*, the *kgb-1 (um3)* and *mlk-1 (ok2471)* single mutants showed no significant increase in ADE anterior migration defect. However, the *dlk-1(tm4024)* single mutant showed significant (*) increase and the *cebp-1* and *kgb-1 (um3) kgb-2(km16)* mutants showed (**) significant increase in ADE anterior migration defect compared to the wild type. For the genes that code for vesicle associated proteins, both *arf-6 (tm1447)*, and *efa-6 (tm3124)* showed a significant (*) increase in ADE anterior migration defect. The *unc-26 (e205)* and *unc-57 (e1190)* single mutants also showed a significant (***/*), respectively) increase in ADE anterior migration (See Graph 23). As for the double

mutants, *dlk-1 (tm4024) I*; *dat-1mch*; *pttx-3 mch (otIs181) III*; *kgb-1 (um3) IV* showed no significant change in ADE growth defects when compared to the single mutants. For *dlk-1 (tm4024) I*; *dat-1mch*; *pttx-3 mch (otIs181) III*; *kgb-1 (um3) IV kgb-2 (km16) IV*, the mutant showed no significant increase in ADE growth defects compared to the *dlk-1 (tm4024)* single mutant, but showed significant (*) increase when compared to the *dat-1mch*; *pttx-3 mch (otIs181) III*; *kgb-1 (um3) IV kgb-2 (km16) IV* mutant (See Graph 24). Defects were seen in the AIY as well. The AIY defects showed posterior migration. Of the strains that showed AIY defects, *arf-6 (tm1447)* did not show a significant increase in AIY defect, while *kgb-1 (um3)* and *kgb-1 (um3) kgb-2(km16)* showed significant (*) increase in AIY defects. Also, the *dlk-1 (tm4024)* single mutant showed significant (***) increase in AIY defects. Both double mutants showed no significant increase in defect when compared to the single mutants (See Graph 25).

In looking at the genes to see if their function is conserved in the PDE for axon regeneration, we can see that the genes do not show very much difference in total average regrowth compared to the wild type control. For the genes in the DLK-1 MAPKKK and JNK MAPK pathway, the only strain to show significant increase in total average regrowth in comparison to the wild type control was *cebp-1(tm2807)* (See Graph 26). The double mutants constructed, *dlk-1 (tm4024) I*; *dat-1mch*; *pttx-3 mch (otIs181) III*; *kgb-1 (um3) IV* and *dlk-1 (tm4024) I*; *dat-1mch*; *pttx-3 mch (otIs181) III*; *kgb-1 (um3) IV kgb-2 (km16) IV*, showed no significant change in average total regrowth when compared to the single mutants (See Graph 27). As for the genes that code for vesicle associated proteins, *unc-26 (e205)*, *unc-57 (e1190)*, *arf-6 (tm1447)*, and *efa-6 (tm3124)*, *unc-26 (e205)* showed no significant decrease in total axon regrowth, while *unc-57 (e1190)* showed

significant (*) decrease in total axon regrowth compared to the wild type control. In contrast, both *arf-6 (tm1447)*, and *efa-6 (tm3124)* showed a significant (*) increase in total average regrowth when compared to the wild type (See Graph 26).

Chapter 3: Testing New Genes for Molecular Function in Axon Growth and Regeneration

To further the understanding of axon growth and regeneration, we are now testing new genes to figure out their molecular function in axon growth and regeneration. We will also test some of the new strains together to see if they interact with one another to figure out pathways. To determine if the genes play a role in developmental growth, we observed the ALM, AVM, PLM, and PVM for defects and compared them to the wild type control and any double mutants that we made. The defects will be the same as described in earlier chapters. We will also be cutting the same PLM axon to determine the genes role in axon regeneration.

The first set of new genes we looked at were the temperature sensitive strains (See Table for list of strains). For the temperature sensitive strains, the proteins remain active at 15 degrees. Upon shifting the strains up to 25 degrees, the strains proteins become inactive leading to the strains For defect in the growth patterns, all but *muIs32 II; par-2 (or373) III* showed no significant changes in PLM defects compared to the wild type control (See graphs 28 and 29). *muIs32 II; par-2 (or373) III* showed a significant (*) decrease in PLM defects (See Graph 28). Also, all the genes showed no other defects in the ALM, AVM, or PVM.

For roles in axon regeneration, *lit-1 (or393)*, *spd-2 (or293)*, *spd-2 (or493)*, *zyg-1 (297)*, *zyg-1 (409)*, *mei-1 (or642)*, *spd-5 (or213)*, and *zdIs5; dnc-1 (or404)*, all showed no significant change in axon regrowth compared to the wild type control (See Graphs 32, 38-41, and 44-48). As for *muIs32 II; dnc-1 (or404)* and *muIs32 II; mel-26 (or543)* the strains show a significant (*) decrease in axon regeneration (See Graph 46 and 48). For the rest of the strains, there was some discrepancy so we will go into a little more depth

for those strains. For *mulS32 II; dnc-4 (or633) IV*, the original axotomy data showed that the strain showed significant (*) increase in regeneration, but the second cut the strain shows a slight reduction in regeneration that is not significant (See Graph 28). For *dnc-4 (or633) IV* in the *zdis5* background, the strain showed a significant (*) decrease in axon regrowth (See Graph 31). The overall trend for *dnc-4 (or633) IV* is that the strains show a decrease in axon regeneration. For *mulS32; par-2 (or640)*, the strain shows mixed results. The first two cuts showed no significant increase in regeneration, while the last cut showed no significant decrease in regeneration (See Graph 33). *mulS32; par-2 (or373)* was cut twice and showed significant (**/***) decrease in regeneration (See Graph 34), while *zdis5; par-2 (or373)* showed only a slight reduction in regeneration that was not significant (See Graph 35). The overall trend that fits *par-2* is that *par-2* is considered to show a decrease in axon regeneration. For *rsa-1, rsa-1(or598); mulS32 II* shows significant (***) increase in regeneration during the first cut and no significant increase in regeneration for the next two cuts (See Graph 42). While *zdis5 rsa-1 (or598)* shows that the first cut shows significant (*) decrease in regeneration and the second cut shows no significant increase in regeneration (See graph 43). The overall trend for *rsa-1 (or598)* is that *rsa-1 (or598)* shows no effect on regeneration. Lastly, for *plk-1, mulS32; plk-1 (or683)* showed significant (***) increase in regeneration during the first cut, but showed no significant decrease in regeneration for the next two cuts (See Graph 36). The last cut showed significant (**) decrease in regeneration. For *zdis5; plk-1 (or683)*, the strain showed a significant (**) decrease in axon regeneration (See Graph 37). The overall trend for *plk-1* is that *plk-1* shows a significant (**) decrease in axon regeneration.

After looking at the temperature sensitive genes, we looked at the new genes that coded for reticulons (RET) dealing with vesicle-associated proteins. For growth defects, the reticulon associated protein, *yop-1* (*tm3367*), showed no significant decrease in PLM overshoot defect (See Graph 52). As for the reticulon genes, *mulS32; ret-1* (*gk242*) *V* showed no significant increase in PLM overshooting defect, while *mulS32; ret-1* (*tm0390*) *V* showed significant (*) decrease in PLM overshooting defect. *mulS32; lnp-1* (*tm1247*) showed similar PLM overshooting defect percentages as the wild type. In comparing the *mec-7-GFP* (*mulS32*) *II*; *ret-1*(*gk242*) *V*; *lnp-1* (*tm1247*)*X* double mutant to the two single mutants, the double mutant shows a significant (**) decrease in PLM defects when compared to the *ret-1* (*gk242*) single mutant and similar PLM defects as the *lnp-1* (*tm1247*) single mutant. When comparing *mec-7-GFP* (*mulS32*) *II*; *ret-1* (*tm0390*) *V*; *lnp-1* (*tm1247*)*X* to the two single mutants, the double mutant showed significant (*) increase in PLM defects compared to *lnp-1* (*tm1247*) single mutant and no significant increase in PLM defect compared to the *ret-1* (*tm0390*) single mutant (See Graph 49). Double mutants were also made with *arf-6* (*tm1447*) and *lnp-1* (*tm1247*) or *ret-1* (*tm0390*). The *arf-6* (*tm1447*) single mutant, like the *lnp-1* (*tm1247*) single mutant, showed similar PLM growth defects as the wild type control. The *mulS32* *II*; *arf-6* (*tm1447*) *IV*; *lnp-1* (*tm1247*) *X* double mutant showed similar amounts of PLM overshooting defects as both the single mutants and the wild type control. As for the *mec-7-GFP* (*mulS32*) *II*; *arf-6* (*tm1447*) *IV*; *ret-1* (*tm0390*) *V* double mutant, the strain showed no significant decrease in PLM overshooting defect compared to the *arf-6* (*tm1447*) single mutant and no significant increase when compared to the *ret-1* (*tm0390*) *V* single mutant (See Graph 50).

For the reticulons function in axon regeneration, *muIs32; ret-1 (gk242) V* showed a significant (*) decrease in axon regeneration. This strain was cut twice and showed similar results both times. As for *muIs32; ret-1 (tm0390) V*, this strain was cut twice as well. For the first cut, strain showed a significant (*) decrease in axon regeneration (See Graph 51). For the second cut, the strain showed no significant decrease in axon regeneration. *lnp-1 (tm1247)* should have been cut to be used as a control, but was not cut. However the gene appears to have no affect on axon regeneration in the *arf-6 (tm1447)* and *ret-1 (tm0390)* backgrounds (See Graph 51). As for *yop-1 (tm3367)*, which interacts with *ret-1*, the strain showed no significant increase in axon regeneration compared to the wild type control (See Graph 53). For the double mutants, *mec-7-GFP(muIs32) II; ret-1 (tm0390) V; lnp-1 (tm1247)X*, *mec-7-GFP(muIs32) II; ret-1(gk242) V; lnp-1 (tm1247)X*, and *muIs32 II; arf-6 (tm1447) IV; lnp-1 (tm1247) X*, all three showed no significant change in total average regrowth when compared to the single mutants as well as the wild type control (See Graph 51).

The last genes we looked at were *pinn-1* and *svh-2*. The only developmental growth defects seen in both *pinn-1 (tm2235)* and *svh-2 (tm0737)* were seen in the PLM, but the defect percentage is so low that the amount was noted and now will be disregarded (See Graph 54). As for their roles in axon regeneration, both the single mutants and the double mutant showed similar total average regrowth as the wild type control (See Graph 55).

After looking at all the data, we can now go on to discuss the roles of all the genes in axon growth and regeneration and how they can potentially interact with each other.

We can also go on to talk about whether the functions of some of the genes are conserved in different neuron.

IV.

Discussion

Better Understanding of Genes Pathways

A goal of my project is to test genes, known to be moderately involved in axon regeneration, with each other- via double mutants- in order to determine if the two genes have genetic interactions. We wanted to be able to determine the pathways, if any, these genes work in to affect axon developmental growth and regeneration. We thought that the double mutants might interact and be involved in similar pathways since they both of the genes in the double mutants have roles in axon regeneration.

For *mec-4-GFP (zdIs5) unc-57 (e1190) I; pxn-2 (ju358) X*, it appears that the genes work in two different parallel pathways. However, for developmental growth, from the data, it appears that these two parallel pathways do not interact with each other. While for axotomy, the data shows that the two parallel pathways probably have opposite effects, meaning that the genes serve reverse roles. In the double mutant, the two genes cancel the other gene's effect. As for the double mutant *mec-4-GFP (zdIs5) I; arf-6 (tm1447) IV; pxn-2 (ju358) X*, we can conclude that PXN-2 can potentially work downstream from ARF-6 in the PLM and the ALM. There were defects seen in the AVM as well, however, the defects seen were at a very low percentage, so we concluded that the genes had no effect on the developmental growth of the AVM. In regards to axon regeneration, the double mutant showed similar regrowth to the wild type control and the *pxn-2 (ju358)* control, so the genes most likely do not interact together to affect regrowth.

In testing other double mutants to see if the genes interacted in the same pathways as each other, we also tested *mec-7-GFP(muIs32) II; arf-6 (tm1447) IV; sec-22 (ok3053) X* and *mec-4-GFP(zdIs5)I; snb-1 (md247)V; sec-22 (ok 3053) X*. For *mec-7-GFP(muIs32) II; arf-6 (tm1447) IV; sec-22 (ok3053) X*, we have concluded that we

cannot really determine anything from the score or the axotomy data, but we think the genes probably have no effects on each other. For *mec-4-GFP(zdIs5)I; snb-1 (md247)V; sec-22 (ok 3053) X*, we did conclude that SEC-22 could work downstream from SNB-1 in both axon growth and regeneration. For axon growth, we believe that the pathway work by SNB-1 activating SEC-22, which then goes on to promote proper developmental growth of the PLM. While in axon regeneration, we believe that SNB-1 inhibits SEC-22, which goes on to inhibit axon regeneration.

In determining if our rescues worked using the transgenes *Prgef-1-arf-6::gfp (juEx4082)* or *Pmec-7-arf-6::gfp (juEx4084)*, we could not determine if the transgenes could rescue axon growth development defects since the single mutants were never scored. However, we could determine whether or not the transgene could rescue the axon regeneration results. We will now continue on to discuss each of the rescues in more detail. We will start with the *Pmec-7-arf-6::gfp (juEx4084)* rescues. For *muIs32; unc-26 (e205) IV arf- 6 (tm1447) IV; juEx4084*, while the rescue strain did not show similar results to *muIs32; unc-26 (e205) IV* and showed a non-significant increased total average regrowth, the strain showed a reduction in total average regrowth when compared to *muIs32; unc-26 (e205) IV arf- 6 (tm1447) IV*. This data would suggest that *Pmec-7-arf-6::GFP(juEx4084)* rescued the strain as expected. For *muIs32; unc-26 (e205) IV arf- 6 (tm1447) IV; juEx4084*, while this rescue strain did not show similar results to *muIs32; unc-26 (e205) IV* and showed a non-significant increased total average regrowth, the strain showed a reduction in total average regrowth when compared to *muIs32; unc-26 (e205) IV arf- 6 (tm1447) IV*. This data would suggest that *Pmec-7-arf-6::GFP(juEx4084)* rescued the strain as expected. As to why *Pmec-7-arf-6::gfp*

(juEx4084) did not show total rescue in both the strains, ARF-6 is a GTPase that needs to be activated in order to function properly, so ARF-6 may not have been activated leading to a lesser rescue of the strains.

Now going on to the *Prgef-1-arf-6::gfp (juEx4082)* rescues, for *muIs32 II; unc-26 (e205) IV arf-6 (tm1447) IV; juEx4082* and *zDis5 I; arf-6 (tm1447) IV; unc-51 (ky347) V; juEx4082*, if the strains showed a rescue, the axon regrowth would be similar to the *muIs32; unc-26 (e205) IV* single mutant. However, since the regrowth was similar to the double mutant without the extrachromosomal array, the strains were not rescued by *Prgef-1-arf-6::GFP (juEx4082)* as expected. From all the data, we could conclude that *Pmec-7-arf-6::gfp (juEx4084)* could rescue the strains as expected, but *Prgef-1-arf-6::gfp (juEx4082)* could not rescue the strains.

The next step for this step of the project is to continue generating double mutants to determine the genes interactions with one another. Also, further testing should be done for any genes that are determined to interact with one another to understand how the genes fully work together.

The Molecular Function of Genes May Not Be Conserved In PDE Neurons

Our next goal was to test genes that were previously determined to have a significant affect on axon regeneration to see if their role is conserved in different neurons. Since we already know that genes can have different function in different neurons, the classic example being the CNS and the PNS, we thought that there might be potential for the genes to act differently in the new neurons, so that is why we are testing them. In looking at the genes to see if there function is conserved in the PDE for axon regeneration, we can see a significant difference from what we saw in the PLM.

For the genes in the DLK-1 MAPKKK and JNK MAPK pathway, we determined the molecular functions of the genes to not be conserved in the PDE. Although *cebp-1* showed a significant increase in regrowth, the *otIs181* wild type control did not regrow to the usual total average, which is about 120um. The regrowth seen in *cebp-1* is probably not significant like the other single mutants. From this data, we can conclude that the DLK-1 MAPKKK and JNK MAPK pathway genes are not essential in the PDE for axon regeneration like they are in the PLM. In the PLM, upon knocking out any of the genes in these parallel pathways, axon regeneration would not been seen in the mutants [(Yan et al., 2009) and (Chen et al., 2012)]. However, all of the strains in the *otIs181* background showed regrowth that would be around the usual total regrowth length of the wild type control.

For the genes that coded for vesicle-associated proteins, we determined, yet again, that the molecular functions of the genes are not conserved in the PDE. While *unc-57* (*e1190*) showed significant (*) decrease in total axon regrowth compared to the wild type control, the decrease was not as significant (***) as it was in the PLM (Chen et al., 2012).

With that being stated, both *unc-26 (e205)* and *unc-57 (e1190)* appear to not be required for PDE regeneration like they are in the PLM. As for *arf-6 (tm1447)*, and *efa-6 (tm3124)*, while they appear to show significant (*) increase in total average regrowth, the *otIs181* wild type control did not regrow to the usual total average. Both *arf-6 (tm1447)*, and *efa-6 (tm3124)* regrew to around the total average regrowth of the usual wild type control, so realistically their increase in regrowth is not actually significant. In the PLM, *efa-6 (tm3124)* shows significant (***) increase in PLM regrowth, meaning that ARF-6 and EFA-6 inhibit axon regeneration since they interact together (Chen et al., 2012). Since *arf-6 (tm1447)*, and *efa-6 (tm3124)* total regrowth is not significant, they are not required in the PDE for axon regeneration like they are in the PLM.

As to whether or not the genes interactions were conserved for axon growth, we looked at two double mutants, *dlk-1 (tm4024) I; dat-1mch; ptx-3 mch (otIs181) III; kgb-1 (um3) IV* and *dlk-1 (tm4024) I; dat-1mch; ptx-3 mch (otIs181) III; kgb-1 (um3) IV kgb-2 (km16) IV*. For the ADE, in looking at the double mutants, which uses the DLK-1 MAPKKK and JNK pathway genes, and comparing them to the single mutants, it appears that the genes may work together in parallel and downstream from one another. However, for the AIY, it appears that the genes work in the same pathway downstream from one another.

The next step for this step of the project is to test the other genes in DLK-1 MAPKKK and JNK pathways to see if the other genes are not conserved in the PDE as well. If they are not conserved, the genes serve a different purpose in the PDE or they are not expressed there.

The Roles of New Genes in Axon Growth and Regeneration

Our last goal in this project was to determine the function of new, not previously tested, genes on axon growth and regeneration. We selected genes based off of their known functions in mechanism other than axon growth or regeneration. We assumed these genes might have an affect on both axon growth and regeneration.

For the temperature sensitive genes, we wanted to determine if the essential maternal genes have any effect on adult axon growth and regeneration. Any discrepancies seen in the axotomy, was determined to be caused by increases in branching in the strain that did not fit the other cuts of the same strain or was caused by an unknown factor. For *lit-1 (or393)*, *zyg-1* in both the *or297* and *or409* alleles, *spd-2* in both the *or293* and *or493* alleles, and *mei-1 (or642)* appear to have no affects on axon growth patterns or axon regeneration. However, *spd-2 (or493)* when compared to *spd-2 (or293)* did show opposite results. However, the results both concluded that the strains did not effect regeneration since the regrowth pattern in both were not significant. The discrepancy between the two alleles can be caused by *spd-2 (or293)* having a lower branching average than *spd-2 (or493)*. This can lead to less total average regrowth.

For the axon growth patterns, *dnc-4 (or633)* appears to have no effect on axon growth patterns. As for the *dnc-4 (or633)* and axon regeneration, *dnc-4 (or633)* shows a small discrepancy between the *mul32* and *zdl5* strains. One shows no significant decrease in regeneration, while the other shows significant (*) decrease. The reason for the difference between the two strains cannot be determined. Overall, *dnc-4 (or633)* is considered to show a decrease in regeneration. For axon growth patterns, *par-2 (or640)* and *par-2 (373)* appear to have no effects on axon growth patterns. *par-2 (or640)* showed

no discrepancy but *par-2 (or373)* did. *par-2 (or373)* in the *muIs32* background shows a significant (*) decrease in PLM overshooting defects from 15 degrees to 25 degrees, but shows an insignificant increase in PLM overshooting defect from 15 degrees to 25 degrees in the *zdIs5* background. The reason for the difference between the strain in the different backgrounds cannot be determined. Although *par-2 (or373)* in the *muIs32* background shows a significant (*) decrease in PLM overshooting defect at 25 degrees when compared to the wild type control at 25 degrees, the results are not seen in the *zdIs5* background. Also the results for *par-2 (or373)* in both backgrounds are not significant from 15 degrees to 25 degrees. Therefore, *par-2 (or373)* appears to have no effect on axon growth patterns. For effects on developmental growth, *plk-1 (or683)* appears to have no effect on axon growth patterns. As for regeneration, the final result of the *muIs32* background cut is consistent with the *zdIs5* background. The average regrowth of each of the strains is similar (~80.4). Overall, *plk-1 (or683)* is considered to have an effect on regeneration. *plk-1 (or683)* probably is required for axon regeneration.

For axon growth in *rsa-1 (or598)*, the strain in both backgrounds appeared to have no effect on axon growth patterns. For the axotomy data, the strain had some discrepancy. However, the final cuts of the strain in both backgrounds showed a similar increase in regrowth (~147.1), which was not significant. Overall, *rsa-1 (or598)* shows no effect on regeneration. As for *dnc-1 (or404)*, the strain appears to have no effect on axon growth patterns. For axon regeneration, the results were not the same in the *zdIs5* and *muIs32* background. However, the average total regrowth for the control of the strain in the *muIs32* regrew a little more than the normal average 120, so strain in both the *zdIs5* and *muIs32* background most likely have no significant effect on axon regeneration.

Lastly, *mel-26 (or543)* appears to have no effect on axon growth patterns, but is considered to have a slight effect on axon regeneration.

Next, for the new genes that code for reticulons that interact with vesicle-associated proteins, the results are inconsistent between the *ret-1* alleles. The difference between the two *ret-1* alleles is most likely an experimental error. However, due to the fact that there is inconsistency we cannot conclude anything from the data since the defect results for the single mutants is most likely incorrect. For *yop-1 (tm3367)* we can conclude that the strain has no affect on axon growth patterns. For axon regeneration, since *ret-1* in both the *gk242* and *tm0390* alleles have shown a significant decrease or a decrease that is almost comparable to the significant decreases in axon regeneration, *ret-1* is considered to possibly have some mild effect in axon regeneration. *lnp-1 (tm1247)*, on the other hand, probably has no affect on axon regeneration since *lnp-1 (tm1247)* appears to have no affect on axon regeneration in the *arf-6 (tm1447)* and *ret-1 (tm0390)* backgrounds. *yop-1 (tm3367)* appears to have no affect on axon regeneration as well. Potentially, if a double mutant was constructed with *yop-1 (tm3367)* and *ret-1*, it could potentially show that the two genes work together not only to interfere with the formation of the endoplasmic reticulum, but in axon regeneration as well.

Lastly, for *pinn-1 (tm2235)* and *svh-2 (tm0737)*, both genes appear to have no affect on axon growth patterns or axon regeneration and appear to not interact with each other.

The next step for this step of the project is to continue on testing new genes to see their functions in axon growth and regeneration, and then testing the new genes with other genes to identify gene interactions and pathways.

V.

Tables, Graphs, and Figures

Table 1: List of Strains Used in Experiments

Vesicle Associated Protein w/ GTPase

	CZ #	Finished Strain Genotype	Starting Strain Genotype
1	CZ15471	<i>mec-7-GFP(muls32) II; arf-6(tm1447) IV; unc-51(e369) V</i>	CZ11970: <i>mec-7-GFP(muls32) II; unc-51 (e369) V</i> CZ14594: <i>arf-6(tm1447) IV</i>
2	CZ15472	<i>mec-7-GFP(muls32) II; unc-26(e205) IV arf-6(tm1447) IV</i>	CZ13002: <i>mec-7-GFP(muls32) II; unc-26 (e205) IV</i> CZ14594: <i>arf-6(tm1447) IV</i>
3	CZ15473	<i>mec-7-GFP(muls32) II; arf-6(tm1447) IV</i>	CZ13002: <i>mec-7-GFP(muls32) II; unc-26 (e205) IV</i> CZ14594: <i>arf-6(tm1447) IV</i>
4	CZ15474	<i>mec-7-GFP(muls32) II; efa-6(tm3124) IV unc-26(e205) IV</i>	CZ13198: <i>mec-4-GFP(zdls5)I; efa-6(tm3124) IV unc-26(e205) IV</i> CZ10969: <i>mec-7-GFP(muls32) II</i>
5	CZ15793	<i>mec-7-GFP(muls32) II; Prgef-1-arf-6::gfp (juEx4082)</i>	CZ15065: <i>Prgef-1-arf-6::gfp (juEx4082)</i> CZ15472: <i>mec-7-GFP(muls32) II; unc-26(e205) IV arf-6 (tm1447) IV</i>
6	CZ15794	<i>mec-7-GFP(muls32) II; unc-26(e205) IV arf-6(tm1447) IV; Prgef-1-arf-6::gfp(juEx4082)</i>	CZ15065: <i>Prgef-1-arf-6::gfp (juEx4082)</i> CZ15472: <i>mec-7-GFP(muls32) II; unc-26(e205) IV arf-6 (tm1447) IV</i>
7	CZ15795	<i>mec-7-GFP(muls32) II; Pmec-7-arf-6::gfp (juEx4084)</i>	CZ15067: <i>Pmec-7-arf-6::gfp (juEx4084)</i> CZ15472: <i>mec-7-GFP(muls32) II; unc-26(e205) IV arf-6 (tm1447) IV</i>
8	CZ15796	<i>mec-7-GFP(muls32) II; unc-26(e205) IV arf-6(tm1447) IV; Pmec-7-arf-6::gfp (juEx4084)</i>	CZ15067: <i>Pmec-7-arf-6::gfp (juEx4084)</i> CZ15472: <i>mec-7-GFP(muls32) II; unc-26(e205) IV arf-6 (tm1447) IV</i>
9	CZ15797	<i>mec-4-GFP(zdls5)I; arf-6(tm1447) IV; unc-51(ky347) V; Prgef-1-arf-6::gfp (juEx4082)</i>	CZ15065: <i>Prgef-1-arf-6::gfp (juEx4082)</i> CZ13634: <i>mec-4-GFP(zdls5)I; arf-6(tm1447) IV; unc-51 (ky347)V</i>
10	CZ15798	<i>mec-4-GFP(zdls5)I; arf-6(tm1447) IV; unc-51(ky347) V; Pmec-7-arf-6::gfp (juEx4084)</i>	CZ15067: <i>Pmec-7-arf-6::gfp (juEx4084)</i> CZ13634: <i>mec-4-GFP(zdls5)I; arf-6(tm1447) IV; unc-51 (ky347) V</i>
11	CZ16150	<i>mec-4-GFP(zdls5)I; snb-1 (md247)V; F55A4.1(ok 3053) X</i>	CZ10728: <i>mec-4-GFP(zdls5)I; F55A4.1(ok 3053) X</i> XNM467: <i>snb-1 (md247)V</i>
12	CZ16073	<i>mec-7-GFP(muls32) II; arf-6 (tm1447) IV; F55A4.1 (ok3053) X</i>	CZ13681: <i>mec-7-GFP (muls32) II; F55A4.1 (ok3053) X</i> CZ5066: <i>arf-6 (tm1447) IV</i>
13	CZ16584	<i>mec-7-GFP (muls32) II; ret-1 (gk242) V</i>	CZ10969: <i>mec-7-GFP (muls32) II</i> VC441: <i>ret-1 (gk242) V</i>
14	CZ16585	<i>mec-7-GFP (muls32) II; ret-1 (tm0390) V</i>	CZ10969: <i>mec-7-GFP (muls32) II</i> FX00390: <i>ret-1 (tm0390) V</i>
15	CZ16583	<i>mec-7-GFP(muls32) II; lnp-1 (tm1247)X</i>	CZ13835: <i>mec-4-GFP (zdls5) I; lnp-1 (tm1247) X</i> CZ10969: <i>mec-7-GFP (muls32) II</i>
16	CZ17287	<i>yop-1 (tm3667) I; muls32 II</i>	FX03667: <i>yop-1 (tm3667) I</i> CZ10969: <i>mec-7-GFP (muls32) II</i>

Table 1: List of Strains Used in Experiments (Continued)

16	CZ16889	<i>mec-7-GFP(muls32) II; ret-1(gk242) V; lnp-1 (tm1247)X</i>	CZ10969: <i>mec-7-GFP (muls32) II</i> VC441: <i>ret-1 (gk242) V</i> CZ13835: <i>mec-4-GFP (zlds5) I; lnp-1 (tm1247) X</i>
17	CZ16890	<i>mec-7-GFP(muls32) II; ret-1 (tm0390) V; lnp-1 (tm1247)X</i>	CZ10969: <i>mec-7-GFP (muls32) II</i> FX00390: <i>ret-1 (tm0390) V</i> CZ13835: <i>mec-4-GFP (zlds5) I; lnp-1 (tm1247) X</i>
18	CZ16891	<i>mec-7-GFP(muls32) II; arf-6(tm1447) IV; ret-1 (tm0390) V</i>	CZ10969: <i>mec-7-GFP (muls32) II</i> CZ5066: <i>arf-6 (tm1447) IV</i> FX00390: <i>ret-1 (tm0390) V</i>
19	CZ17299	<i>muls32 II; arf-6 (tm1447) IV; lnp-1 (tm1247) X</i>	CZ5066: <i>arf-6 (tm1447) IV</i> CZ16583: <i>muls32 II; lnp-1 (tm1247) X</i>

Vesicle Associated Protein/ Developmental

	CZ #	Finished Strain Genotype	Starting Strain Genotype
1	CZ13720	<i>mec-4-GFP(zlds5) unc-57(e1190) I; pxn-2 (ju358) X</i>	incorrectCZ13720: <i>mec-4-GFP (zlds5) unc-57(e1190) I</i> CZ5772: <i>pxn-2 (ju358) X</i>
2	CZ16410	<i>mec-4-GFP (zlds5)I; arf-6 (tm1447) IV; pxn-2 (ju358) X</i>	CZ5066: <i>arf-6 (tm1447) IV</i> CZ12125: <i>mec-4-GFP (zlds5) I; pxn-2 (ju358) X</i>

Temperature Sensitive Mutants in Essential Genes

	CZ #	Finished Strain Genotype	Starting Strain Genotype
1	CZ16399	<i>mec-7-GFP (muls32) II; dnc-4 (or633ts) IV</i>	CZ10969: <i>mec-7-GFP (muls32) II</i> EU1506: <i>dnc-4 (or633ts) IV</i>
2	CZ17097	<i>mec-4-GFP (zlds5) I; dnc-4 (or633ts) IV</i>	CZ10175: <i>mec-4-GFP (zlds5) I</i> EU1506: <i>dnc-4 (or633ts) IV</i>
3	CZ16400	<i>mec-7-GFP (muls32) II; lit-1 (or393ts) III</i>	CZ10969: <i>mec-7-GFP (muls32) II</i> EU920: <i>lit-1 (or393ts) III; him-8 (e1489) IV</i>
4	CZ16401	<i>mec-7-GFP (muls32) II; par-2 (or640ts) III</i>	CZ10969: <i>mec-7-GFP (muls32) II</i> EU1327: <i>par-2 (or640ts) III</i>
5	CZ16402	<i>mec-7-GFP (muls32) II; par-2 (or373ts) III</i>	CZ10969: <i>mec-7-GFP (muls32) II</i> EU822: <i>par-2 (or373ts) III; lin-2(e1309) X</i>
6	CZ17098	<i>mec-4-GFP (zlds5) I; par-2 (or373ts) III</i>	CZ10175: <i>mec-4-GFP (zlds5) I</i> EU822: <i>par-2 (or373ts) III; lin-2(e1309) X</i>
7	CZ16403	<i>mec-7-GFP (muls32) II; plk-1 (or683ts) III</i>	CZ10969: <i>mec-7-GFP (muls32) II</i> EU1441: <i>plk-1 (or683ts) III</i>

Table 1: List of Strains Used in Experiments (Continued)

8	CZ17099	<i>mec-4-GFP (zdl5) I; plk-1 (or683ts) III</i>	CZ10175: <i>mec-4-GFP (zdl5) I</i> EU1441: <i>plk-1 (or683ts) III</i>
9	CZ16405	<i>spd-2 (or493ts) I; mec-7-GFP (muls32) II</i>	EU2005: <i>spd-2 (or493ts) I</i> CZ10969: <i>mec-7-GFP (muls32) II</i>
10	CZ16405	<i>spd-2 (or293ts) I; mec-7-GFP (muls32) II</i>	EU780: <i>spd-2 (or293ts) I; him-8 (e1489) IV</i> CZ10969: <i>mec-7-GFP (muls32) II</i>
11	CZ16406	<i>mec-4-GFP (zdl5) I; zyg-1 (or297ts) II</i>	CZ10175: <i>mec-4-GFP (zdl5) I</i> EU782: <i>zyg-1 (or297ts) II</i>
12	CZ16407	<i>mec-4-GFP (zdl5) I; zyg-1 (or409ts) II</i>	CZ10175: <i>mec-4-GFP (zdl5) I</i> EU2009: <i>zyg-1 (or409ts) II</i>
13	CZ 16408	<i>rsa-1 (or598ts) I; mec-7-GFP (muls32) II</i>	EU1999: <i>rsa-1 (or598ts) I</i> CZ10969: <i>mec-7-GFP (muls32) II</i>
14	CZ17100	<i>mec-4-GFP (zdl5) rsa-1 (or598ts) I</i>	CZ10175: <i>mec-4-GFP (zdl5) I</i> EU1999: <i>rsa-1 (or598ts) I</i>
15	CZ16409	<i>mei-1 (or642ts) I; mec-7-GFP(muls32) II</i>	EU1334: <i>mei-1 (or642ts) I</i> CZ10969: <i>mec-7-GFP (muls32) II</i>
16	CZ16892	<i>spd-5 (or213) I; mec-7-GFP (muls32) II</i>	CZ10969: <i>mec-7-GFP (muls32) II</i> EU856: <i>spd-5 (or213) I</i>
17	CZ16893	<i>mel-26 (or543) I; mec-7-GFP (muls32) II</i>	CZ10969: <i>mec-7-GFP (muls32) II</i> EU1077: <i>mel-26 (or543) I; him-8 (e1489) IV</i>
18	Re-make CZ12150	<i>mec-7-GFP (muls32) II; dnc-1(or404) IV</i>	CZ10969: <i>mec-7-GFP (muls32) II</i> EU1006: <i>dnc-1(or404) IV</i>
19	Re-make CZ12037	<i>mec-4-GFP (zdl5) I; dnc-1(or404) IV</i>	CZ10175: <i>mec-4-GFP (zdl5) I</i> EU1006: <i>dnc-1(or404) IV</i>

Table 1: List of Strains Used in Experiments (Continued)

MAPK Pathway

	CZ #	Finished Strain Genotype	Starting Strain Genotype
1	CZ17286	<i>mec-4-GFP (zcls5) I; Y110A2AL1.3 (tm2235) II</i>	CZ10175: <i>mec-4-GFP (zcls5) I</i> FX02235: <i>Y110A2AL1.3 (tm2235) II</i>
2	CZ17285	<i>mec-4-GFP (zcls5) I; T14E8.1a (tm0737) X</i>	CZ10175: <i>mec-4-GFP (zcls5) I</i> FX00737: <i>T14E8.1a (tm0737) X</i>
3	CZ17288	<i>mec-4-GFP (zcls5) I; Y110A2AL1.3 (tm2235) II; T14E8.1a (tm0737) X</i>	CZ10175: <i>mec-4-GFP (zcls5) I</i> FX02235: <i>Y110A2AL1.3 (tm2235) II</i> FX00737: <i>T14E8.1a (tm0737) X</i>

PDE Dopaminergic Neurons

	CZ #	Finished Strain Genotype	Starting Strain Genotype
1	CZ16076	<i>otls181III</i>	OH8483: <i>dat-1mch; pttx-3mch (otls181); him-8 (e1489)</i>
2	CZ16413	<i>otls181III; arf-6 (tm1447) IV</i>	OH8483: <i>dat-1mch; pttx-3mch (otls181); him-8 (e1489)</i> CZ13636: <i>mec-7-GFP (muls32) II; arf-6 (tm1447) IV</i>
3	CZ16412	<i>otls181 III ; unc-26 (e205) IV</i>	OH8483: <i>dat-1mch; pttx-3mch (otls181); him-8 (e1489)</i> CZ15472: <i>mec-7-GFP(muls32) II; unc-26 (e205) arf-6 (tm1447) IV</i>
4	CZ16411	<i>unc-57 (e1190) I; otls181 III</i>	OH8483: <i>dat-1mch; pttx-3mch (otls181); him-8 (e1489)</i> CZ13720: <i>mec-4-GFP (zcls5) unc-57 (e1190) I</i>
5	CZ16475	<i>otls181 III; cebp-1 (tm2807) X</i>	OH8483: <i>dat-1mch; pttx-3mch (otls181); him-8 (e1489)</i> CZ8920: <i>cebp-1 (tm2807) X</i>
6	CZ16476	<i>dlk-1(tm4024) I; otls181 III</i>	OH8483: <i>dat-1mch; pttx-3 mch (otls181); him-8 (e1489)</i> FX04024: <i>dlk-1 (tm4024) I</i>
7	CZ16477	<i>otls181 III; efa-6 (tm3124) IV</i>	OH8483: <i>dat-1mch; pttx-3mch (otls181); him-8 (e1489)</i> CZ10891: <i>efa-6 (tm3124) IV</i>
8	CZ16894	<i>otls181 III; kgb-1 (um3) IV</i>	OH8483: <i>dat-1mch; pttx-3mch (otls181); him-8 (e1489)</i> CZ3481: <i>kgb-1 (um3) IV</i>

Table 1: List of Strains Used in Experiments (Continued)

9	CZ17000	<i>otls181 III; kgb-1 (um3) kgb-2(km16) IV</i>	OH8483: <i>dat-1mch; pttx-3mch (otls181); him-8 (e1489)</i> KB7: <i>kgb-1 (um3) kgb-2 (km16) IV</i>
10	CZ17282	<i>dlk-1 (tm4024) I; otls181 III; kgb-1 (um3) IV</i>	CZ16476: <i>dlk-1 (tm4024) I;</i> <i>otls181 III</i> CZ3481: <i>kgb-1 (um3) IV</i>
11	CZ17283	<i>dlk-1 (tm4024) I; otls181 III; kgb-1(um3) kgb-2 (km16) IV</i>	CZ16476: <i>dlk-1 (tm4024) I;</i> <i>otls181 III</i> KB7: <i>kgb-1 (um3) kgb-2(km16) IV</i>
12	CZ17834	<i>otls181 III; mlk-1 (ok2471)</i>	CZ16076: <i>dat-1mch; pttx-3mch (otls181) III</i>

Table 2: List of Primers Used for Strain Construction.**Vesicle Associated Protein w/ GTPase**

	CZ #	Finished Strain Genotype	Finished Strain Gross Phenotypes	*Primers *NT change and AA change *PCR, Seq, or RE digest
1	CZ15471	<i>mec-7-GFP(muls32) II; arf-6(tm1447) IV; unc-51(e369) V</i>	Strain is obviously unc.	Emily Grossman's Primers <i>arf-6</i> F1: gcaaattccgacgatggctc <i>arf-6</i> R1: cgccaaccatcatgtgcttc <i>arf-6</i> R2: gattgcccgagcttcagtttg PCR (deletion) Band Sizes: WT: 808bp MT: 641bp
2	CZ15472	<i>mec-7-GFP(muls32) II; unc-26(e205) IV arf-6(tm1447) IV</i>	Strain is obviously unc.	Emily Grossman's Primers <i>arf-6</i> F1: gcaaattccgacgatggctc <i>arf-6</i> R1: cgccaaccatcatgtgcttc <i>arf-6</i> R2: gattgcccgagcttcagtttg PCR (deletion) Band Sizes: WT: 808bp MT: 641bp
3	CZ15473	<i>mec-7-GFP(muls32) II; arf-6(tm1447) IV</i>	Strain is slow growing.	Emily Grossman's Primers <i>arf-6</i> F1: gcaaattccgacgatggctc <i>arf-6</i> R1: cgccaaccatcatgtgcttc <i>arf-6</i> R2: gattgcccgagcttcagtttg PCR (deletion) Band Sizes: WT: 808bp MT: 641bp
4	CZ15474	<i>mec-7-GFP(muls32) II; efa-6(tm3124) IV unc-26(e205) IV</i>	Strain is obviously unc.	<i>efa-6</i> F: YJ6452: gttggtgctgcgctcttgat <i>efa-6</i> R: YJ6453: cgtcgaacattcagtggt PCR (deletion)
5	CZ15793	<i>mec-7-GFP(muls32) II; Prgef-1-arf-6::gfp (juEx4082)</i>	Strain appears artificially WT	N/A
6	CZ15794	<i>mec-7-GFP(muls32) II; unc-26(e205) IV arf-6(tm1447) IV; Prgef-1-arf-6::gfp(juEx4082)</i>	Strain is obviously unc.	Emily Grossman's Primers <i>arf-6</i> F1: gcaaattccgacgatggctc <i>arf-6</i> R1: cgccaaccatcatgtgcttc <i>arf-6</i> R2: gattgcccgagcttcagtttg PCR (deletion) Band Sizes: WT: 808bp MT: 641bp

Table 2: List of Primers Used for Strain Construction (Continued)

7	CZ15795	<i>mec-7-GFP(muls32) II; Pmec-7-arf-6::gfp (juEx4084)</i>	Strain appear artificially WT	N/A
8	CZ15796	<i>mec-7-GFP(muls32) II; unc-26(e205) IV arf-6(tm1447) IV; Pmec-7-arf-6::gfp (juEx4084)</i>	Strain is obviously unc.	Emily Grossman's Primers <i>arf-6</i> F1: gcaaattccgacgatggctc <i>arf-6</i> R1: cgccaaccatcatgtgcttc <i>arf-6</i> R2: gattgcccgagcttcagtttg PCR (deletion) Band Sizes: WT: 808bp MT: 641bp
9	CZ15797	<i>mec-4-GFP(zdls5)I; arf-6(tm1447) IV; unc-51(ky347) V; Prgef-1-arf-6::gfp (juEx4082)</i>	Strain is obviously unc.	Emily Grossman's Primers <i>arf-6</i> F1: gcaaattccgacgatggctc <i>arf-6</i> R1: cgccaaccatcatgtgcttc <i>arf-6</i> R2: gattgcccgagcttcagtttg PCR (deletion) Band Sizes: WT: 808bp MT: 641bp
10	CZ15798	<i>mec-4-GFP(zdls5)I; arf-6(tm1447) IV; unc-51(ky347) V; Pmec-7-arf-6::gfp (juEx4084)</i>	Strain is obviously unc.	<i>arf-6</i> (tm1447): F1: YJ8994: gcaaattccgacgatggctc <i>arf-6</i> (tm1447): R1: YJ8995: gaagcacatgatggtggacg <i>arf-6</i> (tm1447): R2: YJ8996: gattgcccgagcttcagtttg PCR (deletion)
11	CZ16150	<i>mec-4-GFP(zdls5)I; snb-1(md247)V; F55A4.1(ok3053) X</i>	Strain is sluggish and unc. Strain has jerky backward movement.	<i>F55A4.1</i> (ok3053) F1: YJ6079: atgcacatcccacaacacat <i>F55A4.1</i> (ok3053) R1: YJ6226: gtggcgactggcttaaaaat PCR (deletion)

Table 2: List of Primers Used for Strain Construction (Continued)

12	CZ16073	<i>mec-7-GFP(muls32) II</i> ; <i>arf-6 (tm1447) IV</i> ; <i>F55A4.1 (ok3053) X</i>	Strain appears to grow a little slower than WT.	Emily Grossman's Primers <i>arf-6</i> F1: gcaaattccgacgatggctc <i>arf-6</i> R1: cgccaaccatcatgtgcttc <i>arf-6</i> R2: gattgcccgagcttcagttg PCR (deletion) Band Sizes: WT: 808bp MT: 641bp
				<i>F55A4.1 (ok3053)</i> F1: YJ6079: atgcacatcccaacacat <i>F55A4.1 (ok3053)</i> R1: YJ6226: gtggcgactggcttaaaaat PCR (deletion)
13	CZ16584	<i>mec-7-GFP (muls32) II</i> ; <i>ret-1 (gk242) V</i>	Strain moves artificially like WT and grows similar to WT, but looks small. Brood size average for strain is 175 compared to 216 for WT.	F1:YJ8955:tcggttcggcactcttcc R1:YJ8956:cgaacacatcagcttagcg PCR (deletion) Band sizes: WT: 310bp MT: 292bp
14	CZ16585	<i>mec-7-GFP (muls32) II</i> ; <i>ret-1 (tm0390) V</i>	Strain moves artificially like WT and grows similar to WT, but looks small. Brood size average for strain is 71 compared to 216 for WT.	F1:YJ8953:tgctcagtgtagaaagcgag R1:YJ8954:ccacgaagcagatgtatgtcaaag PCR (deletion) Band sizes: WT: 386bp MT: 415bp
15	CZ16583	<i>mec-7-GFP(muls32) II</i> ; <i>lnp-1 (tm1247)X</i>	weakly abnormal thertotaxis when raised to 23 C Moves artificially like WT and grows similar to WT. Brood size average for strain is 206 compared to 216 for WT.	<i>lnp-1 (tm1247)</i> F: YJ7400: cacagagcttgagcgagttg <i>lnp-1 (tm1247)</i> IF: YJ7401: acgaattgggacagcatttc <i>lnp-1 (tm1247)</i> R: YJ7402: tcagacggaccaactcttcc PCR (deletion) Band sizes: WT: 391bp MT: 409bp

Table 2: List of Primers Used for Strain Construction (Continued)

16	CZ16889	<i>mec-7-GFP(muls32) II;</i> <i>ret-1(gk242) V; lnp-1</i> <i>(tm1247)X</i>	Strain appears slightly unc. Strain grows similar to WT. Brood size average for strain is 191 compared to 216 for WT.	<p><i>lnp-1 (tm1247) F:</i> YJ7400: cacagagcttgagcgagttg <i>lnp-1 (tm1247) IF:</i> YJ7401: acgaattgggacagcatttc <i>lnp-1 (tm1247) R:</i> YJ7402: tcagacggaccaactcttcc PCR (deletion)</p> <p>Band sizes: WT: 391bp MT: 409bp</p> <p><i>ret-1(gk242) F1:</i> YJ8955:tcgttccggcactcttctcc <i>ret-1(gk242)R1:</i> YJ8956: cgaacacatcagcttgagcg <i>ret-1(gk242)Del:</i> YJ9011: ggctgacttctggcatcgcg PCR (deletion)</p> <p>Band sizes: WT: 310bp MT: 292bp</p>
17	CZ16890	<i>mec-7-GFP(muls32) II;</i> <i>ret-1 (tm0390) V; lnp-1</i> <i>(tm1247)X</i>	Strain moves artificially like WT and grows similar to WT. Strain has protruding vulvas and is small	<p><i>lnp-1 (tm1247) F:</i> YJ7400: cacagagcttgagcgagttg <i>lnp-1 (tm1247) IF:</i> YJ7401: acgaattgggacagcatttc <i>lnp-1 (tm1247) R:</i> YJ7402: tcagacggaccaactcttcc PCR (deletion)</p> <p>Band sizes: WT: 391bp MT: 409bp</p> <p><i>ret-1 (tm0390) F1:</i> YJ8953:tgctaggtcagaaaggcg ag <i>ret-1 (tm0390) R1:</i> YJ8954:cttgacatacatcgcttctg gg <i>ret-1 (tm0390)Del:</i> YJ9012:cttctgctctgttcttctg ccaagt PCR (deletion)</p> <p>Band sizes: WT: 386bp MT: 415bp</p>

Table 2: List of Primers Used for Strain Construction (Continued)

18	CZ16891	<i>mec-7-GFP(muls32) II</i> ; <i>arf-6(tm1447) IV</i> ; <i>ret-1(tm0390) V</i>	Strain is slower growing. Strain moves like WT. Strain has protruding vulvas. Brood size average for strain is 20 compared to 216 for WT.	Emily Grossman's Primers <i>arf-6</i> F1: gcaaattccgacgatggctc <i>arf-6</i> R1: cgccaaccatcatgtgcttc <i>arf-6</i> R2: gattgcccgagcttcagttg PCR (deletion) Band Sizes: WT: 808bp MT: 641bp <hr/> <i>ret-1 (tm0390) F1</i> : YJ8953:tgtcagtgtcagaaaggc ag <i>ret-1 (tm0390) R1</i> : YJ8954:cttgacatacatcgcttcg gg <i>ret-1 (tm0390)Del</i> : YJ9012:cttctcgctctgttcgttctg ccaagt PCR (deletion) Band sizes: WT: 386bp MT: 415bp
19	CZ17299	<i>muls32 II</i> ; <i>arf-6 (tm1447) IV</i> ; <i>lnp-1 (tm1247) X</i>	Worms appear slightly unc and look sick with protruding vulvas. Worms move like WT and grow similar to WT. Brood size average for strain is 28 compared to 216 for WT.	Emily Grossman's Primers <i>arf-6</i> F1: gcaaattccgacgatggctc <i>arf-6</i> R1: cgccaaccatcatgtgcttc <i>arf-6</i> R2: gattgcccgagcttcagttg PCR (deletion) Band Sizes: WT: 808bp MT: 641bp <hr/> <i>lnp-1 (tm1247) F</i> : YJ7400: cacagagcttgagcgagttg <i>lnp-1 (tm1247) IF</i> : YJ7401: acgaattgggacagcatttc <i>lnp-1 (tm1247) R</i> : YJ7402: tcagacggaccaactcttc PCR (deletion) Band sizes: WT: 391bp MT: 409bp
20	CZ17287	<i>yop-1(tm3667) I</i> ; <i>muls32 II</i>	Strain moves like WT. Strain grows similar to WT.	<i>yop-1</i> (tm3667) F: YJ9076: ggattcgtctaccggcttac <i>yop-1</i> (tm3667) R: YJ9077: ggcactgttctactatcggc PCR (deletion) Band Sizes: WT: 993bp MT: 355bp

Table 2: List of Primers Used for Strain Construction (Continued)**Vesicle Associated Protein/ Developmental**

	CZ #	Finished Strain Genotype	Finished Strain Gross Phenotypes	*Primers *NT change and AA change *PCR, Seq, or RE digest
1	CZ13720	<i>mec-4-GFP(zdIs5) unc-57(e1190) I; pxn-2 (ju358) X</i>	Some of the worms have kinks and bends. The strain is unc.	Phenotyped. <i>unc-57</i> worms are unc. <i>pxn-2</i> worms have kinks and bends. <i>pxn-2 (ju358)</i> F1: AC1743:ggagcattctgcaataga ac <i>pxn-2 (ju358)</i> R1: AC1744:gaaaagttacgacggcaa tc <i>pxn-2</i> NT change:G→A AA change: glutamic acid→ lysine PCR → seq Band size: 436bp
2	CZ16410	<i>mec-4-GFP (zdIs5) I; arf-6 (tm1447) IV; pxn-2 (ju358) X</i>	<i>pxn-2 (ju358)</i> worms appear to have bends and kinks. Small percentage of worms (~10%) appear superficially WT	<i>pxn-2 (ju358)</i> F1: AC1743:ggagcattctgcaataga ac <i>pxn-2 (ju358)</i> R1: AC1744:gaaaagttacgacggcaa tc <i>pxn-2</i> NT change:G→A AA change: glutamic acid→ lysine PCR → seq Band size: 436bp Emily Grossman's Primers <i>arf-6</i> F1: gcaaattccgacgatggctc <i>arf-6</i> R1: cgtccaacctcatgtgcttc <i>arf-6</i> R2: gattgcccagcttcagtttg PCR (deletion) Band Sizes: WT: 808bp MT: 641bp <i>arf-6 (tm1447)</i>

Table 2: List of Primers Used for Strain Construction (Continued)**Temperature Sensitive Mutations in Essential Genes**

	CZ #	Finished Strain Genotype	Finished Strain Gross Phenotypes	*Primers *NT change and AA change *PCR, Seq, or RE digest
1	CZ16399	<i>mec-7-GFP (muls32) II;</i> <i>dnc-4 (or633ts) IV</i>	At 25°, <i>dnc-4 (or633ts)</i> worms have smaller brood sizes and is embryonic lethal (~97% lethal)	F1:YJ8912:acatttaggagcggttgcgg R1:YJ8913:gacgcttgatggttcaaggc NT change:G→A Altered splice donor site after 1st exon PCR→ seq Band size: 267bp
2	CZ17097	<i>mec-4-GFP (zdl5) I;</i> <i>dnc-4 (or633ts) IV</i>	At 25°, <i>dnc-4 (or633ts)</i> worms have smaller brood sizes and is embryonic lethal (~97% lethal)	F1:YJ8912:acatttaggagcggttgcgg R1:YJ8913:gacgcttgatggttcaaggc NT change:G→A Altered splice donor site after 1st exon PCR→ seq Band size: 267bp
3	CZ16400	<i>mec-7-GFP (muls32) II;</i> <i>lit-1 (or393ts) III</i>	At 25°, <i>lit-1 (or393ts)</i> worms are embryonic lethal (~98.5% lethal). Worms are sick. Few eggs hatch and make it to adult stages.	F1:YJ8895:atggttcgtcacaccacgtg R1:YJ8896:gtctcgatgcaggatgtttgc NT change: A→T AA change: Isoleucine→phenylalanine PCR→ seq Band size: 798bp
4	CZ16401	<i>mec-7-GFP (muls32) II;</i> <i>par-2 (or640ts) III</i>	At 25°, <i>par-2 (or640ts)</i> worms are sterile.	N/A Mutation site not reported.
5	CZ16402	<i>mec-7-GFP (muls32) II;</i> <i>par-2 (or373ts) III</i>	At 25°, <i>par-2 (or373ts)</i> worms are embryonic lethal (~98% lethal)	F1:YJ8914:ttgagctcggaactcctctg R1:YJ8915:ccacggtttccggggtaaaaactgtcg NT change:G→A AA change: Cysteine→tyrosine PCR→ RE digest with NdeI Band Sizes: WT: 1525bp MT: 187bp + 1338bp

Table 2: List of Primers Used for Strain Construction (Continued)

6	CZ17098	<i>mec-4-GFP (zdl5) I;</i> <i>par-2 (or373ts) III</i>	At 25°, <i>par-2 (or373ts)</i> worms are embryonic lethal (~98% lethal)	F1:YJ8914:ttgagctcggaactcct ctg R1:YJ8915:ccacggtttccggggt aaaaactgtcg NT change: G→A AA change: Cysteine→ tyrosine PCR→ RE digest with NdeI Band Sizes: WT: 1525bp MT: 187bp + 1338bp
7	CZ16403	<i>mec-7-GFP (muls32) II;</i> <i>plk-1 (or683ts) III</i>	At 25°, <i>plk-1 (or683ts)</i> worms are sterile with protruding vulvas. At 15°, worms are sick. Very few eggs hatch and make it to adult stages.	F1:YJ8957:ttatcaatcaccagagt gcctcc R1:YJ8958:gaacaatcttcagcgc aatgg NT change: T→A AA change: methionine → lysine PCR→ seq Band size: 571bp
8	CZ17099	<i>mec-4-GFP (zdl5) I;</i> <i>plk-1 (or683ts) III</i>	At 25°, <i>plk-1 (or683ts)</i> worms are sterile with protruding vulvas. At 15°, worms are sick. Very few eggs hatch and make it to adult stages.	F1:YJ8957:ttatcaatcaccagagt gcctcc R1:YJ8958:gaacaatcttcagcgc aatgg NT change: T→A AA change: methionine → lysine PCR→ seq Band size: 571bp
9	CZ16405	<i>spd-2 (or493ts) I;</i> <i>mec- 7-GFP (muls32) II</i>	At 25°, <i>spd-2 (or493ts)</i> worms have smaller brood sizes and are embryonic lethal (~98.5%)	F1:YJ8897:cattcggtgtgtgca gtcg R1:YJ8898:cacttaatcatcgcaa agccgtc NT change: G→A AA change: glycine → serine PCR→ seq Band size: 594bp
10	CZ16405	<i>spd-2 (or293ts) I;</i> <i>mec- 7-GFP (muls32) II</i>	At 25°, <i>spd-2 (or293ts)</i> worms are sterile and have protruding vulvas	F1:YJ8897:cattcggtgtgtgca gtcg R1:YJ8898:cacttaatcatcgcaa agccgtc NT change: G→A AA change: arginine→ histidine PCR→ seq Band size: 594bp

Table 2: List of Primers Used for Strain Construction (Continued)

11	CZ16406	<i>mec-4-GFP (zdl5) I</i> ; <i>zyg-1 (or297ts) II</i>	At 25°, <i>zyg-1 (or297ts)</i> worms are embryonic lethal (~99.5% lethal)	F1:YJ8916:aattcgctcacctagtgtgg ctc R1:YJ8917:gcatatgaagtaagagga aac NT change: G→A AA change: aspartic acid→ asparagine PCR→ seq Band sizes: 346bp
12	CZ16407	<i>Mec-4-GFP (zdl5) I</i> ; <i>zyg-1 (or409ts) II</i>	At 25°, <i>zyg-1 (or409ts)</i> worms have smaller broods and are embryonic lethal (~100% lethal)	F1:YJ8916:aattcgctcacctagtgtgg ctc R1:YJ8917:gcatatgaagtaagagga aac NT change: G→A AA change: aspartic acid→ asparagine PCR→ seq Band sizes: 346bp
13	CZ16408	<i>rsa-1 (or598ts) I</i> ; <i>mec-7-GFP (muls32) II</i>	At 25°, <i>rsa-1 (or598ts)</i> worms are sterile	F1:YJ8901:cgattcctgactccaac g R1:YJ8902:cttcgggacgtaactctgg c NT change: A→G AA change: aspartic acid→ glycine PCR→ seq Band size: 446bp
14	CZ 17100	<i>mec-4-GFP (zdl5) rsa-1 (or598ts) I</i>	At 25°, <i>rsa-1 (or598ts)</i> worms are sterile	F1:YJ8901:cgattcctgactccaac g R1:YJ8902:cttcgggacgtaactctgg c NT change: A→G AA change: aspartic acid→ glycine PCR→ seq Band size: 446bp
15	CZ16409	<i>mei-1 (or642ts) I</i> ; <i>mec-7-GFP(muls32) II</i>	At 25°, <i>mei-1 (or642ts)</i> worms are embryonic lethal (~99.75% lethal)	F1:YJ8899:tccaacacaaggaataact gcctc R1:YJ8900:gaatcaccagccacttgc NT change: A→C AA change: lysine→ glutamine PCR→ RE digest with BstAPI Band size: WT: 202bp +204bp MT: 190bp+204bp

Table 2: List of Primers Used for Strain Construction (Continued)

16	CZ16892	<i>spd-5 (or213) I; mec-7-GFP (muls32) II</i>	Keep at 15 degrees. Worms are embryo lethal at 25 degrees.	F1: YJ9015: caattcgtaatgccaccacc R1: YJ9016: Gcagcctgataactacgac NT change: G→A AA change: arginine → lysine PCR→ RE digest with BstBI Band sizes: WT: 272bp + 340bp MT: 612bp
17	CZ16893	<i>mel-26 (or543) I; mec-7-GFP (muls32) II</i>	Keep at 15 degrees. Strain is temperature sensitive.	F1: YJ9013: gtagtaatggagtaccggcac R1: YJ9014: gtctcaactgcaacatcaattccacattc NT change: C→T AA change: Arginine→ cysteine PCR→ seq Band Size: 487bp
18	Re-make CZ12150	<i>mec-7-GFP (muls32) II; dnc-1(or404) IV</i>	Keep at 15 degrees. Strain is temperature sensitive. At 15C, 100% viable. At 25C, 10% viable. At 26C, 2% viable. At higher temperatures, strain has smaller brood sizes. Worms	F1: AC2735: ttcatcaggatctccatccgt R1: AC2736: tgggtgccacagtacttac NT change: C→T AA change: arginine → cysteine PCR→ RE digest with Hyp99I Band size: WT: 146bp + 286bp MT: 432bp
19	Re-make CZ12037	<i>mec-4-GFP (zdl5) I; dnc-1(or404) IV</i>	Keep at 15 degrees. Strain is temperature sensitive. At 15C, 100% viable. At 25C, 10% viable. At 26C, 2% viable. At higher temperatures, strain has smaller brood sizes.	F1: AC2735: ttcatcaggatctccatccgt R1: AC2736: tgggtgccacagtacttac NT change: C→T AA change: arginine → cysteine PCR→ RE digest with Hyp99I Band size: WT: 146bp + 286bp MT: 432bp

Table 2: List of Primers Used for Strain Construction (Continued)**MAPK Pathway**

	CZ #	Finished Strain Genotype	Finished Strain Gross Phenotypes	*Primers *NT change and AA change *PCR, Seq, or RE digest
1	CZ17286	<i>mec-4-GFP (zcls5) I;</i> <i>Y110A2AL1.3 (tm2235) II</i>	Strain moves like WT. Strain grows similar to WT. Brood size average for strain is 208 compared to 216 for WT.	F1: YJ9080: ccctcaatgttccgacgcatc R1: YJ9081: gagtcgataattcgctgc PCR (deletion)
2	CZ17285	<i>mec-4-GFP (zcls5) I;</i> <i>T14E8.1a (tm0737) X</i>	Strain is slightly unc and small. Strain grows similar to WT. Brood size average for strain is 201 compared to 216 for WT.	F1: YJ9078: gacagatcaactgcacact R1: YJ9079: ttgtcaacgcgaggttctt PCR (deletion)
3	CZ17288	<i>mec-4-GFP (zcls5) I;</i> <i>Y110A2AL1.3 (tm2235) II;</i> <i>T14E8.1a (tm0737) X</i>	Strain is slightly unc and small. Strain grows similar to WT. Brood size average for strain is 150 compared to 216 for WT.	Y110A2AL1.3 (tm2235): F1: YJ9080: ccctcaatgttccgacgcatc Y110A2AL1.3 (tm2235): R1: YJ9081: gagtcgataattcgctgc PCR (deletion) T14E8.1a (tm0737): F1: YJ9078: gacagatcaactgcacact T14E8.1a (tm0737): R1: YJ9079: ttgtcaacgcgaggttctt PCR (deletion)

PDE Dopaminergic Neurons

	CZ #	Finished Strain Genotype	Finished Strain Gross Phenotypes	*Primers *NT change and AA change *PCR, Seq, or RE digest
1	CZ16076	<i>otIs181III</i>	WT	N/A
2	CZ16413	<i>otIs181III; arf-6 (tm1447) IV</i>	Strain moves like WT	Emily Grossman's Primers <i>arf-6</i> F1: gcaaattccgacgatgctc <i>arf-6</i> R1: cgtccaaccatcatgtgcttc <i>arf-6</i> R2: gattgcccgagcttcagtttg PCR (deletion) Band Sizes: WT: 808bp MT: 641bp
3	CZ16412	<i>otIs181 III ; unc-26 (e205) IV</i>	Strain is unc	N/A
4	CZ16411	<i>unc-57 (e1190) I; otIs181 III</i>	Strain is unc	N/A
5	CZ16475	<i>otIs181 III; cebp-1 (tm2807) X</i>	Strain moves like WT	Kai Kim's Primers F: gcagctggttgctaaatcgcgcg Raacttaagggtttattctgact PCR (deletion) Band Sizes: WT: 1171bp MT: 692bp

Table 2: List of Primers Used for Strain Construction (Continued)

6	CZ16476	<i>dlk-1(tm4024) I; otIs181 III</i>	Strain moves like WT	Dong's Primers F1:ggaacttgcttagcttag R1:gtataatcatgtcgaggttt PCR (deletion) Band sizes: WT: 1504bp MT: 1044bp
7	CZ16477	<i>otIs181 III; efa-6 (tm3124) IV</i>	Strain moves like WT	F1:YJ6452:ggttgctgccccttgat R1:YJ6453:ccgtcgaacattcagtggt PCR (deletion)
8	CZ16894	<i>otIs181 III; kgb-1 (um3) IV</i>	Keep at 15 or 20 degrees. Worms are sterile at 26 degrees. Strain moves like WT. Brood size average for strain is 134 compared to 216 for WT.	F1:YJ9008: acacacaattgacagagg R1: YJ9009:gtcggcttgatagcgttg PCR (deletion)
9	CZ17000	<i>otIs181 III; kgb-1 (um3) kgb-2(km16) IV</i>	Keep at 15 or 20 degrees. Worms are sterile at 26 degrees. Strain moves like WT. Brood size average for strain is 132 compared to 216 for WT.	F1: YJ9010: ggtctaccagagttgtgggaatc R1: YJ1350: gatagccttgacttcgttg PCR (deletion) Band size: WT: MT: no visible bands
10	CZ17282	<i>dlk-1 (tm4024) I; otIs181 III; kgb-1 (um3) IV</i>	Strain moves like WT. Brood size average for strain is 198 compared to 216 for WT.	Dong's Primers F1:ggaacttgcttagcttag R1:gtataatcatgtcgaggttt PCR (deletion) Band sizes: WT: 1504bp MT: 1044bp kgb-1 (um3): F1:YJ9008: acacacaattgacagagg kgb-1 (um3) R1: YJ9009: gtcggcttgatagcgttg PCR (deletion)

Table 2: List of Primers Used for Strain Construction (Continued)

11	CZ17283	<i>dlk-1 (tm4024) I; otls181 III; kgb-1(um3) kgb-2 (km16) IV</i>	Strain moves like WT and grows like WT. Brood size average for strain is 150 compared to 216 for WT.	<p>Dong's Primers F1:ggaacttgcttagcttag R1:gtataatcatgtcgaggtt</p> <p>PCR (deletion)</p> <p>Band sizes: WT: 1504bp MT: 1044bp</p> <hr/> <p>kgb-1 (um3) kgb-2(km16): F1: YJ9010: ggtctaccagagtttggggaatc kgb-1 (um3) kgb-2(km16): R1: YJ1350: gatagcctgcacttcgttg PCR (deletion)</p>
12	CZ17834	<i>otls181 III; mlk-1 (ok2471)</i>		<p>YJ9265: F: CTGGTCACTGTTGAAACgtagg YJ9266:IF: CGACACTATCACTGAGCAGTCC YJ9267: R: GTAGTTTAGCCCAGGCTTTGA</p> <p>Band Sizes: WT: 382bp MT: 782bp</p>

Table 3: List Of Average Branch Number For Each Axotomy Group
(Done by Zilu Wu)

Group #	Strain CZ#	Genotype	N#	Branch Average	Average Regrowth
G1869	CZ10175	<i>mec-4-GFP (zdIs5) I</i>	13	0.769231	91.846
G1870	CZ15797	<i>mec-4-GFP(zdIs5)I; arf-6(tm1447) IV; unc-51(ky347) V; Prgef-1-arf-6::gfp (juEx4082)</i>	16	0.125	64
G1871	CZ15797 w/o juEx4082	<i>mec-4-GFP(zdIs5)I; arf-6(tm1447) IV; unc-51(ky347) V</i>	18	0.277778	51.944
G1873	CZ10969	<i>mec-7-GFP (muIs32) II</i>	15	1.6	104.533
G1874	CZ13002	<i>mec-7-GFP(muIs32) II; unc-26 (e205) IV</i>	15	1.066667	92.4
G1896	CZ10969	<i>mec-7-GFP (muIs32) II</i>	16	1.375	99.875
G1898	CZ15796 w/o juEx4084	<i>mec-7-GFP(muIs32) II; unc-26(e205) IV arf-6(tm1447) IV</i>	12	1	98.083
G1899	CZ15796	<i>mec-7-GFP(muIs32) II; unc-26(e205) IV arf-6(tm1447) IV; Pmec-7-arf-6::gfp (juEx4084)</i>	16	0.5625	78.313
G1900	CZ15795	<i>mec-7-GFP(muIs32) II; Pmec-7-arf-6::gfp (juEx4084)</i>	14	0.71429	106.571

Table 3: List Of Average Branch Number For Each Axotomy Group
(Done by Zilu Wu) [Cont.]

G1901	CZ15793	<i>mec-7-GFP(muIs32) II; Prgef-1-arf-6::gfp (juEx4082)</i>	12	1.58333	108
G1902	CZ15794	<i>mec-7-GFP(muIs32) II; unc-26(e205) IV arf-6(tm1447) IV; Prgef-1-arf-6::gfp(juEx4082)</i>	13	1.076923	80.615
G1903	CZ15794 w/o juEx4082	<i>mec-7-GFP(muIs32) II; unc-26(e205) IV arf-6(tm1447) IV</i>	16	0.75	72.875
G1904	CZ15798 w/o juex4084	<i>mec-4-GFP(zdIs5)I; arf-6(tm1447) IV; unc-51(ky347) V</i>	15	0.13333	45.267
G1905	CZ15798	<i>mec-4-GFP(zdIs5)I; arf-6(tm1447) IV; unc-51(ky347) V; Pmec-7-arf-6::gfp (juEx4084)</i>	15	0	32.333
G1906	CZ10175	<i>mec-4-GFP (zdIs5) I</i>	15	0.53333	100.067
G1916	CZ10969	<i>mec-7-GFP (muIs32) II</i>	15	1.33333	99.6
G1920	CZ16075	<i>mec-7-GFP(muIs32) II; PF25B33-FLAG::DLK-1 (k162A) (juIs227)</i>	17	0	18.706
G1931	CZ10175	<i>mec-4-GFP (zdIs5) I</i>	17	0.588235	119.529

Table 3: List Of Average Branch Number For Each Axotomy Group
(Done by Zilu Wu) [Cont.]

G1932	CZ15837	<i>mec-4-GFP(zdIs5) I; usp-46(ok2232) III; Pusp-46:usp-46 + sur-5-mch + ttx-3-rfp (juEx4460) [line 1]</i>	17	0	55.529
G1933	CZ16150	<i>mec-4-GFP(zdIs5)I; snb-1 (md247)V; F55A4.1(ok3053) X</i>	12	0.25	100.833
G1934	CZ13608	<i>mec-4-GFP(zdIs5)I; ark-1 (sy247) IV</i>	14	0.78571	111.214
G1935	CZ16076	<i>otIs181 III; cebp-1 (tm2807) X</i>	Not Clear	Not Clear	Not Clear
G1936	CZ16074	<i>otIs181 III; cebp-1 (tm2807) X</i>	Not Clear	Not Clear	Not Clear
G1941	CZ10969	<i>mec-7-GFP (muIs32) II</i>	14	0.85714	91.214
G1942	CZ13681	<i>mec-7-GFP (muIs32) II; F55A4.1 (ok3053) X</i>	14	1.5	119.214
G1944	CZ16073	<i>mec-7-GFP(muIs32) II; arf-6 (tm1447) IV; F55A4.1 (ok3053) X</i>	15	1.26667	116.733
G1950	CZ16401	<i>mec-7-GFP (muIs32) II; par-2 (or640ts) III</i>	14	1	150.285
G1951	CZ16405	<i>spd-2 (or493ts) I; mec-7-GFP (muIs32) II</i>	13	1	100.54

Table 3: List Of Average Branch Number For Each Axotomy Group
(Done by Zilu Wu) [Cont.]

G1952	CZ16400	<i>mec-7-GFP (muIs32) II; lit-1 (or393ts) III</i>	13	1	133.31
G1953	CZ16403	<i>mec-7-GFP (muIs32) II; plk-1 (or683ts) III</i>	12	2	187.42
G1954	CZ16409	<i>mei-1 (or642ts) I; mec-7-GFP(muIs32) II</i>	14	1.07143	138.14
G1955	CZ16399	<i>mec-7-GFP (muIs32) II; dnc-4 (or633ts) IV</i>	16	2.375	149.81
G1956	CZ16408	<i>rsa-1 (or598ts) I; mec-7-GFP (muIs32) II</i>	16	1.6875	174.31
G1957	CZ10969	<i>mec-7-GFP (muIs32) II</i>	15	1	122.53
G1958	CZ10175	<i>mec-4-GFP (zdIs5) I</i>	15	0.4	102.27
G1959	CZ16406	<i>mec-4-GFP (zdIs5) I; zyg-1 (or297ts) II</i>	12	0.5	106.5
G1960	CZ16407	<i>mec-4-GFP (zdIs5) I; zyg-1 (or409ts) II</i>	17	1	117.59
G1961	CZ10175	<i>mec-4-GFP (zdIs5) I</i>	16	0.06667	128.25
G1965	CZ10969	<i>mec-7-GFP (muIs32) II</i>	14	0.64286	143.71
G1966	CZ16401	<i>mec-7-GFP (muIs32) II; par-2 (or640ts) III</i>	14	1.21429	157.29
G1967	CZ16400	<i>mec-7-GFP (muIs32) II; lit-1 (or393ts) III</i>	16	0.625	131.94
G1968	CZ16399	<i>mec-7-GFP (muIs32) II; dnc-4 (or633ts) IV</i>	16	2	119.69

Table 3: List Of Average Branch Number For Each Axotomy Group
(Done by Zilu Wu) [Cont.]

G1969	CZ16403	<i>mec-7-GFP (muIs32) II; plk-1 (or683ts) III</i>	13	1.38461	130.31
G1970	CZ16409	<i>mei-1 (or642ts) I; mec-7-GFP(muIs32) II</i>	16	1.0625	168.38
G1971	CZ16408	<i>rsa-1 (or598ts) I; mec-7-GFP (muIs32) II</i>	12	2.16667	172.5
G1972	CZ16404	<i>spd-2 (or293ts) I; mec-7-GFP (muIs32) II</i>	15	0.666667	83.67
G1973	CZ16405	<i>spd-2 (or493ts) I; mec-7-GFP (muIs32) II</i>	16	0.875	134.44
G1974	CZ10969	<i>mec-7-GFP (muIs32) II</i>	15	0.73333	108.27
G1975	CZ16403	<i>mec-7-GFP (muIs32) II; plk-1 (or683ts) III</i>	16	0.875	103.06
G1976	CZ16405	<i>spd-2 (or493ts) I; mec-7-GFP (muIs32) II</i>	17	1.76471	143.71
G1977	CZ16402	<i>mec-7-GFP (muIs32) II; par-2 (or373ts) III</i>	17	0.4117647	66.41
G1978	CZ10969	<i>mec-7-GFP (muIs32) II</i>	13	0.84615	121
G1979	CZ10175	<i>mec-4-GFP (zdIs5) I</i>	16	0.375	129.94
G1980	CZ13720	<i>mec-4-GFP (zdIs5) unc-57 (e1190) I</i>	11	0.09091	76
G1981	CZ16237		17	0	38.12
G1982	CZ16410	<i>mec-4-GFP (zdIs5)I; arf-6 (tm1447) IV; pxn-2 (ju358) X</i>	8	0.5	160.88
G1983	CZ12125	<i>CZ12125: mec-4-GFP (zdIs5); pxn-2 (ju358) X</i>	9	0.44444	135.33

Table 3: List Of Average Branch Number For Each Axotomy Group
(Done by Zilu Wu) [Cont.]

G1986	OH8483	<i>dat-1mch;</i> <i>pttx-3 mch</i> <i>(otIs181); him-</i> <i>8 (e1489)</i>	5	0.8	40.8
G1987	CZ16476	<i>dlk-1 (tm4024)</i> <i>I; otIs181 III</i>	8	1.125	80.37
G1988	CZ16475	<i>otIs181</i> <i>III;cebp-1</i> <i>(tm2807) X</i>	6	2.16667	151.33
G1989	CZ16477	<i>otIs181 III;</i> <i>efa-6 (tm3124)</i> <i>IV</i>	6	0.66667	88.17
G1990	CZ16413	<i>otIs181III; arf-</i> <i>6 (tm1447) IV</i>	6	1.3333	95.33
G1991	OH8483	<i>dat-1mch;</i> <i>pttx-3 mch</i> <i>(otIs181); him-</i> <i>8 (e1489)</i>	6	2.16667	123.83
G1992	CZ16412	<i>otIs181 III ;</i> <i>unc-26 (e205)</i> <i>IV</i>	8	0.5	93.25
G1993	CZ16411	<i>unc-57 (e1190)</i> <i>I; otIs181 III</i>	7	0.85714	76
G2001	CZ16076	<i>dat-1mch;</i> <i>pttx-3mch</i> <i>(otIs181)III</i>	20	0.95	125.4
G2002	CZ16476	<i>dlk-1 (tm4024)</i> <i>I; otIs181 III</i>	10	0.6	96.1
G2003	CZ16475	<i>otIs181</i> <i>III;cebp-1</i> <i>(tm2807) X</i>	8	1.375	98.25
G2007	CZ10969	<i>mec-7-GFP</i> <i>(muIs32) II</i>	15	1.4	143.73
G2008	CZ12150	<i>mec-7-GFP</i> <i>(muIs32) II;</i> <i>dnc-1(or404)</i> <i>IV</i>	18	1.61111	115.06
G2009	CZ16893	<i>mel-26 (or543)</i> <i>I; mec-7-GFP</i> <i>(muIs32) II</i>	15	0.53333	100.4
G2010	CZ16892	<i>spd-5 (or213)</i> <i>I; mec-7-GFP</i> <i>(muIs32) II</i>	13	1	143.31

Table 3: List Of Average Branch Number For Each Axotomy Group
(Done by Zilu Wu) [Cont.]

G2011	CZ16076 (6hr)	<i>otIs181 III; cebp-1</i>	8	0.875	64
G2012	CZ10175	<i>mec-4-GFP (zds5) I</i>	17	0.76471	66.41
G2013	CZ12037	<i>mec-4-GFP (zds5) I; dnc-1(or404) IV</i>	16	0.875	67.06
G2017	CZ16965	<i>mec-7-GFP (muIs32) II; dlk-1 (tm4024); dat-1mch; pttx-3mch (otIs181)III</i>	15	0.66667	16.73
G2018	CZ16965	<i>mec-7-GFP (muIs32) II; dlk-1 (tm4024); dat-1mch; pttx-3mch (otIs181)III</i>	16	0.5625	26.63
G2019	CZ10969 (12um)	<i>mec-7-GFP (muIs32) II</i>	11	1.636	112.91
G2020	CZ10969	<i>mec-7-GFP (muIs32) II</i>	12	1.25	119.92
G2024	CZ16583	<i>mec-7-GFP(muIs32) II; lnp-1 (tm1247)X</i>	14	1.21429	122.36
G2028	CZ10969	<i>mec-7-GFP (muIs32) II</i>	12	1.33333	109.75
G2030	CZ16584	<i>mec-7-GFP (muIs32) II; ret-1 (gk242) V</i>	14	1.78571	93.5
G2031	CZ16585	<i>mec-7-GFP (muIs32) II; ret-1 (tm0390) V</i>	15	1	88.73
G2035	CZ16076	<i>dat-1mch; pttx-3mch (otIs181)III</i>	12	1.25	143.75
G2036	CZ16894	<i>otIs181 III; kgb-1 (um3) IV</i>	10	1	148.3

Table 3: List Of Average Branch Number For Each Axotomy Group
(Done by Zilu Wu) [Cont.]

G2037	CZ17000	<i>otIs181III; kgb-1 (um3) kgb-2(km16) IV</i>	7	0.28571	90.71
G2053	CZ10969	<i>mec-7-GFP (muIs32) II</i>	15	2.26667	87.4
G2054	CZ12095 (50um) ALM	<i>mec-7-GFP (muIs32) II; dlk-1 (tm4024)</i>	15	0.6	44.6
G2055	CZ12095 (50um) ALM& PLM	<i>mec-7-GFP (muIs32) II; dlk-1 (tm4024)</i>	ALM -17 PLM -17	ALM- 0.88235 PLM-0	79.35
G2056	CZ10969	<i>mec-7-GFP (muIs32) II</i>	15	1.26667	122.6
G2057	CZ16408	<i>rsa-1 (or598ts) I; mec-7-GFP (muIs32) II</i>	11	1.1818	143.18
G2058	CZ16402	<i>mec-7-GFP (muIs32) II; par-2 (or373ts) III</i>	14	0.14286	67.43
G2059	CZ16402	<i>mec-7-GFP (muIs32) II; par-2 (or373ts) III</i>	16	0.8125	106.44
G2076	CZ17099	<i>mec-4-GFP (zdIs5) I; plk-1 (or683ts) III</i>	13	0.30769	72.85
G2077	CZ10175	<i>mec-4-GFP (zdIs5) I</i>	17	0.82353	124.18
G2078	CZ17098	<i>mec-4-GFP (zdIs5) I; par-2 (or373ts) III</i>	16	0.6875	97.13
G2079	CZ17097	<i>mec-4-GFP (zdIs5) I; dnc-4 (or633ts) IV</i>	15	1	76.8
G2080	CZ17100	<i>mec-4-GFP (zdIs5) rsa-1 (or598ts) I</i>	14	0.85714	91.79

Table 3: List Of Average Branch Number For Each Axotomy Group
(Done by Zilu Wu) [Cont.]

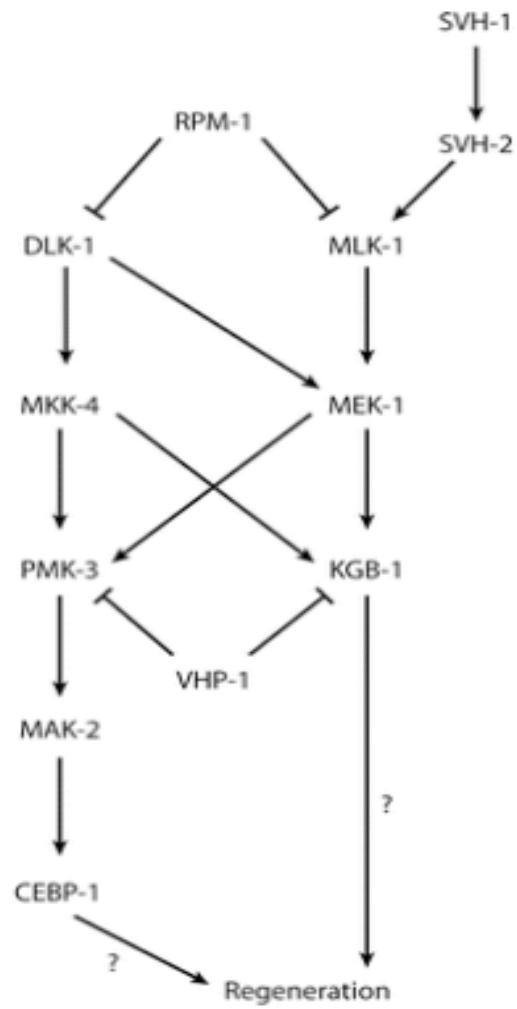
G2081	CZ10969	<i>mec-7-GFP (muIs32) II</i>	15	1.3333	128.87
G2082	CZ16584	<i>mec-7-GFP (muIs32) II; ret-1 (gk242) V</i>	16	2	106.94
G2083	CZ16889	<i>mec-7-GFP(muIs32) II; ret-1(gk242) V; lnp-1 (tm1247)X</i>	16	1.5	107
G2084	CZ16890	<i>mec-7-GFP(muIs32) II; ret-1 (tm0390) V; lnp-1 (tm1247)X</i>	15	1.0667	99.07
G2085	CZ16585	<i>mec-7-GFP (muIs32) II; ret-1 (tm0390) V</i>	13	1.7692	110.77
G2086	CZ17299	<i>muIs32 II; arf-6 (tm1447) IV; lnp-1 (tm1247) X</i>	12	0.75	145.75
G2087	CZ10175	<i>mec-4-GFP (zdIs5) I</i>	11	1	156.18
G2088	CZ17285	<i>mec-4-GFP (zdIs5) I; T14E8.1a (tm0737) X</i>	15	0.13333	89.33
G2089	CZ17286	<i>mec-4-GFP (zdIs5) I; Y110A2AL1.3 (tm2235) II</i>	16	0.625	112.5
G2090	CZ17288	<i>mec-4-GFP (zdIs5) I; Y110A2AL1.3 (tm2235) II; T14E8.1a (tm0737) X</i>	17	0.94118	98.29
G2094	CZ10175	<i>mec-4-GFP (zdIs5) I</i>	13	0.15385	120

Table 3: List Of Average Branch Number For Each Axotomy Group
(Done by Zilu Wu) [Cont.]

G2095	CZ17285	<i>mec-4-GFP</i> (<i>zdIs5</i>) I; <i>T14E8.1a</i> (<i>tm0737</i>) X	15	0.33333	95.27
G2096	CZ17286	<i>mec-4-GFP</i> (<i>zdIs5</i>) I; <i>Y110A2AL1.3</i> (<i>tm2235</i>) II	13	0.84615	113.62
G2097	CZ17288	<i>mec-4-GFP</i> (<i>zdIs5</i>) I; <i>Y110A2AL1.3</i> (<i>tm2235</i>) II; <i>T14E8.1a</i> (<i>tm0737</i>) X	14	0.28571	11.29
G2100	CZ10969	<i>mec-7-GFP</i> (<i>muIs32</i>) II	13	1.3846	113.77
G2102	CZ17287	<i>yop-1(tm3667)</i> I; <i>muIs32</i> II	15	0.93333	128
G2103	CZ16076	<i>dat-1mch</i> ; <i>pttx-</i> <i>3mch</i> (<i>otIs181</i>)III	7	1.2857	130.29
G2104	CZ16476	<i>dlk-1 (tm4024)</i> I; <i>otIs181</i> III	12	0.83333	106.08
G2105	CZ17282	<i>dlk-1 (tm4024)</i> I; <i>otIs181</i> III; <i>kbg-1 (um3)</i> IV	11	0.83333	123.82
G2106	CZ17283	<i>dlk-1 (tm4024)</i> I; <i>otIs181</i> III; <i>kbg-1(um3)</i> <i>kbg-2 (km16)</i> IV	11	0.83333	114.73
G2107	CZ16894	<i>otIs181</i> III; <i>kbg-</i> <i>1 (um3)</i> IV	4	0.83333	125.5
G2108	CZ17000	<i>otIs181</i> III; <i>kbg-</i> <i>1 (um3)</i> <i>kbg-</i> <i>2(km16)</i> IV	4	0.83333	102
G2132	CZ16403	<i>mec-7-GFP</i> (<i>muIs32</i>) II; <i>plk-1 (or683ts)</i> III	16	0.83333	88
G2133	CZ16399	<i>mec-7-GFP</i> (<i>muIs32</i>) II; <i>dnc-4 (or633ts)</i> IV	13	0.83333	128.08

Table 3: List Of Average Branch Number For Each Axotomy Group
(Done by Zilu Wu) [Cont.]

G2134	CZ16408	<i>rsa-1 (or598ts)</i> <i>I; mec-7-GFP</i> <i>(muIs32) II</i>	15	0.83333	151.07
G2135	CZ10969	<i>mec-7-GFP</i> <i>(muIs32) II</i>	16	0.83333	142.06




 El Bejjani R, Hammarlund M. 2012.
Annu. Rev. Genet. 46:499–513

Figure 1: DLK-1 MAPKKK and JNK MAPK Pathway

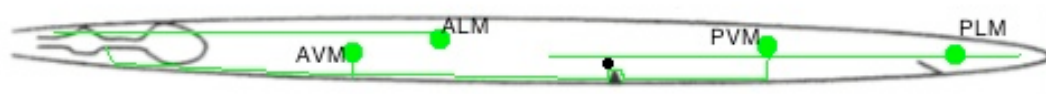
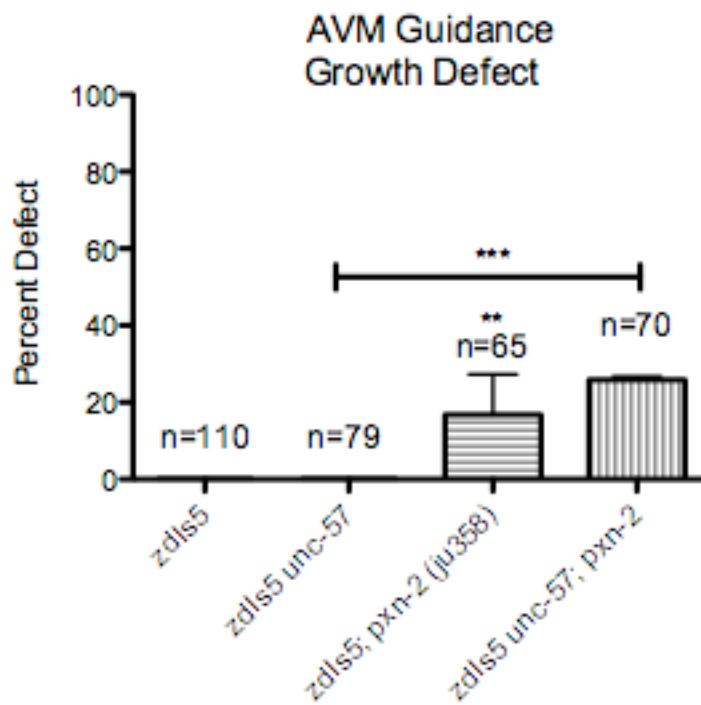


Figure 2: Proper Growth of ALM, AVM, PLM, and PVM Neurons

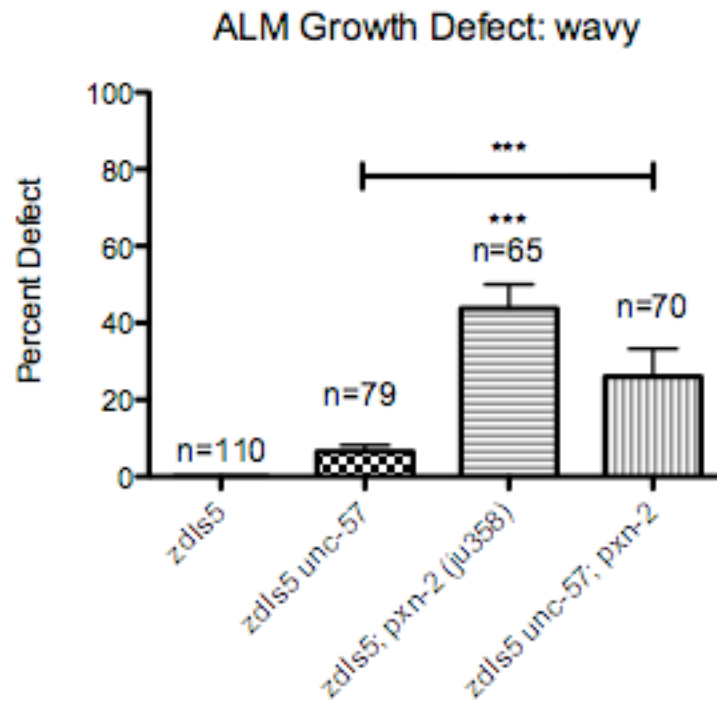


Figure 3: Proper Growth of CEP, AIY, ADE, and PDE Neurons



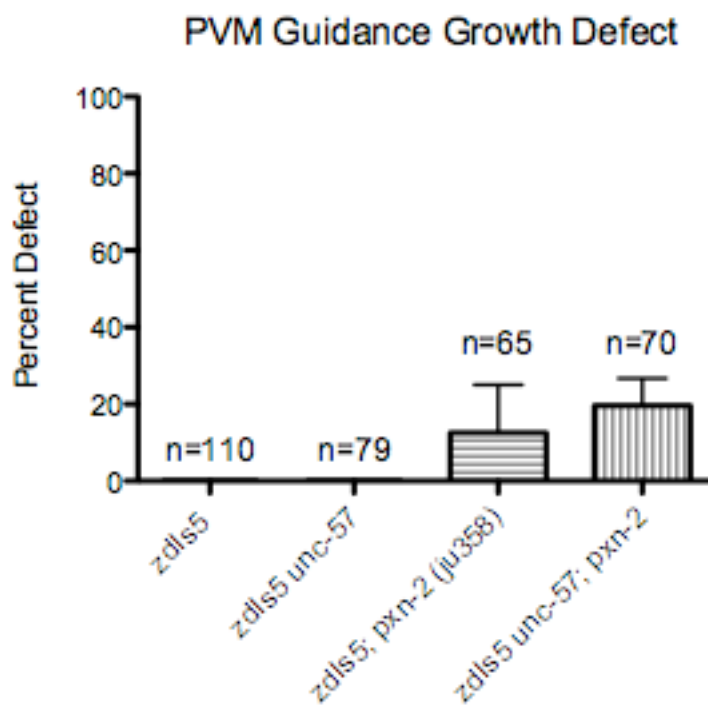
Graph 1: AVM Guidance Growth Defect for double mutant

zdis5 I unc-57 (e1190); pxn-2(ju358)



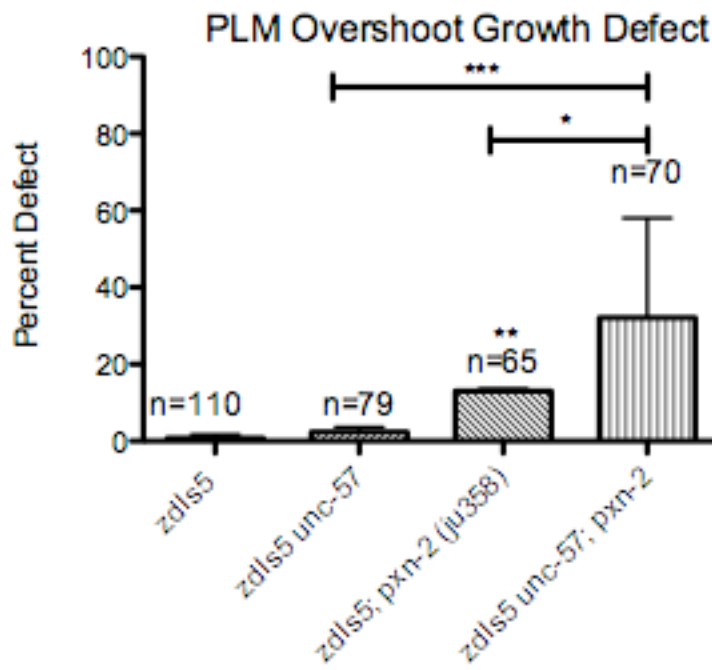
Graph 2: ALM Guidance Growth Defect for double mutant

zdls5 I unc-57 (e1190); pxn-2(ju358)



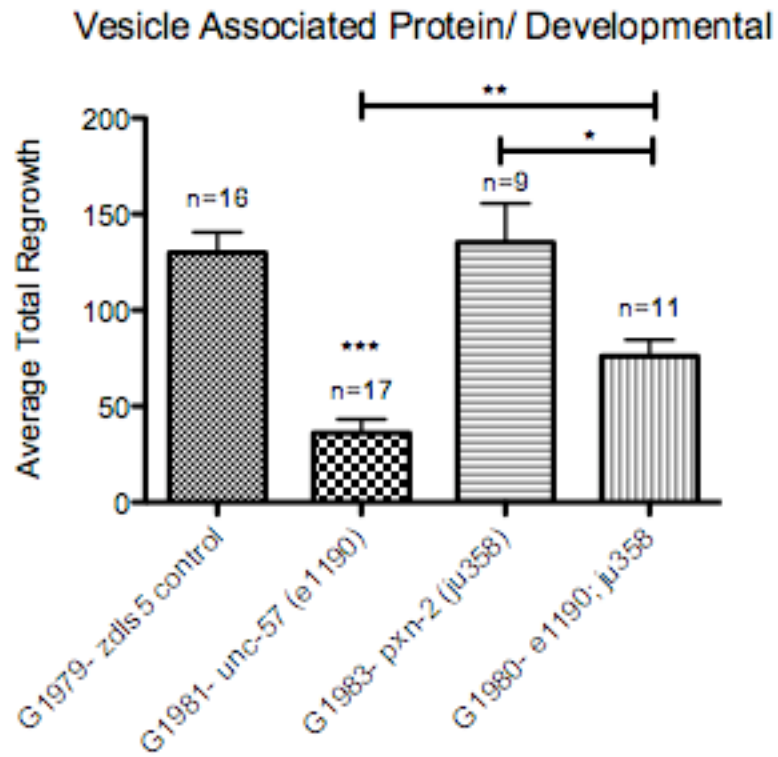
Graph 3: PVM Guidance Growth Defect for double mutant

zdIs5 I unc-57 (e1190); pxn-2(ju358)



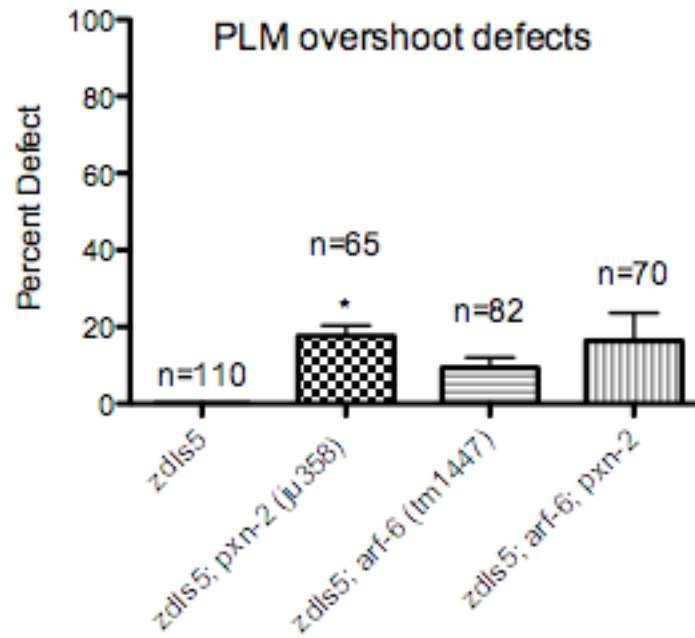
Graph 4: PLM Overshoot Growth Defect for double mutant

zdIs5 I unc-57 (e1190); pxn-2(ju358)



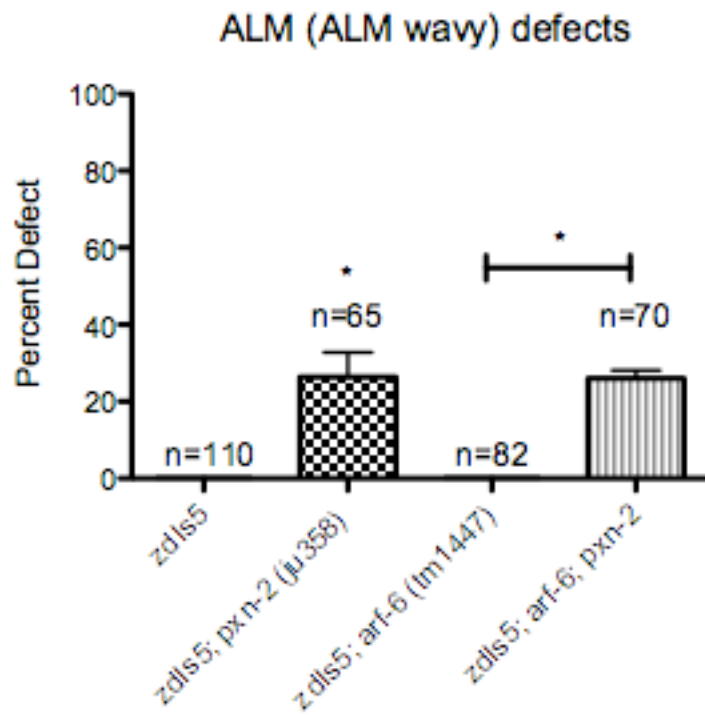
Graph 5: Axotomy Data: Vesicle Associated Protein/ Development

Double mutant *zdl5 I unc-57 (e1190); pxn-2(ju358)*



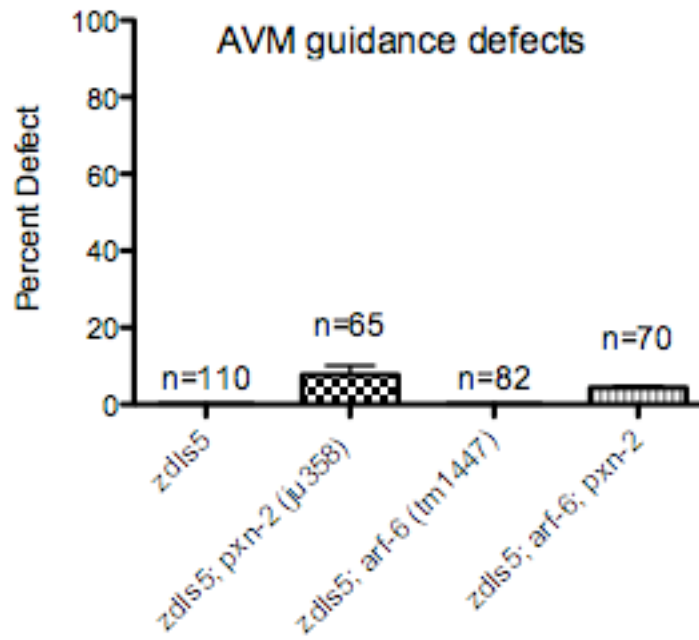
Graph 6: PLM Overshoot Growth Defect for double mutant

zdIs5 I; arf-6 (tm1447); pxn-2(ju358)



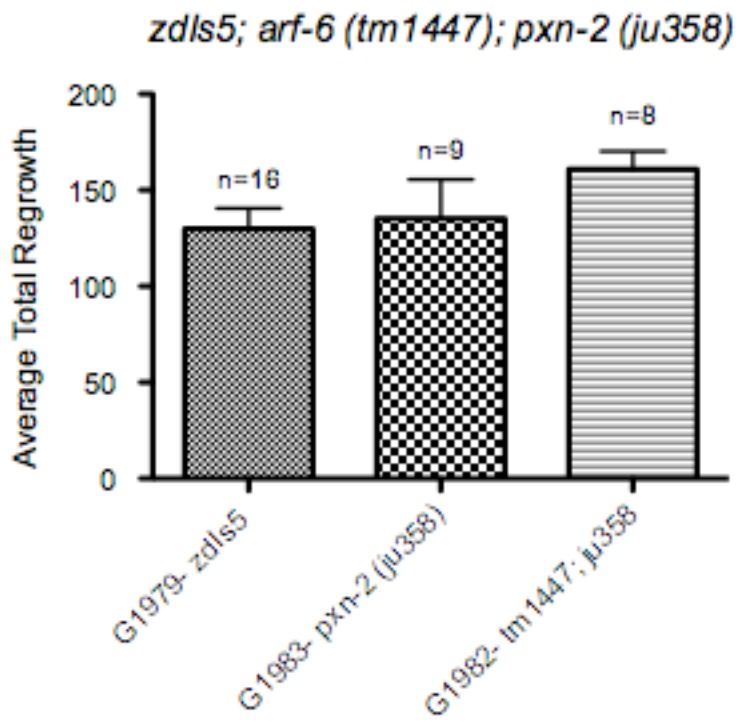
Graph 7: ALM (ALM Wavy) Growth Defect for double mutant

zdIs5 I; arf-6 (tm1447); pxn-2(ju358)



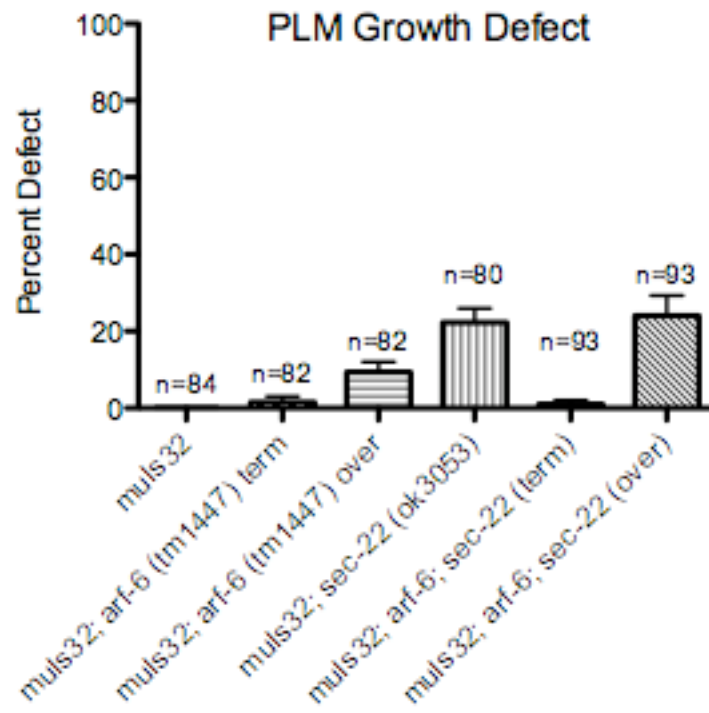
Graph 8: AVM Guidance Growth Defect for double mutant

zdIs5 I; arf-6(tm1447); pxn-2(ju358)



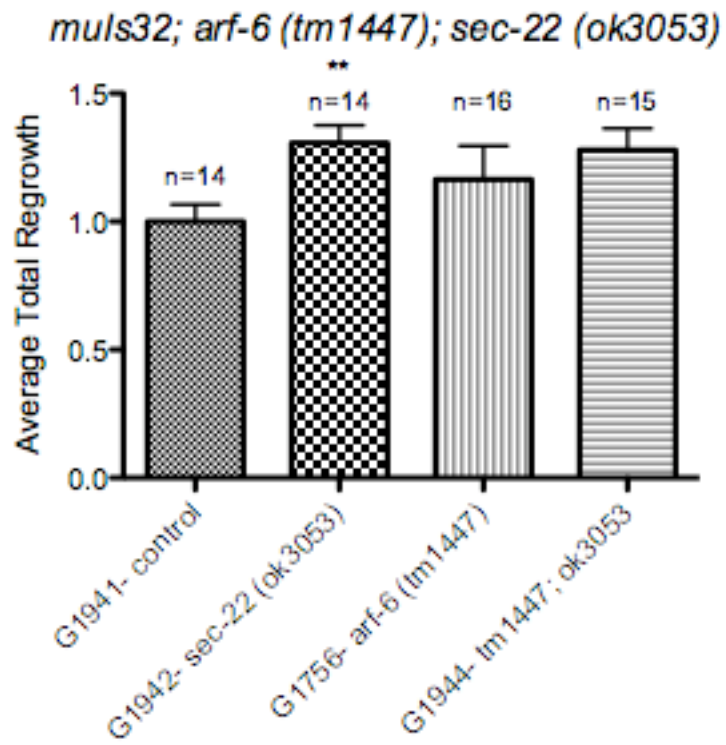
Graph 9: Axotomy Data: for double mutant

zdis5 I; arf-6 (tm1447); pxn-2(ju358)

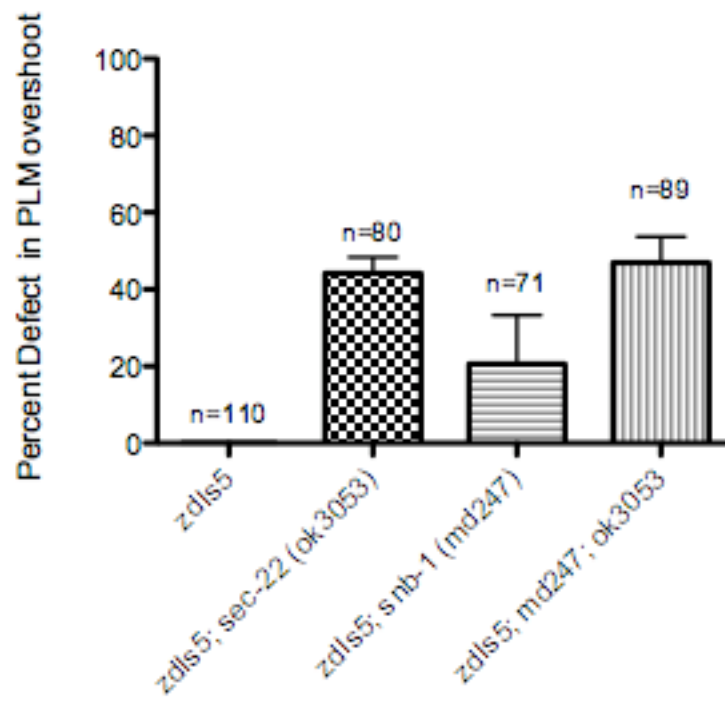


Graph 10: PLM Overshoot Growth Defect for double mutant

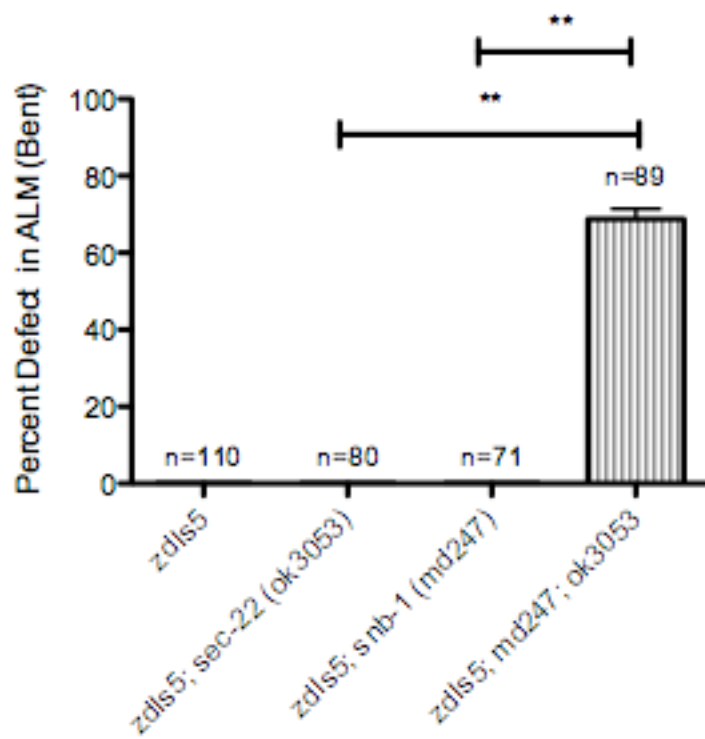
muIs32 II; arf-6(tm1447) IV; sec-22(ok3053) X



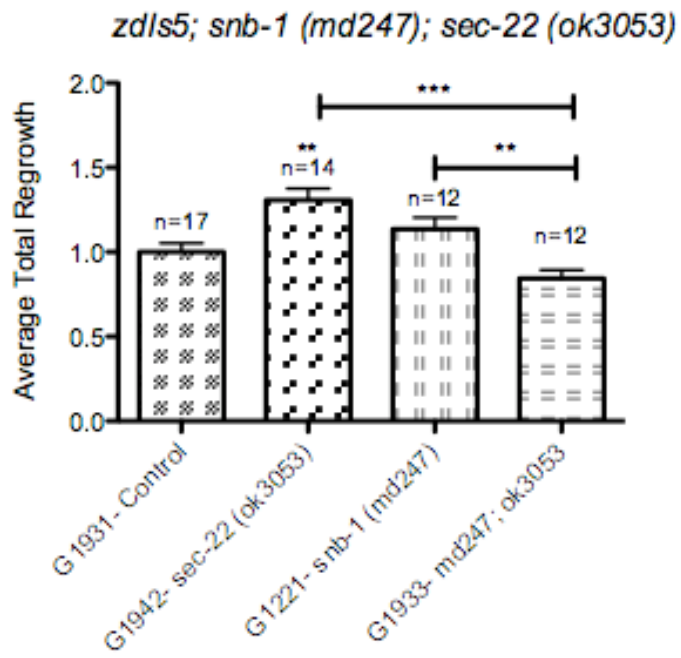
Graph 11: Axotomy Data: for the double mutant
mulS32 II; arf-6 (tm1447) IV; sec-22 (ok3053) X



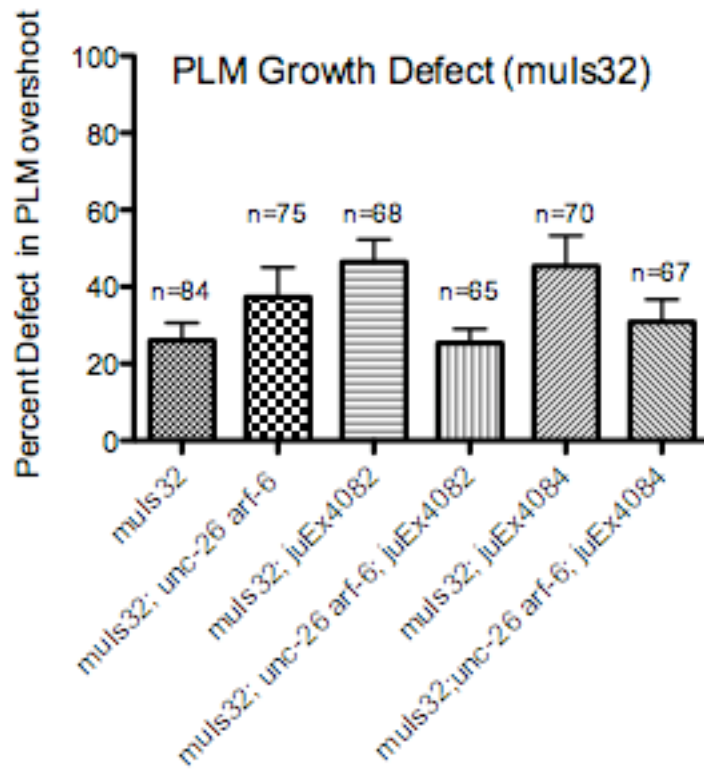
Graph 12: PLM Overshoot Growth Defect for double mutant
mulS32 II; snb-1 (md247) V, sec-22 (ok3053) X



Graph 13: ALM Bent Growth Defect for double mutant
mul532 II; snb-1 (md247) V, sec-22 (ok3053) X

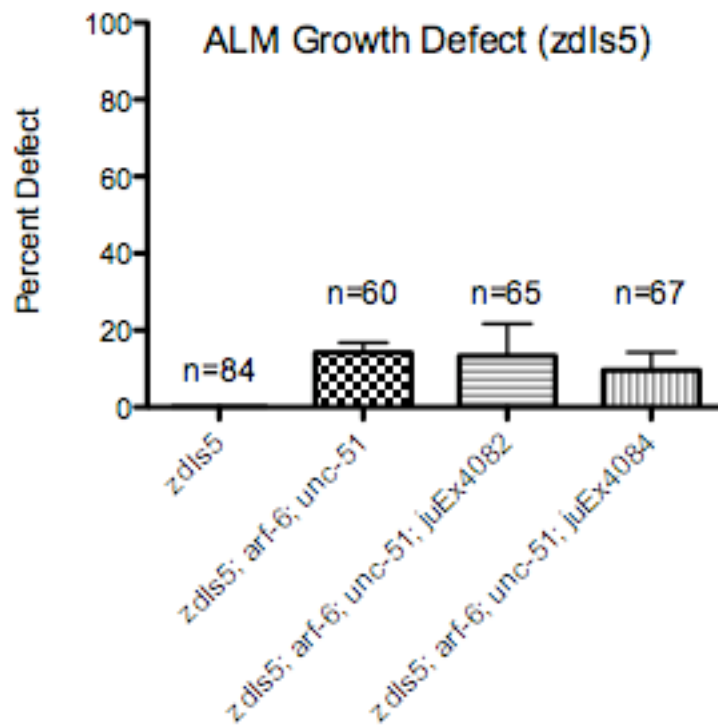


Graph 14: Axotomy Data: for the double mutant
muIs32 II; snb-1 (md247) V, sec-22 (ok3053) X



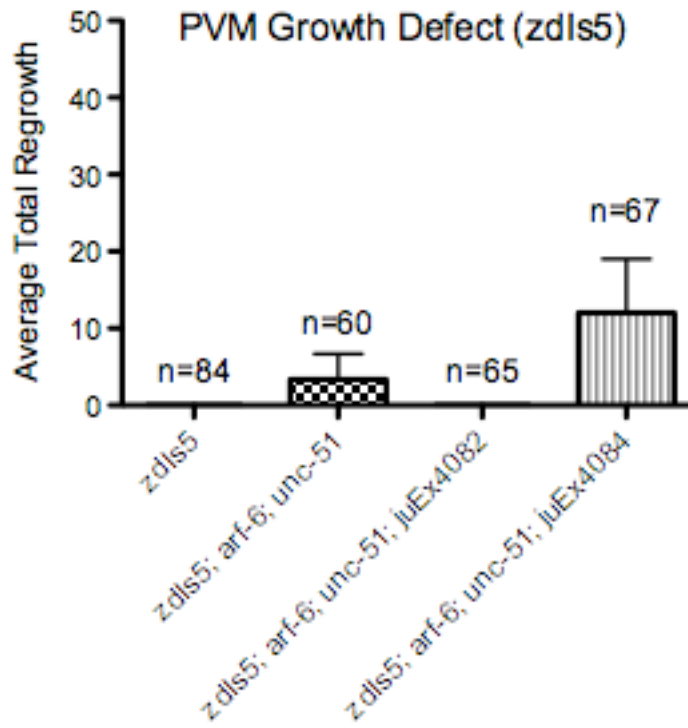
Graph 15: PLM Overshoot Growth Defect: Rescue

muls32 II; unc-26 (e205) IV arf-6 (tm1447) IV



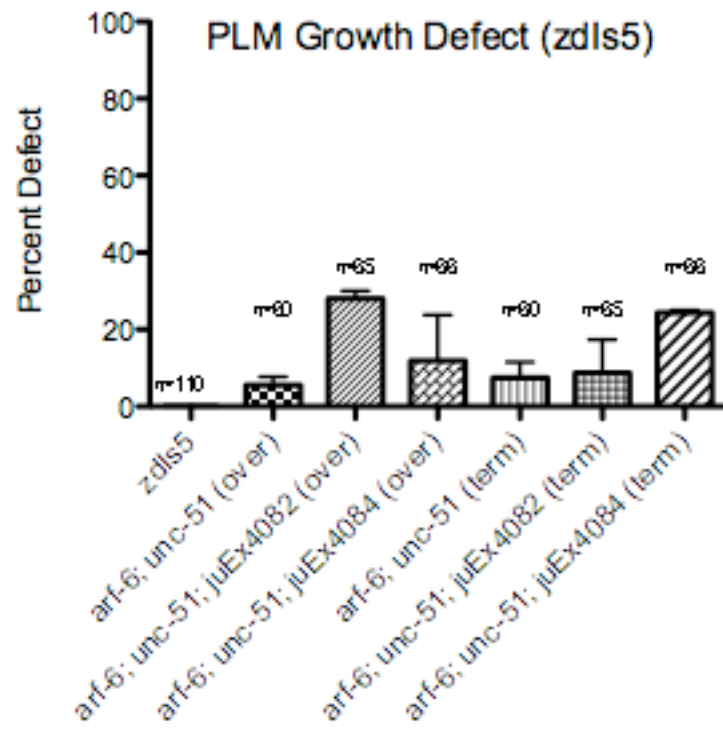
Graph 16: ALM Wavy Growth Defect: Rescue

zdIs5 I; *arf-6* (*tm1447*) IV; *unc-51* (*ky347*) V



Graph 17: PVM Guidance Growth Defect: Rescue

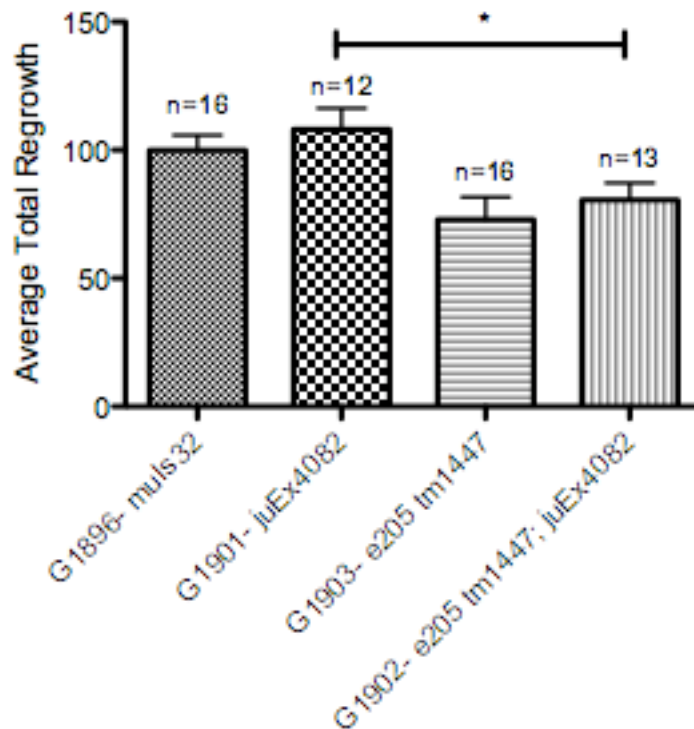
zdis5 I; *arf-6* (*tm1447*) IV; *unc-51* (*ky347*) V



Graph 18: PLM Overshoot Growth Defect: Rescue

zdIs5 I; arf-6 (tm1447) IV; unc-51 (ky347) V

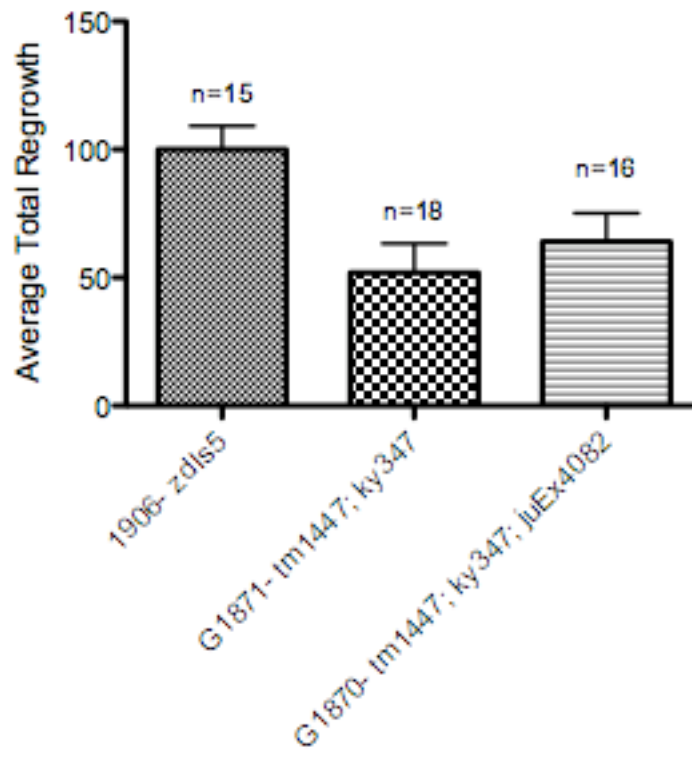
mulS32; unc-26 (e205) arf- 6 (tm1447); juEx4082



Graph 19: Axotomy Data: Rescue:

mulS32 II; unc-26 (e205) IV arf- 6 (tm1447) IV; juEx4082

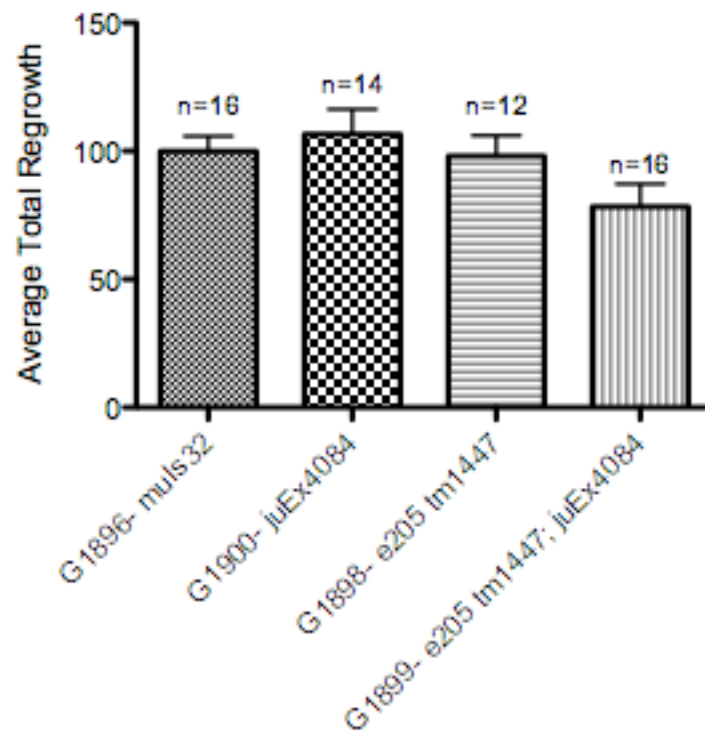
zdis5; arf-6 (tm1447); unc-51 (ky347); juEx4082



Graph 20: Axotomy Data: Rescue:

zdis5 I; arf-6 (tm1447) IV; unc-51 (ky347) V; juEx4082

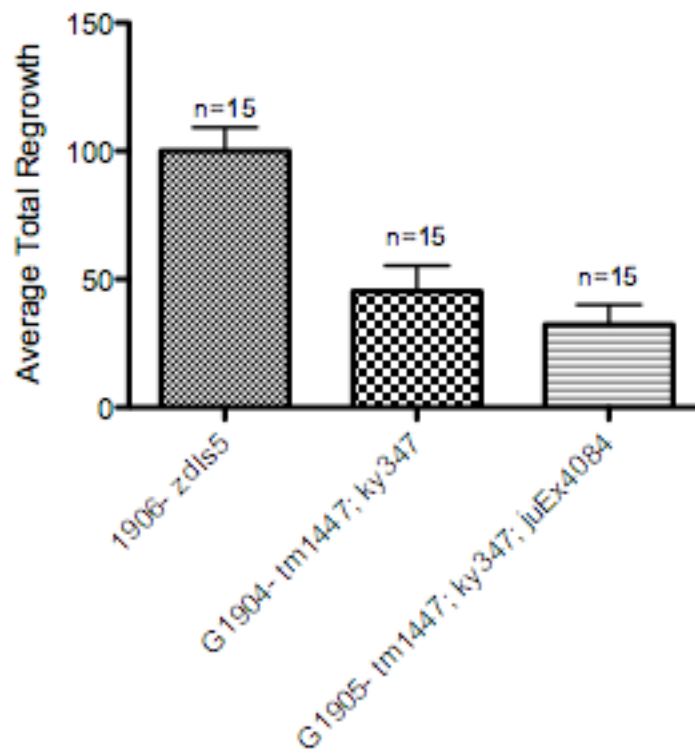
mulS32; unc-26 (e205) arf- 6 (tm1447); juEx4084



Graph 21: Axotomy Data: Rescue:

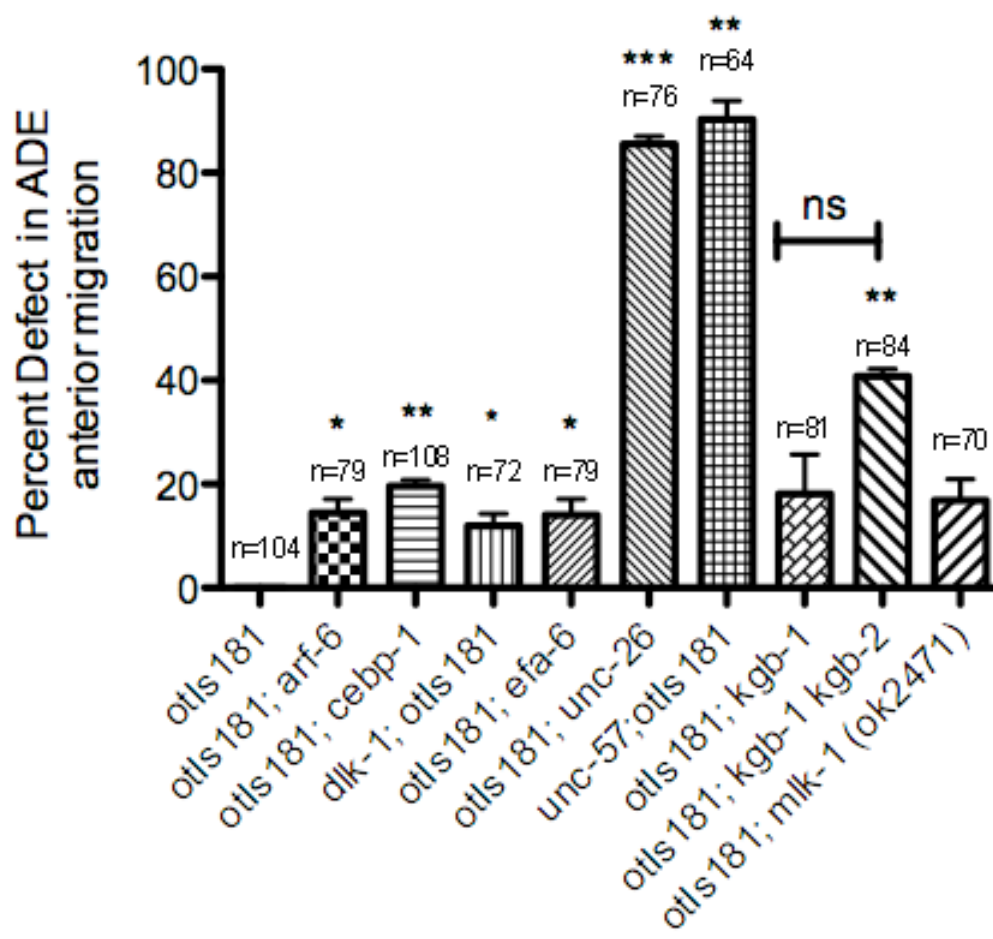
mulS32 II; unc-26 (e205) IV arf- 6 (tm1447) IV; juEx4084

zdis5; arf-6 (tm1447); unc-51 (ky347); juEx4084

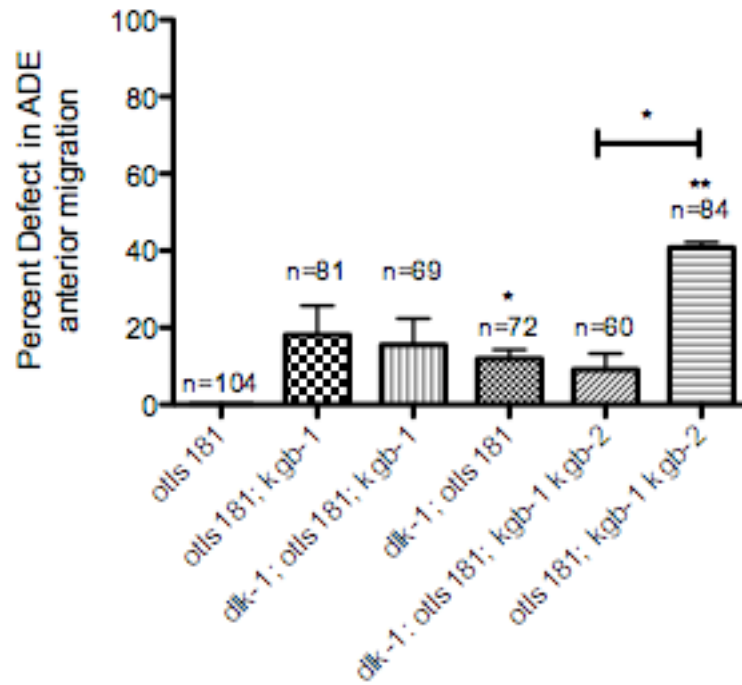


Graph 22: Axotomy Data: Rescue:

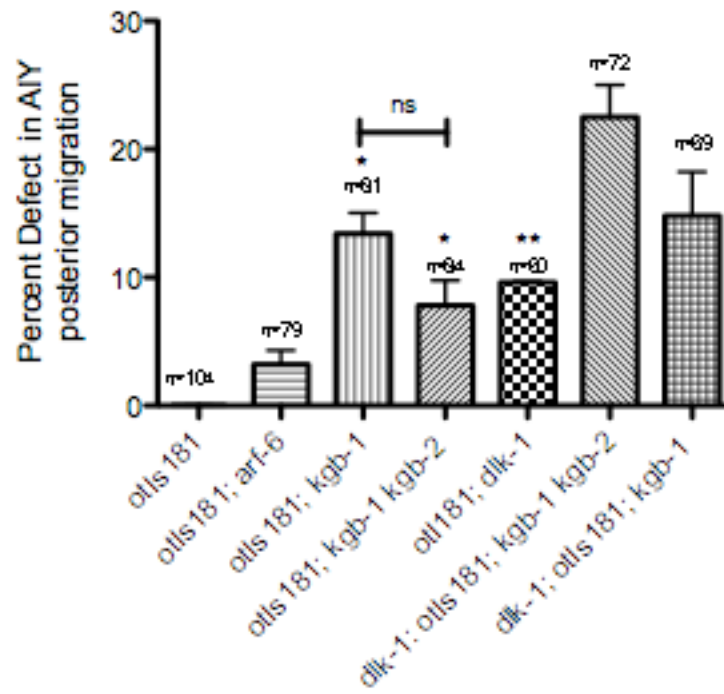
zdis5 I; arf-6 (tm1447) IV; unc-51 (ky347) V; juEx4082



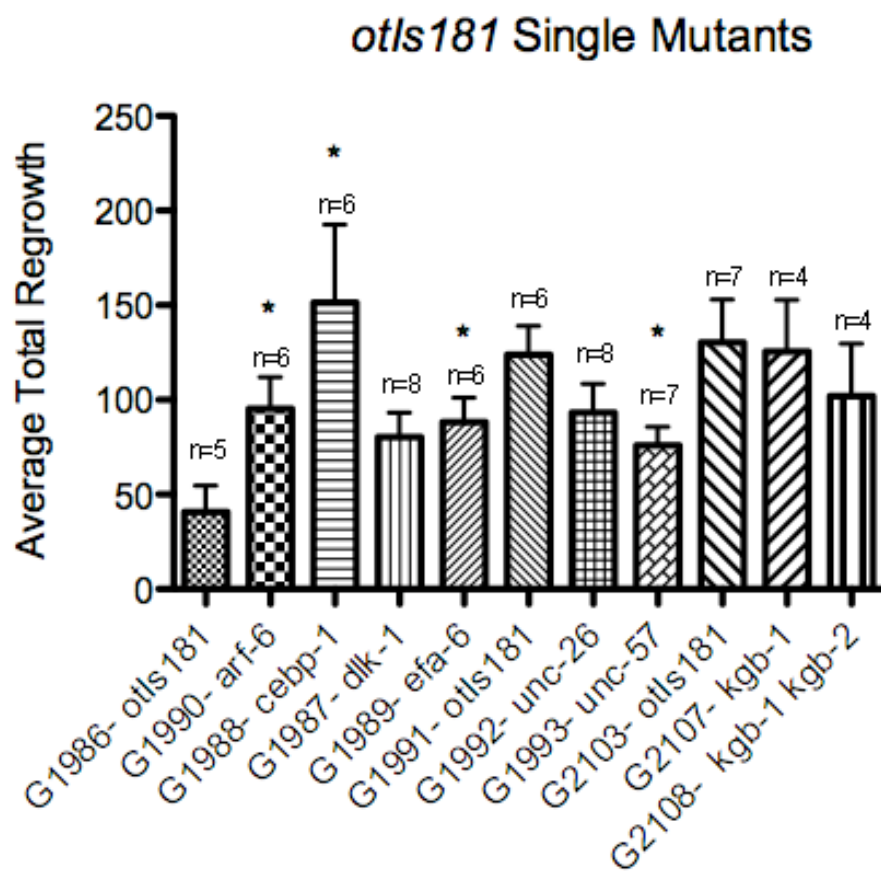
Graph 23: ADE Anterior Migration Defect: *otIs181* Single Mutants



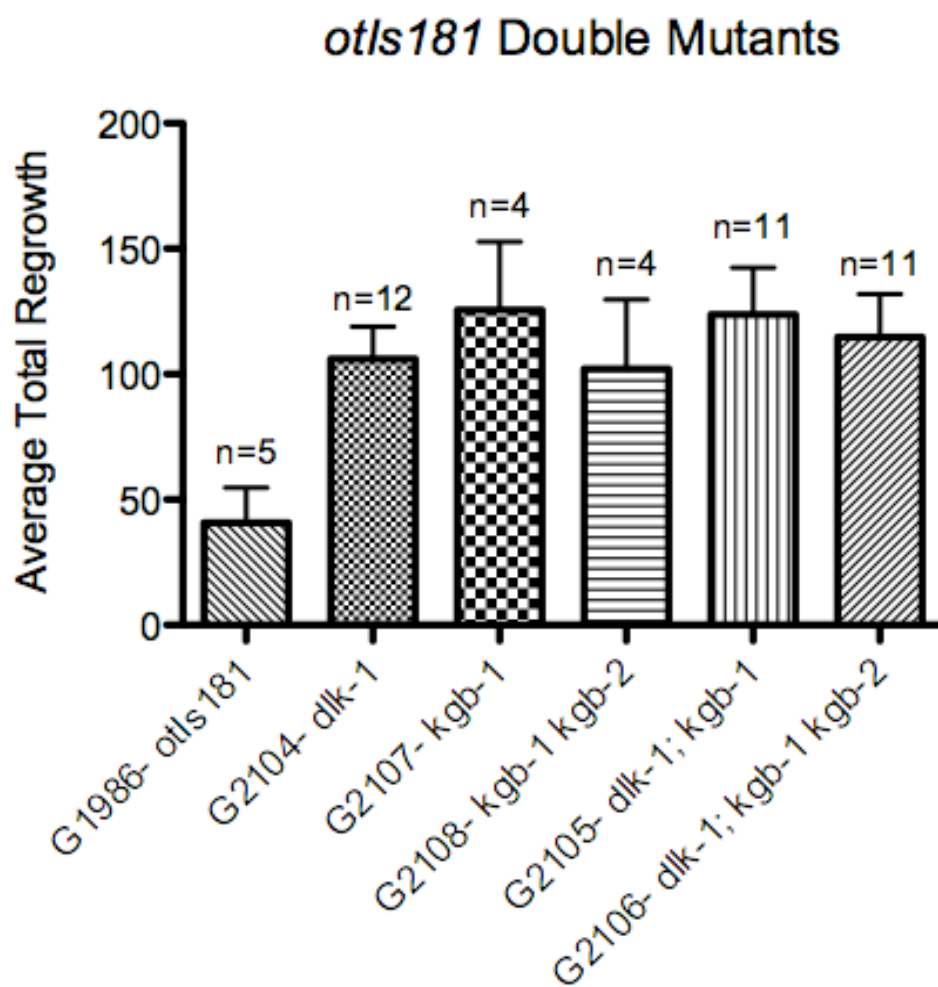
Graph 24: ADE Anterior Migration Defect: *otIs181* Double Mutants



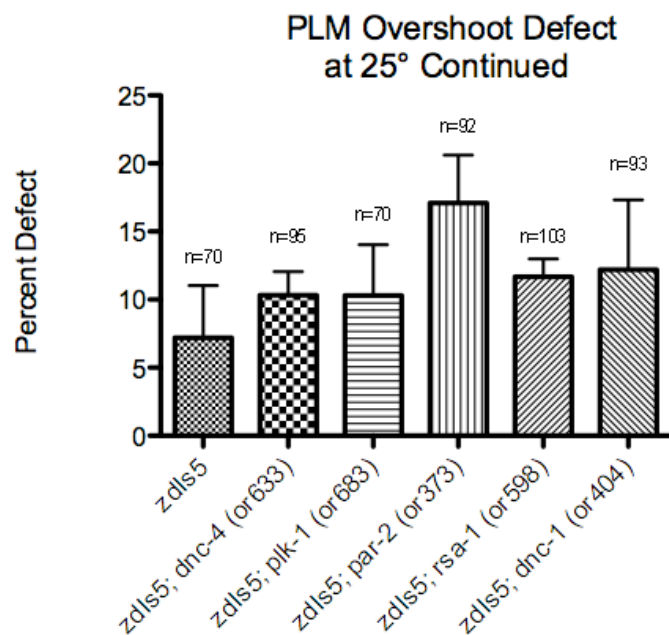
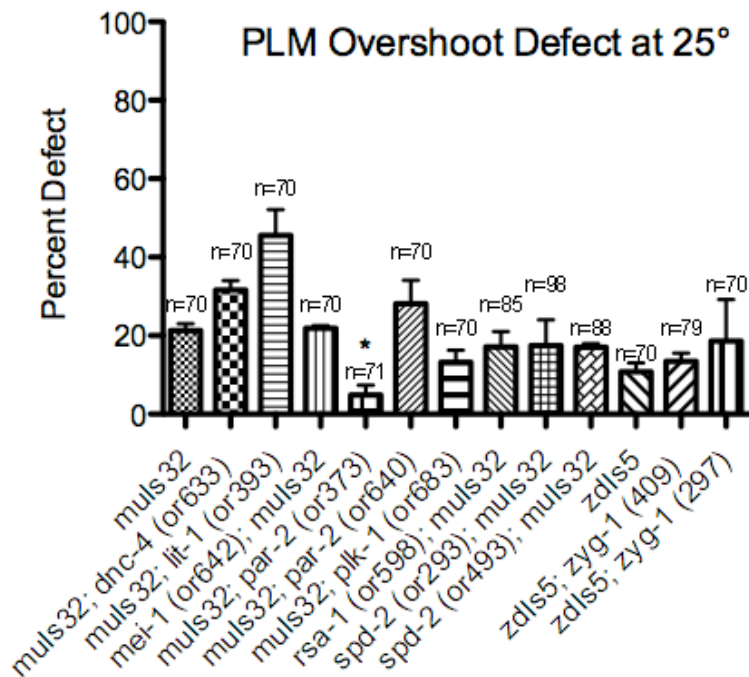
Graph 25: AIY Posterior Migration Defect: *otIs181*



Graph 26: Axotomy Data: *otIs181* Single Mutants

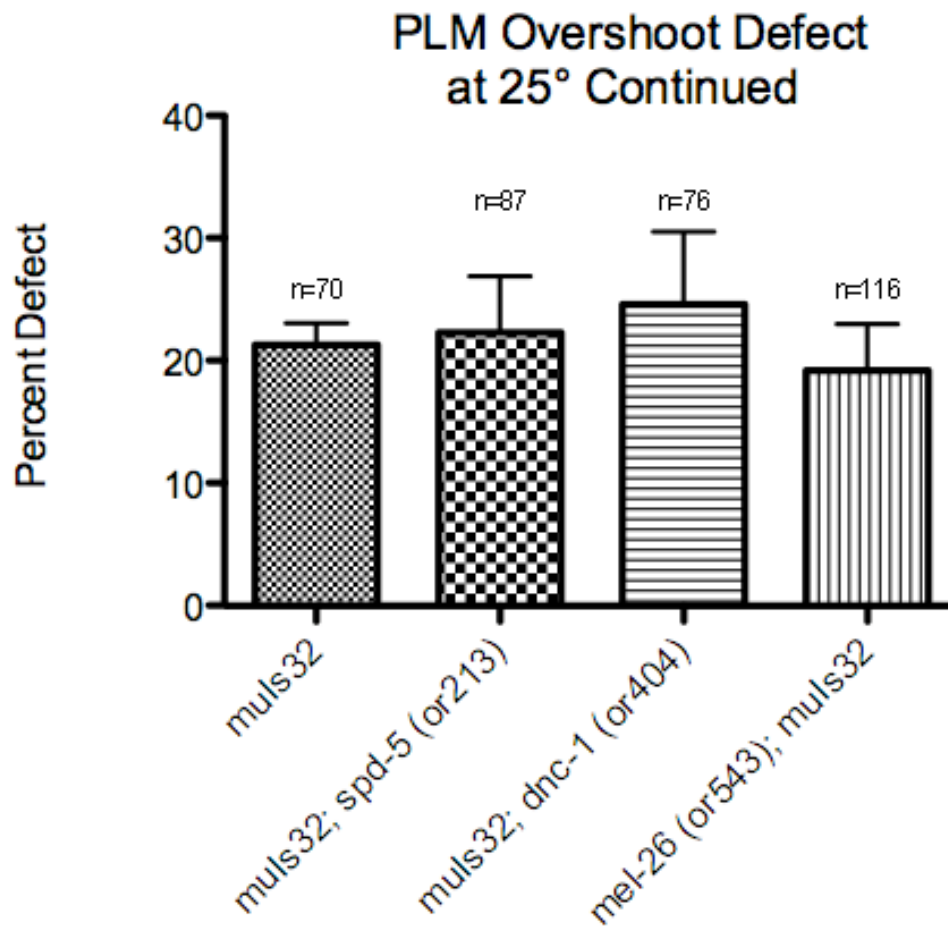


Graph 27: Axotomy Data: *otIs181* Double Mutants

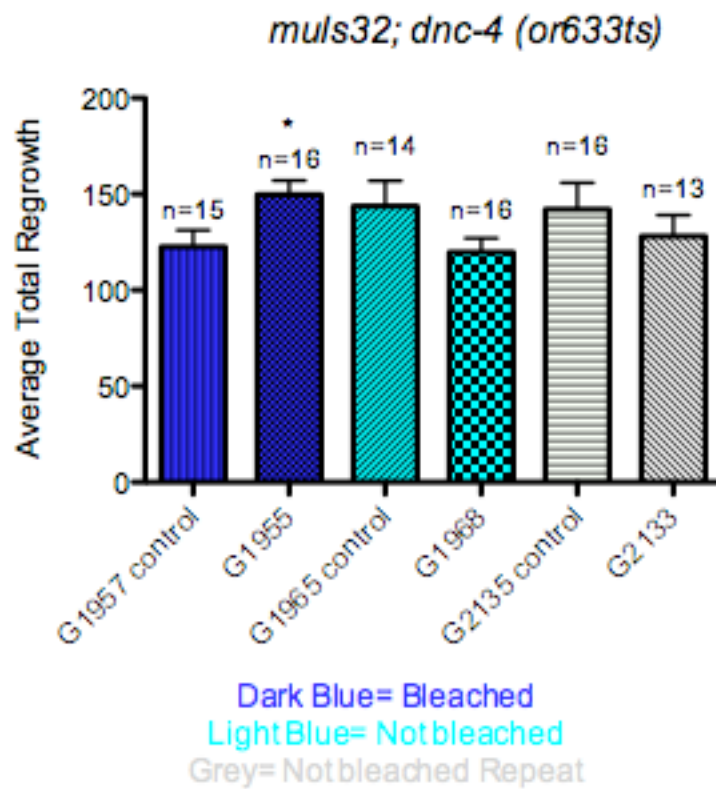


Graph 28: PLM Overshoot Defect: Temperature Sensitive 25 degrees

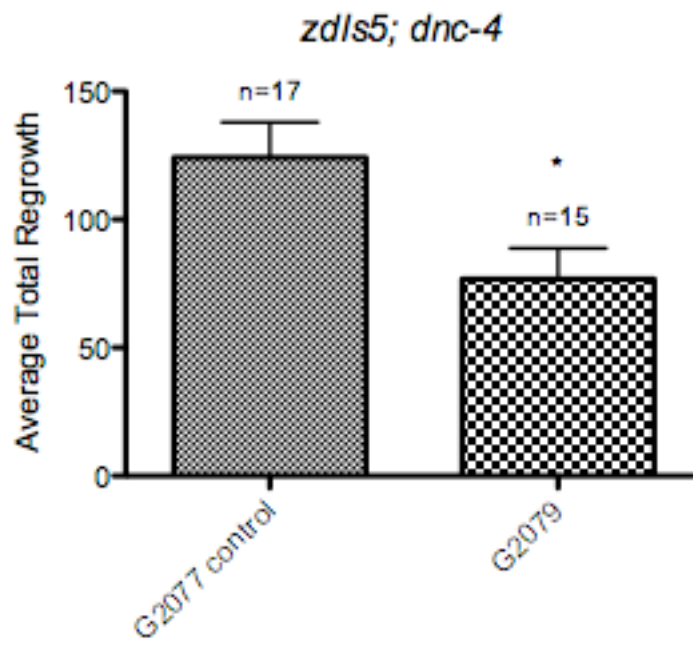
PLM Overshoot Defect: Temperature Sensitive 25 degrees (Cont.)



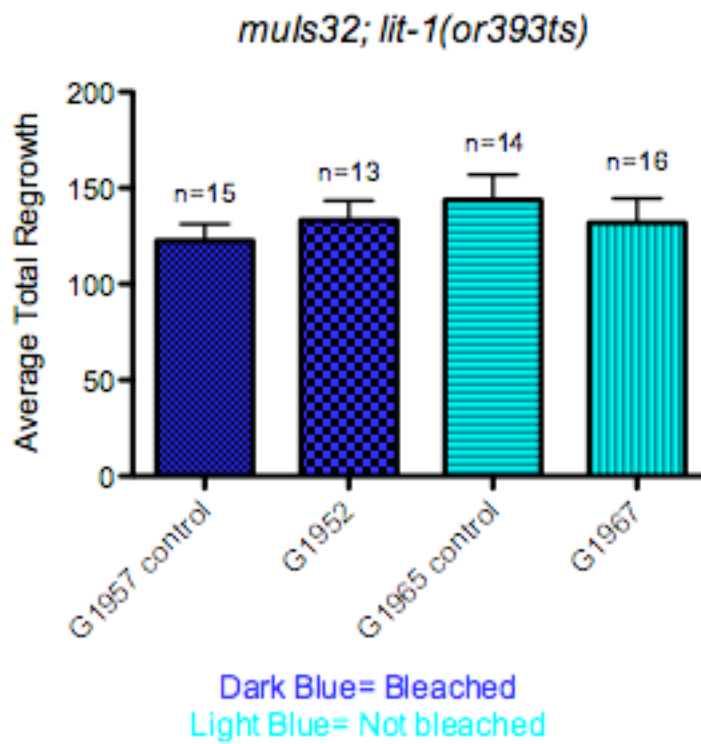
Graph 29: PLM Overshoot Defect: New Temperature Sensitive



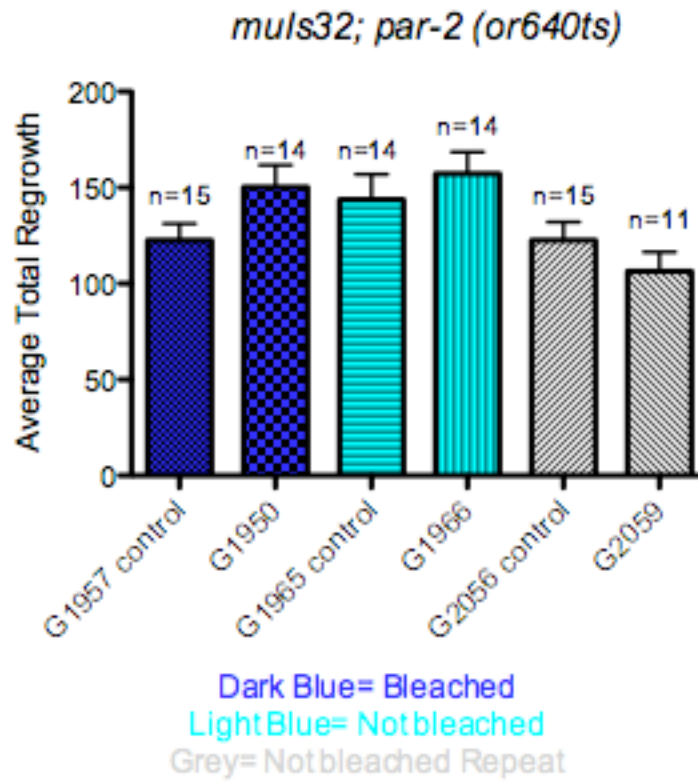
Graph 30: *mulS32 II; dnc-4 (or633) IV* Temperature Sensitive



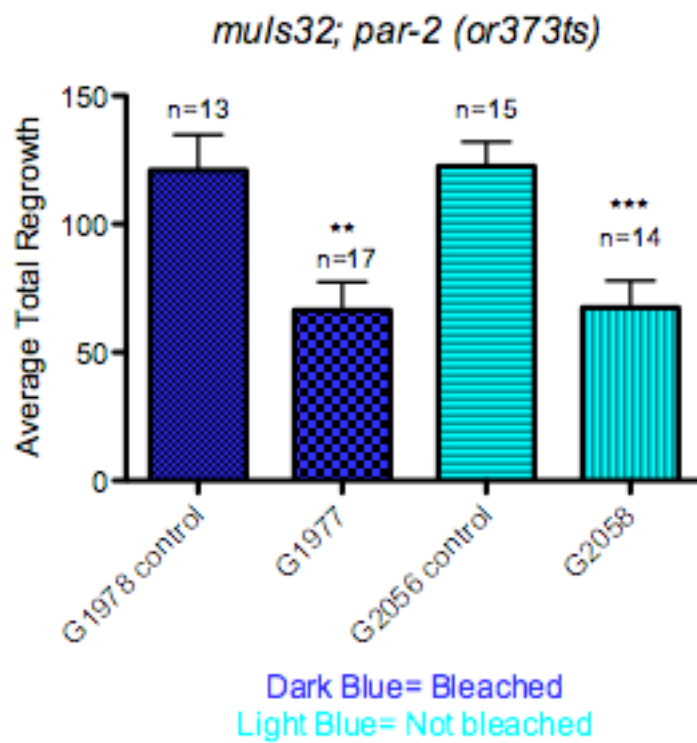
Graph 31: *zdis5 I; dnc-4 (or633) IV* Temperature Sensitive



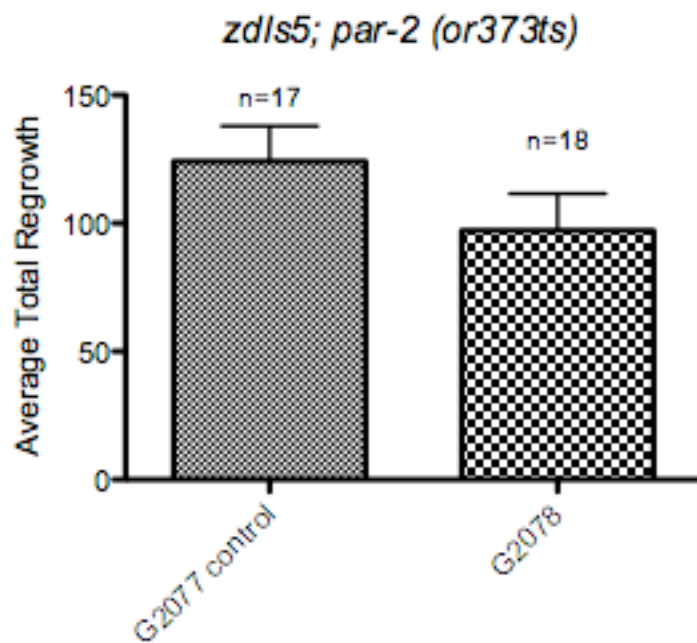
Graph 32: *mul32 II; lit-1 (or393) III* Temperature Sensitive



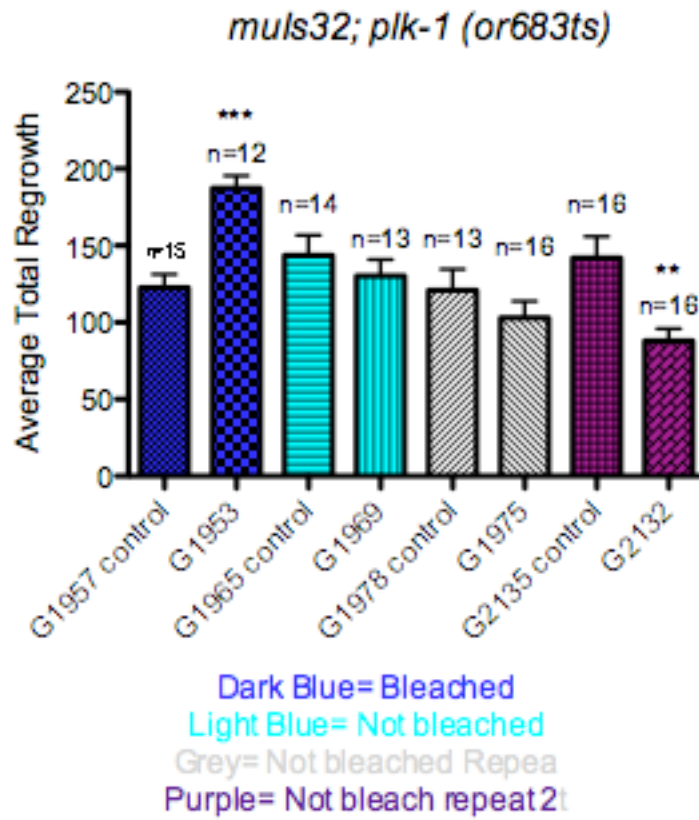
Graph 33: *mulS32 II; par-2 (or640)* Temperature Sensitive



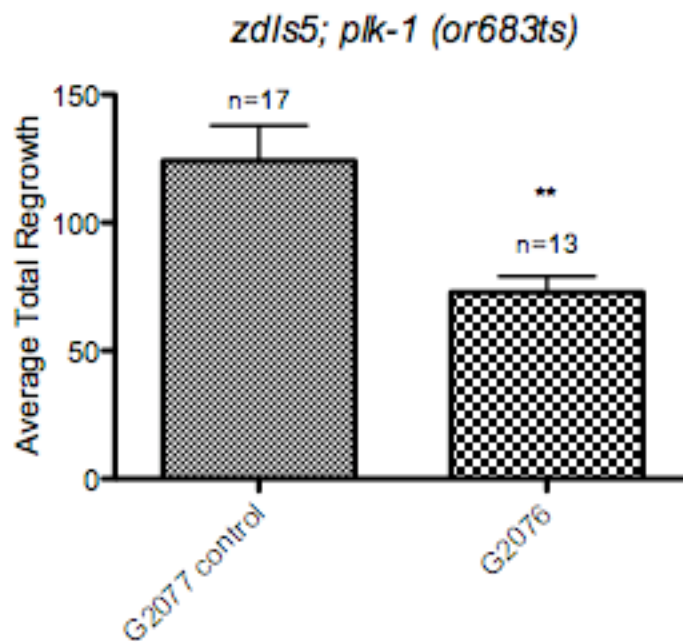
Graph 34: *mulS32 II; par-2 (or373)* Temperature Sensitive



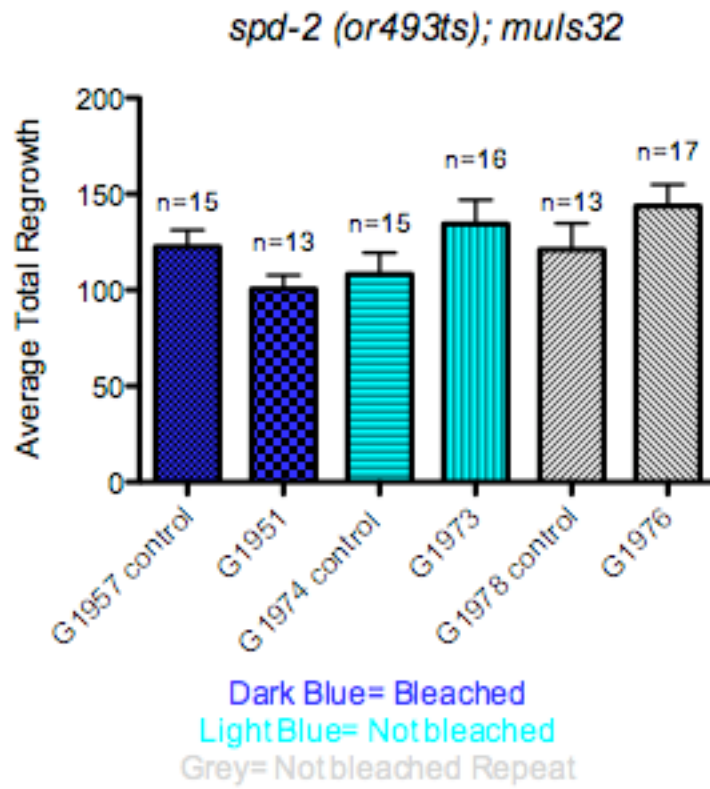
Graph 35: *zdis5 I; par-2 (or373)* Temperature Sensitive



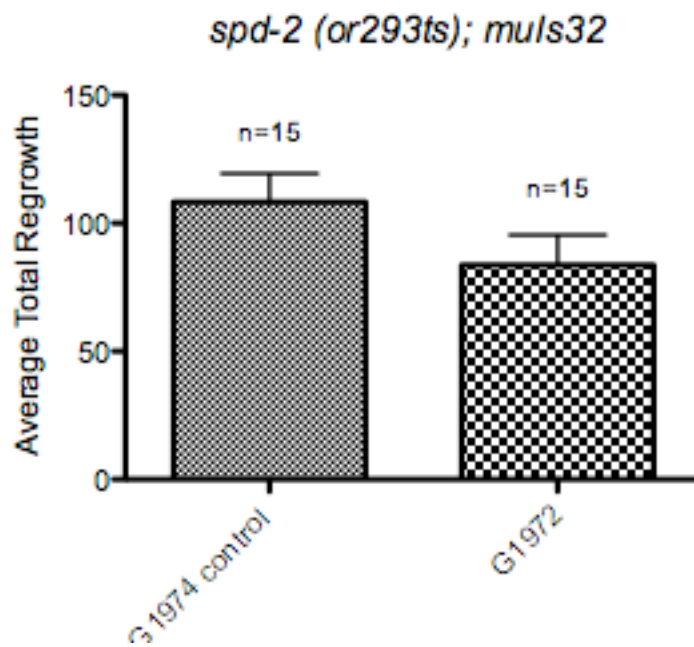
Graph 36: *mul32 II; plk-1 (or683) III* Temperature Sensitive



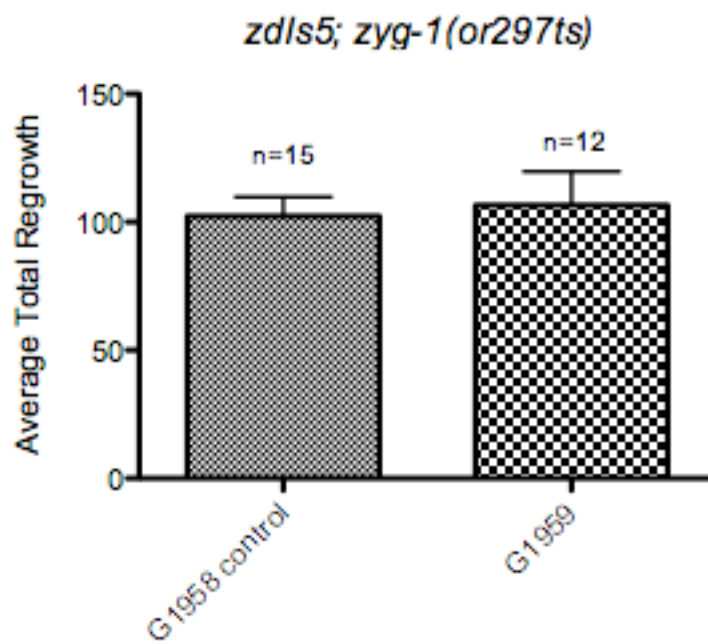
Graph 37: *zdis5 I; plk-1 (or683) III* Temperature Sensitive



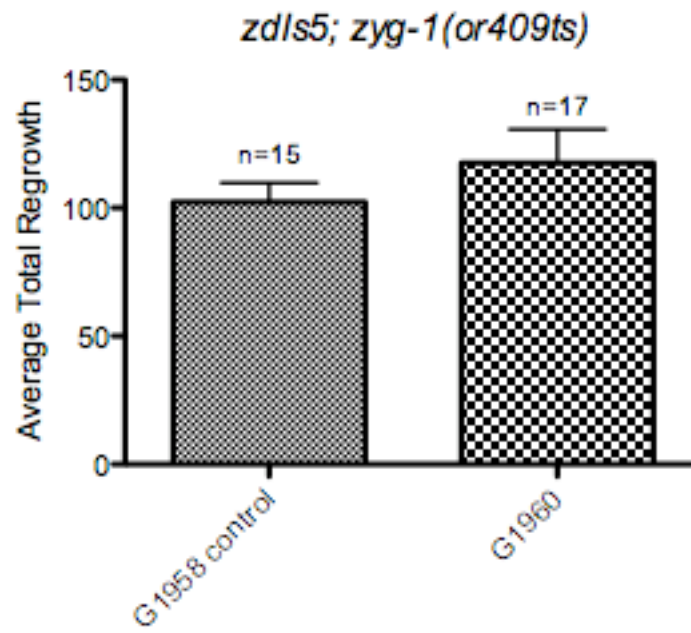
Graph 38: *spd-2 (or492) I; muls32 II* Temperature Sensitive



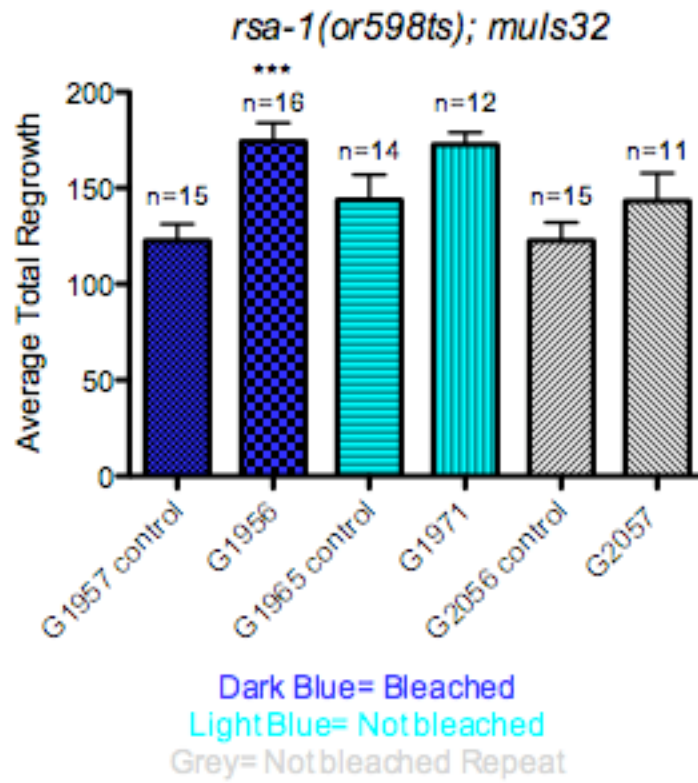
Graph 39: *spd-2 (or293) I; muls32 II* Temperature Sensitive



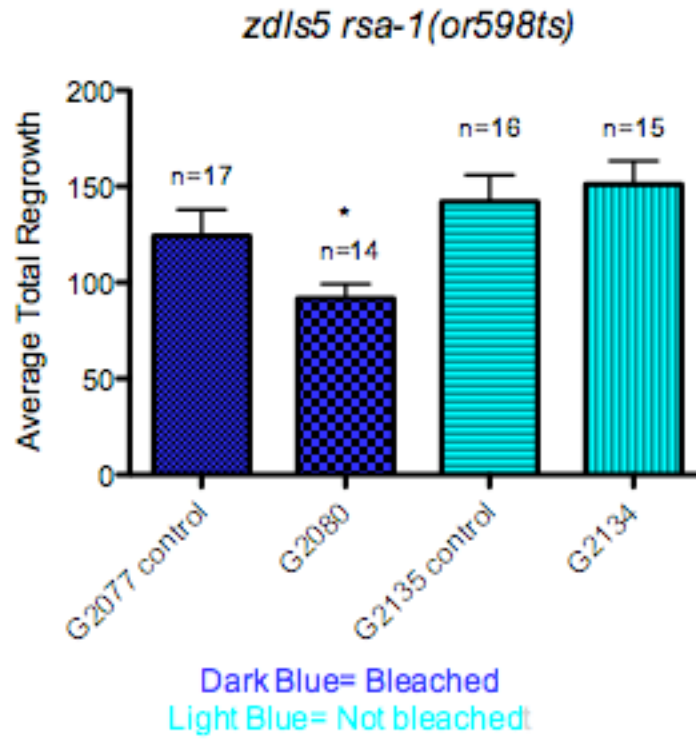
Graph 40: *zdl5 I; zyg-1 (or297) II* Temperature Sensitive



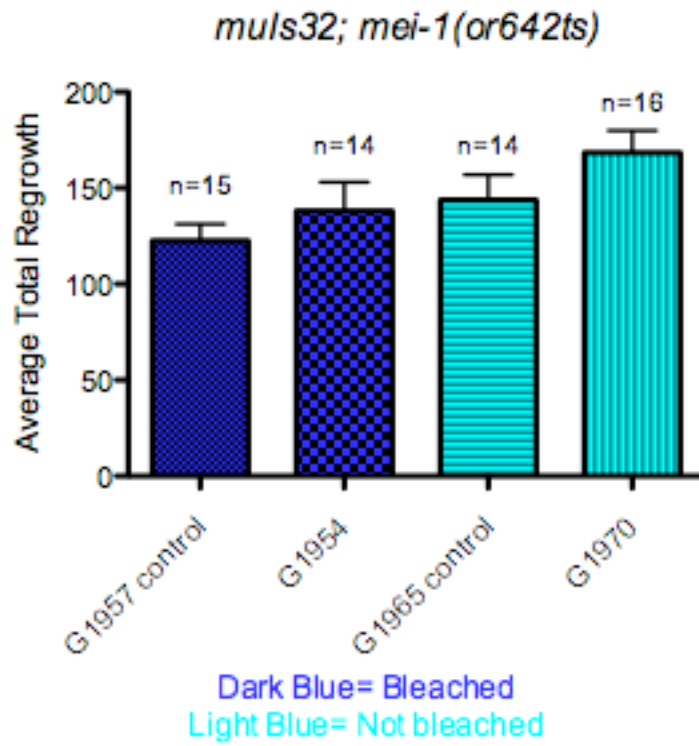
Graph 41: *zdl5 I; zyg-1 (or409) II* Temperature Sensitive



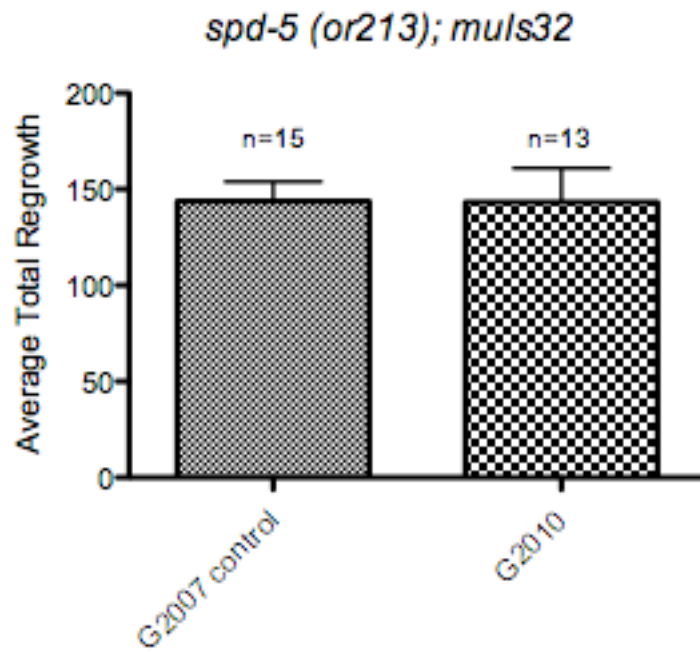
Graph 42: *rsa-1 (or598) I; muls32 II* Temperature Sensitive



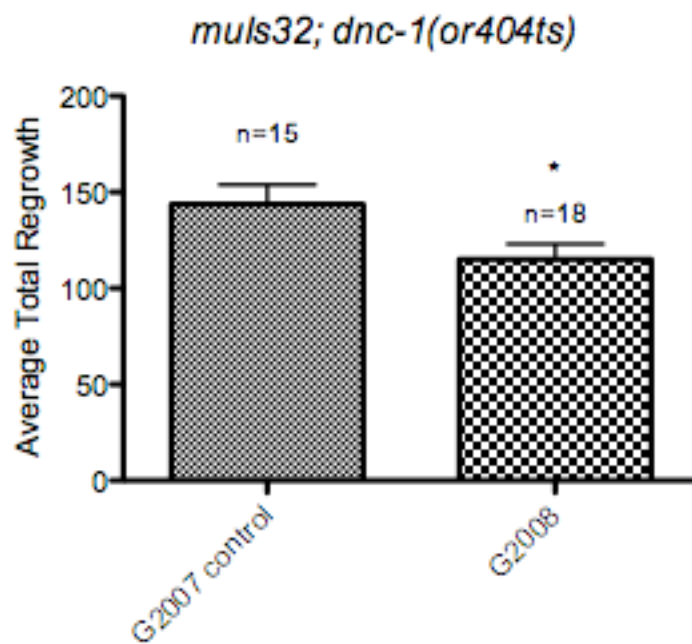
Graph 43: *zdis5 I rsa-1 (or598) I* Temperature Sensitive



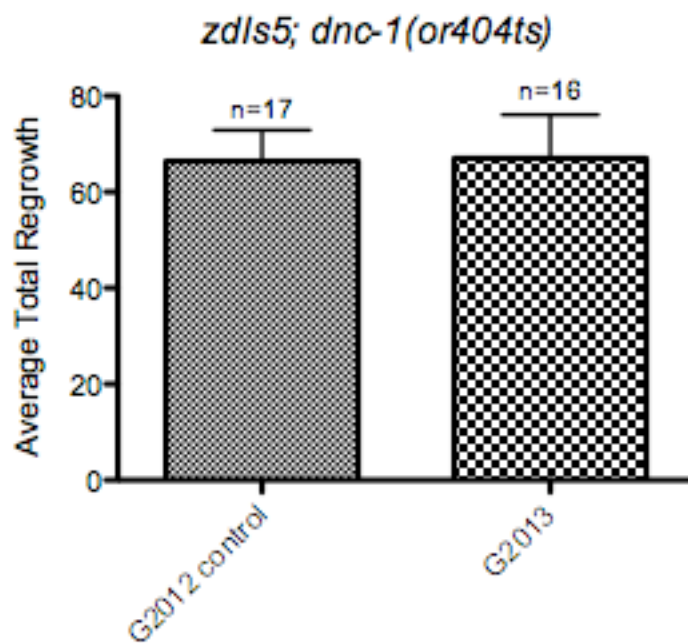
Graph 44: *mei-1 (or642) I; mulS32 II* Temperature Sensitive



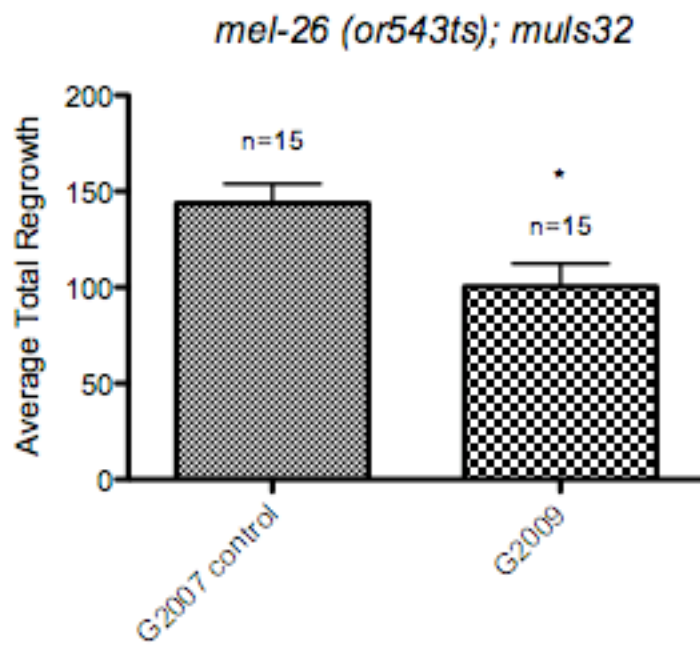
Graph 45: *spd-5 (or213) I; muls32 II* Temperature Sensitive



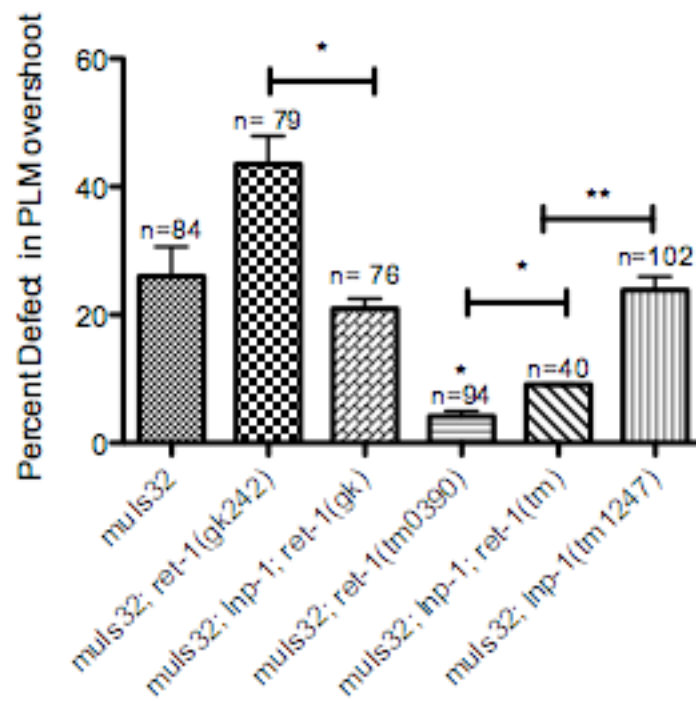
Graph 46: *dnc-1 (or404) I; mulS32 II* Temperature Sensitive



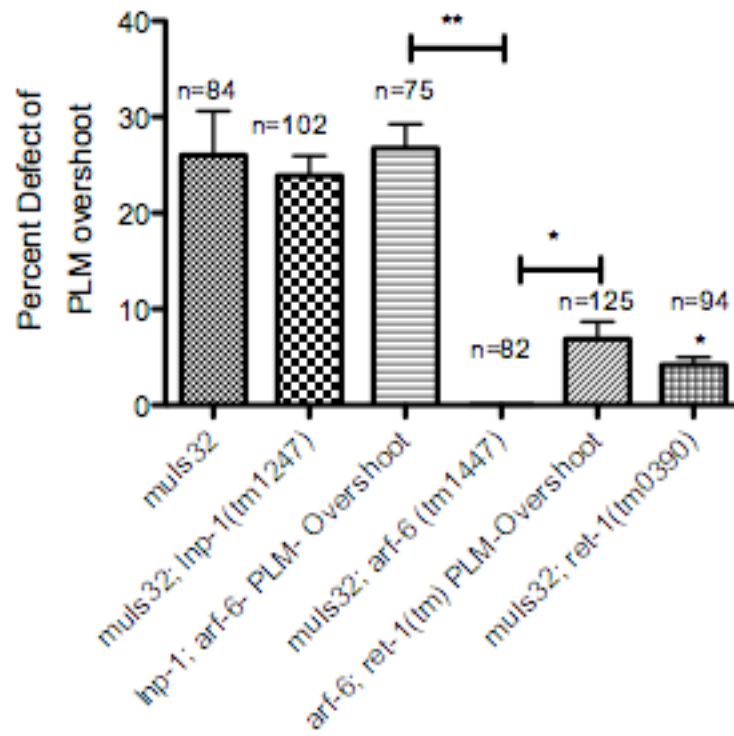
Graph 47: *zdl5* | *dnc-1 (or404)* | Temperature Sensitive



Graph 48: *mel-26 (or543) I; muls32 II* Temperature Sensitive

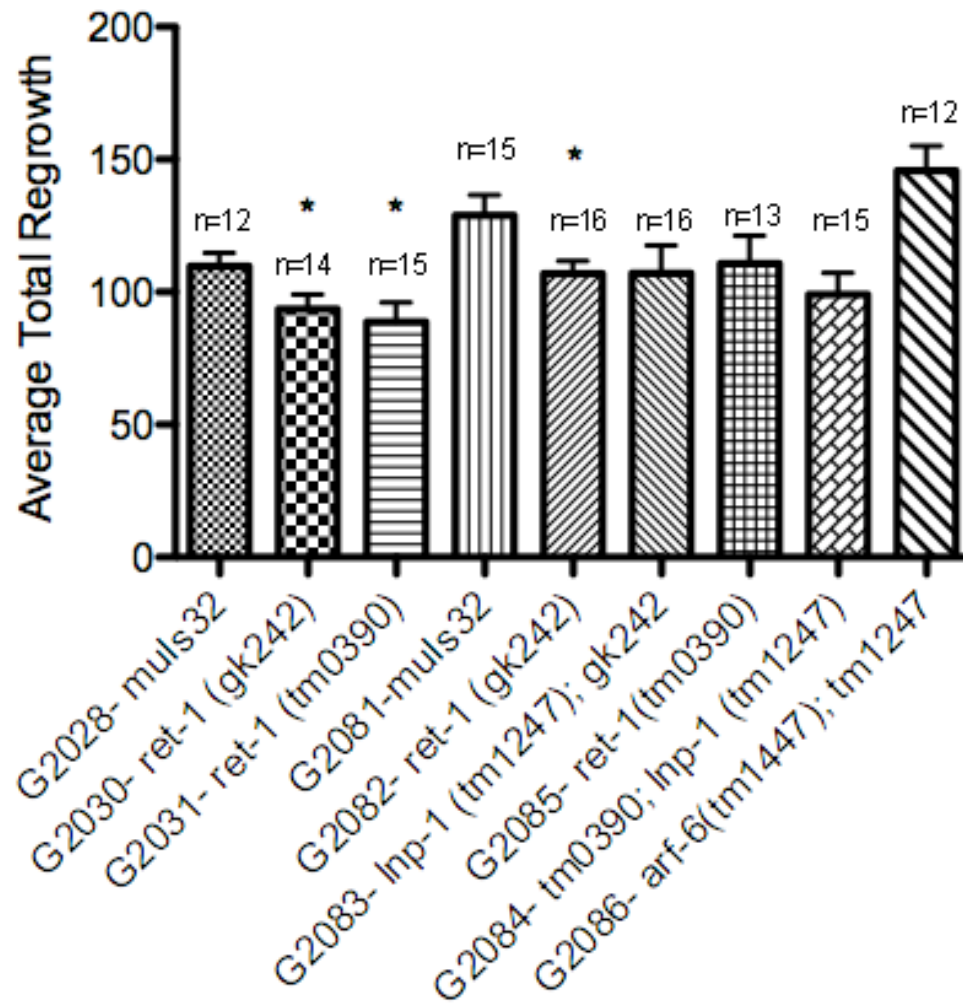


Graph 49: PLM Overshoot Defect: Reticulon (RET) associated

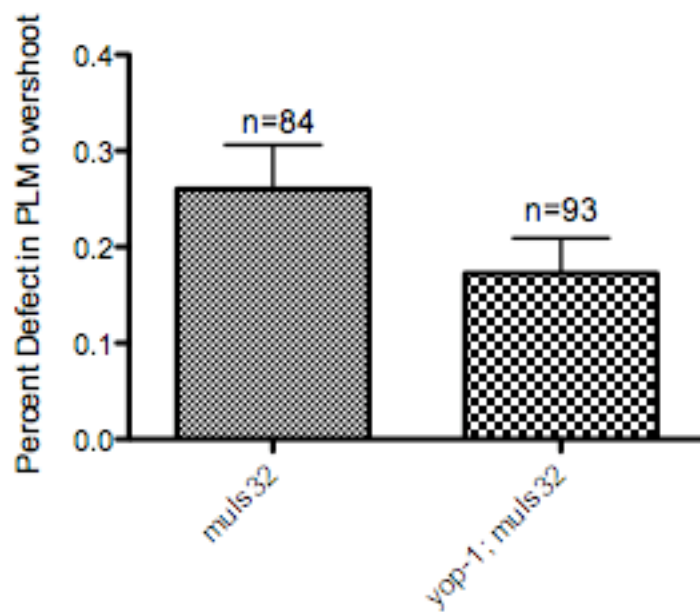


Graph 50: PLM Overshoot Defect: Reticulon (RET)

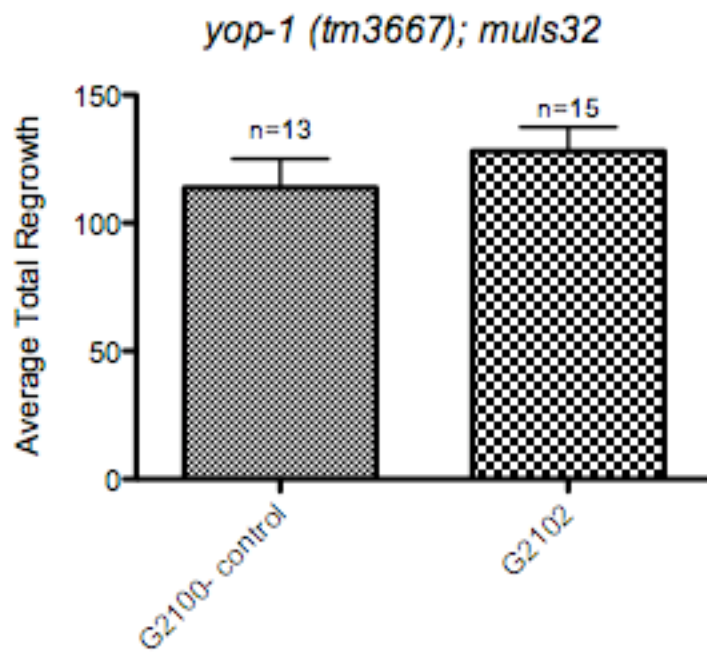
with vesicle- associated genes



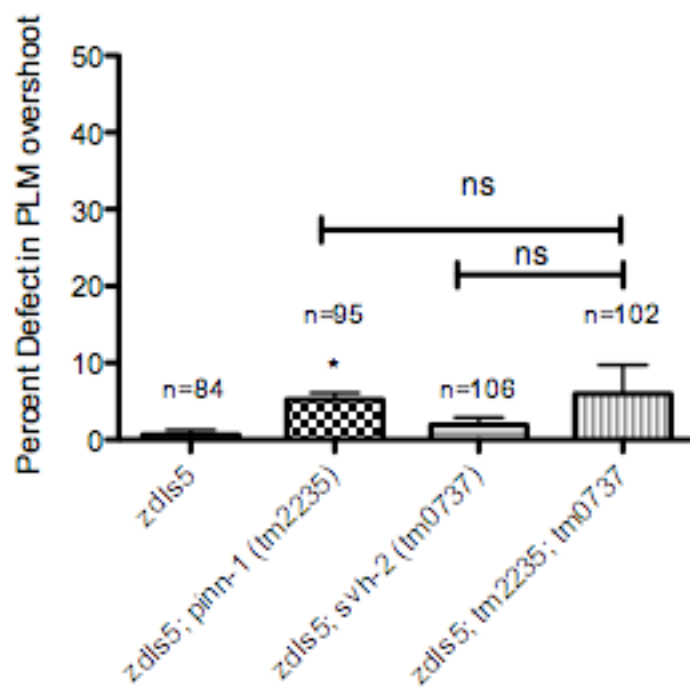
Graph 51: Axotomy Data: Reticulon (RET) associated



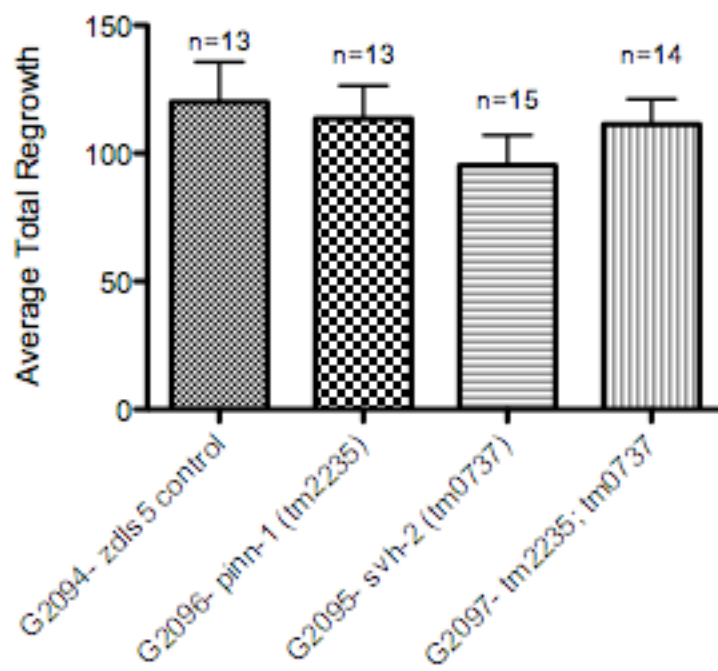
Graph 52: PLM Overshoot Defect: Reticulon (RET) associated 2



Graph 53: Axotomy Data: Reticulon (RET) associated 2



Graph 54: PLM Overshoot Defect: *pinn-1* and *svh-2*



Graph 55: Axotomy Data: *pinn-1* and *svh-2*

References

- Audhya A., Desai A., and Oegema K., 2007. A role for Rab5 in structuring the endoplasmic reticulum. *The Journal of Cell Biology*, 178: 43-55.
- Bejjani R. and Hammarlund M., 2012. Neural Regeneration in *Caenorhabditis elegans*. *Annual Review of Genetics*, 46: 499- 513.
- Brenner S., 1974. The genetics of *Caenorhabditis elegans*. *Genetics*, 77: 71-94.
- Chen L., Wang Z., Ghosh-Roy A., Hubert T., Yan D., O'Rourke S., Bowerman B., Wu Z., Jin Y., and Chisholm A.D., 2011. Axon Regeneration Pathways Identified by Systematic Genetic Screening in *C. elegans*. *Neuron*, 71: 1043-1057.
- Dang H., Li Z., Skolnik E., and Fares H., 2003. Disease-related Myotubularins Function in Endocytic Traffic in *Caenorhabditis elegans*. *Molecular Biology of the Cell*, 15: 189-196.
- Hammarlund M., Nix P., Hauth L., Jorgensen E., and Bastiani M., 2009. Axon Regeneration Requires a Conserved MAP Kinase Pathway. *Science*, 323: 802- 806.
- Gotenstein J.R., Swale R.E., Fukuda T., Wu Z., Giurumescu C.A., Goncharov A., Jin Y., and Chisholm A.D., 2010. The *C. elegans* peroxidase PXN-2 is essential for embryonic morphogenesis and inhibits adult axon regeneration. *Development*, 137: 3603- 3613.
- Harris T.W., Hartweg E., Horvitz H.R., and Jorgensen E.M., 2000. Mutations in Synaptojanin Disrupt Synaptic Vesicle Recycling. *The Journal of Cell Biology*, 150: 589-600.
- Li C., Hisamoto N., Nix P., Kanao S., Mizuno T., Bastiani M., and Matsumoto, 2011. The growth factor SVH-1 regulates axon regeneration in *C. elegans* via the JNK MAPK cascade. *Nature Neuroscience*, 15: 551-557.
- Ogura K., Wicky C., Magnenat L., Tobler H., Mori I., Muller F., and Ohshima Y., 1994. *Caenorhabditis elegans unc-51* gene required for axonal elongation encodes a novel serine/ threonine kinase. *Genes and Development*, 8: 2389- 2400.
- O' Rourke S., Carter C., Carter L., Christensen S., Jones M., Nash B., Price M., Turnbull D., Garner A., Hamill D., Osterberg V., Lyczak R., Madison E., Nguyen M., Sandberg N., Sedghi N., Willis J., Yochem J., Johnson E., and Bowerman B., 2011. A survey of new temperature- sensitive, embryonic- lethal mutations in *C. elegans*: 24 alleles of thirteen genes. *PLoS One*, 6: e16644.
- O' Rourke S., Dorfman M., Carter J., and Bowerman B., 2007. Dynein Modifiers in *C. elegans*: Light Chains Suppress Conditional Heavy Chain Mutants. *PLoS Genetics*, 3:1339- 1354.

Poli M., Gatta L., Dominic R., Lovati C., Mariani C., Albertini A., and Finazzi D., 2005. *Neuroscience Letters*, 389: 66-70.

Schuske K., Richmond J., Matthies D., Davis W., Runz S., Rube D., Van Der Bliet A., and Jorgensen E., 2003. Endophilin is Required for Synaptic Vesicle Endocytosis by Localizing Synaptojanin. *Neuron*, 40: 749- 762.

Schwab M., 2010. Functions of Nogo proteins and their receptors in the nervous system. *Nature Reviews Neuroscience*, 11: 799-811.

Wang Z. and Jin Y., 2011. Genetic dissection of axon regeneration. *Current Opinion Neurobiology*, 21: 189–196.

Wu Z., Ghosh-Roy A., Yanik M.F., Zhang J.Z., Jin Y., and Chisholm A.D., 2007. *Caenorhabditis elegans* neuronal regeneration is influenced by life stage, ephrin signaling, and synaptic branching. *Proceedings of the National Academy of Sciences U.S.A.*, 104: 15132- 15137.

Yan D., Wu Z., Chisholm A.D., and Jin Y., 2009. The DLK-1 Kinase Promotes mRNA Stability and Local Translation in *C. elegans* Synapses and Axon Regeneration. *Cell*, 138: 1005-1018.

Yang Y. and Strittmatter S., 2007. The reticulons: a family of proteins with diverse function. *Genome Biology*, 8: 234.

Yanik M.F., Cinar H., Cinar H.N., Chisholm A.D., Jin Y., and Ben-Yakar A., 2004. Neurosurgery: functional regeneration after laser axotomy. *Nature*, 432: 822.